DISS. ETH NO. 22539

MECHANISMS OF RNA INTERFERENCE IN PNS MYELINATION

A thesis submitted to attain the degree of

DOCTOR OF SCIENCES of ETH ZURICH

(Dr. sc. ETH Zurich)

presented by

DENIZ GÖKBUGET

Diplom-Biochemiker, Johann Wolfgang Goethe-Universität Frankfurt am Main

born on 12.10.1984

citizen of Germany

accepted on the recommendation of

Prof. Ueli Suter

Prof. Markus Stoffel

Prof. Constance Ciaudo

Prof. Jean-Marc Fritschy

2015

To my family.

Contents

Summary

Myelination is a remarkable example of cell differentiation, and ensures fast signal propagation in the nervous system. In peripheral nerves this process is mediated by Schwann cells (SCs). Prior to myelination the SC population needs to expand to match the number of available axons, providing enough SCs to engage with axons in a one-to-one SC-to-axon relation. At this stage myelination is initiated by Krox20 (also known as Egr2)-dependent myelin gene expression, ultimately leading to the consecutive wrapping of multiple compacted layers of myelin around axons. A prominent class of small noncoding RNAs, microRNAs (miRNAs), was shown to be critical for myelination. Mature miRNAs are derived from a primary transcript which is sequentially processed by two RNAse III enzymes, Drosha and Dicer. Drosha is part of the microprocessor complex containing RNA-binding protein DiGeorge syndrome critical region gene 8 (DGCR8), which is necessary for substrate recognition. A detailed mechanism of how the miRNA pathway regulates myelination remains unclear.

The first part of the thesis introduces a crucial miRNA-independent function of the microprocessor in the promotion of SC survival and radial sorting through the suppression of sonic hedgehog (Shh) signalling. We found that conditional SC-specific DGCR8 mutant mice show a pronounced radial sorting defect, which was not observed in Dicer mutants. Using mouse genetics and transcriptomics analysis, we show that this phenotype is miRNA-independent and microprocessor-dependent. Morphological analysis revealed that radial sorting is impaired due to increased SC death in DGCR8 mutants. Comparison of the transcriptomes of DGCR8 and Dicer mutant mice revealed Shh as the most upregulated mRNA in DGCR8 mice. We elucidate a detrimental role of Shh in SCs by showing that the activation of Shh signalling in wildtype mice compromises SC survival, whereas its inhibition rescues SC survival and radial sorting in DGCR8 mutants.

In the second part of the thesis Lin28B-dependent let-7 miRNAs are presented as critical drivers of myelination through the suppression of myelination-inhibitory Notch1 signalling. We found that let-7 miRNAs are expressed prior to the onset of myelination and that their expression is inversely correlated to Lin28B levels. Using conditional transgenic mice, we show that sustained SC-specific Lin28B expression and consequently reduced levels of let-7 impairs the onset of myelination. This impairment is dependent on let-7 miRNAs, as *in vivo* delivery of Lin28B-independent let-7 leads to a rescue of myelination in this mouse model. Finally, we show that let-7 miRNAs promote Neuregulin-1 (Nrg1)-dependent Krox20 expression by suppression of Notch1 mRNA and that inhibition of Notch signalling rescues sustained Lin28B expression *in vivo*.

The newly discovered multifaceted functions of the miRNA pathway contribute to a deeper understanding of developmental myelination in the PNS, and can be beneficial for the development of novel therapeutic approaches in demyelinating diseases.

Kurzfassung

Myelinisierung ist ein beeindruckendes Beispiel für Zelldifferenzierung und ist von fundamentaler Bedeutung für die schnelle Reizleitung im Nervensystem. In peripheren Nerven wird dieser Prozess von Schwann Zellen (SZ) bewältigt. Bevor Myelinisierung beginnen kann muss die SZ-Population zuerst expandieren, um der Zahl der vorhandenen Axone zu entsprechen. Dadurch ist sichergestellt, dass genügend SZ vorhanden sind, um jeweils ein Axon zu umschliessen. In diesem Stadium wird Myelinisierung durch Krox20 (auch bekannt als Egr2)-induzierte Myelin-Genexpression initiiert, welche letztlich zur Bildung mehrerer kompakt gestapelter Myelinmembranschichten um das Axon führt. Frühere Forschungsergebnisse haben gezeigt, dass microRNAs (miRNAs), eine bedeutende Klasse von kleinen nicht-kodierenden RNAs, essentiell für die Myelinisierung sind. Terminal prozessierte miRNAs werden durch sequenzielles Prozessieren eines Primärtranskriptes durch die RNAse III Enzyme Drosha und Dicer generiert. Drosha ist Teil des sogenannten Mikroprozessorkomplexes, welcher auch das RNA-Bindeprotein DiGeorge syndrome critical region gene 8 (DGCR8) enthält. DGCR8 ist notwendig für die Substraterkennung durch den Enzymkomplex. Ein detaillierter Mechanismus des miRNA-Signalweges während der Myelinisierung ist nicht bekannt.

Der erste Teil dieser Arbeit stellt eine grundlegende miRNA-unabhängige Funktion des Mikroprozessorkomplexes vor, welche Überlebenssignale in SZ fördert und so genügend SZ für die Zahl der zu umschliessenden Axone bereitstellt. Diese Funktion basiert auf einer Unterdrückung des Sonic Hedgehog (Shh)-Signalwegs. Unsere Resultate zeigen, dass konditionale SZ-spezifische DGCR8- im Gegensatz zu Dicer-Mausmutanten ein Defizit in der Fähigkeit von SZ, Axone zu sortieren, aufweisen. Durch Analyse verschiedener Mausmutanten und Expressionsmustern konnten wir zeigen, dass der DGCR8 Phänotyp miRNA-unabhängig und Mikroprozessor-abhängig ist. Morphologische Untersuchungen haben aufgezeigt, dass das Defizit beim Sortieren von Axonen auf erhöhten Schwann Zelltod zurückzurühren ist. Durch komparative Analyse der Expressionsmuster von DGCR8- und Dicer-Mausmutanten wurde Shh als die am stärksten hochregulierte mRNA nachgewiesen. Wir konnten zeigen, dass Shh schädlich für das Überleben von SZ ist. Diese Schlussfolgerung resultiert aus dem Ergebnis, dass die Aktivierung des Shh-Signalwegs zu reduziertem Überleben von SZ in Wildtyp Mäusen führt, wohingegen dessen Inhibition zu erhöhtem Überleben von SZ und einer generellen Verbesserung des Phänotyps in DGCR8-Mausmutanten führt.

Der zweite Teil dieser Arbeit präsentiert Lin28B-abhängige let-7 miRNAs als essentielle Antreiber von Myelinisierung. Diese Funktion basiert auf einer Unterdrückung des Notch1-Signalwegs, welcher bekanntlich Myelinisierung inhibiert. Wir konnten zeigen, dass let-7 miRNAs vor dem Beginn der Myelinisierung exprimiert werden und dass ihr Expressionsniveau invers mit dem von Lin28B korreliert ist. Durch Analyse von konditionalen transgenen Mäusen konnten wir nachweisen, dass anhaltende Expression von

Lin28B und daraus resultierende reduzierte Expression von let-7 den Beginn der Myelinisierung behindert. Diese Behinderung basiert auf let-7, da *in vivo* Verabreichung von Lin28B-unabhängigen let-7 zu Myelinisierung in diesen Mausmodellen führt. Ferner konnten wir zeigen, dass let-7 miRNAs Neuregulin-1 (Nrg1)-abhängige Krox20 Expression fördern, indem sie Notch1 mRNA unterdrücken. Zuletzt konnten wir nachweisen, dass die *in vivo* Hemmung des Notch1- Signalwegs, bei anhaltender Expression von Lin28B, Myelinisierung erlaubt.

Die neu entdeckten breitgefächerten Funktionen des miRNA-Signalweges tragen zu einem tieferen Verständnis der Myelinisierung während der Entwicklung bei und können zu neuen therapeutischen Strategien bei demyelinisierenden Erkrankungen beitragen.

List of Abbreviations

BSA .... Bovine serum albumin
cDNA .... Complementary deoxyribonucleic acid
DEPC .... Diethylpyrocarbonate
DMEM .... Dulbecco's Modified Eagle Medium
dNTPs .... Deoxynucleoside triphosphates
DTT .... Dithiothreitol
FBS .... Fetal bovine serum
FEG .... Field emission gun
HBSS .... Hanks' Balanced Salt Solution
HEPES .... 4-(2-hydroxyethyl)-1-piperazineethanesulfonic acid
HRP .... Horseradish peroxidase
MEM .... Modified Eagle Medium
NGF .... Nerve growth factor
PBS .... Phosphate buffered saline
PCR .... Polymerase chain reaction
PDL .... Poly-D-lysine
PFA .... Paraformaldehyde
RNA .... Ribonucleic acid
RT .... Room temperature
SDS .... Sodium dodecyl sulfate
TBS .... Tris buffered saline
TEM .... Transmission electron microscopy
Tris 2-Amino-2-hydroxymethyl-propane-1,3-diol

1 Introduction

1.1 Developmental myelination in the peripheral nervous system

Myelination is an evolutionary conserved process that guarantees electrical insulation to axons allowing efficient spatiotemporal signal propagation in the vertebrate nervous systems [Schweigreiter et al., 2006]. In the peripheral nervous system (PNS) this process is governed by Schwann cells (SCs). These glial cells origin from neural crest migratory stem cells and are directly formed from differentiating Schwann cell precursors (Fig. 1.1) [Jessen and Mirsky, 2005]. Initially they emerge as immature SCs which are still dependent on axonal contact for survival signals, including axonal Nrg1. During this stage the SC population expands to match the number of proximate axon segments. In a process called radial sorting, SCs engage with larger calibre axons (measuring more than 1 µm in diameter in the adult PNS) and sort them out of axon bundles. The resulting 1:1 SC-axon relation is considered as the pro-myelinating stage. To myelinate,
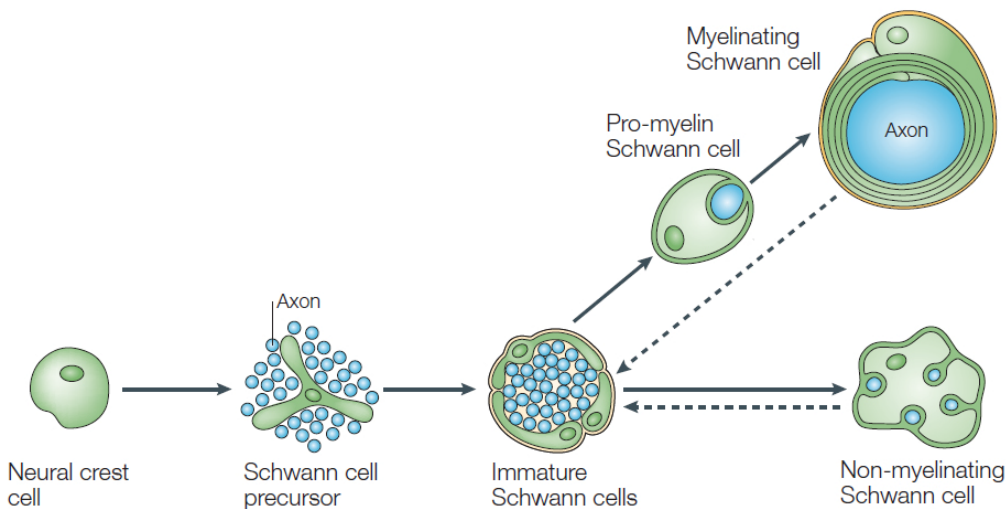
Figure 1.1 | Scheme showing major differentiation stages of the SC lineage. Schwann cell precursors (SCPs) arise from migrating neural crest stem cells at around embryonic day (E) 12-13 in mice. SCPs are tightly tethered to surrounding axons. Around E13-E15 SCPs give rise to immature SCs, which post-natally start to sort individual axonal segments out of the bundles and proceed with myelin production. Axons smaller than 1 µm in diameter on the adult PNS are not myelinated, and instead are engaged by non-myelinating SCs. Adapted from Jessen and Mirsky (2005).

pro-myelinating SCs exit the cell cycle and express the transcription factor Krox20, a master regulator of myelin gene expression [Topilko et al., 1994, Pereira et al., 2012]. After forming multiple consecutive layers of compacted myelin membrane around the axon developmental myelination reaches its mature state. Axons with smaller calibre remain unmyelinated, but are still surrounded by SC processes in so-called Remak bundles [Jessen and Mirsky, 2005].

Radial sorting is a prerequisite for proper myelination to occur [Pereira et al., 2012]. Mechanisms involved in radial sorting include the matching of SC numbers to the number of axonal segments which are to be myelinated and the cytoskeletal rearrangements that lead to the extension of processes in order to sort axons from bundles. Molecules with critical roles in the expansion of the SC pool during radial sorting include FAK (focal adhesion kinase) and Cdc42 [Grove et al., 2007, Benninger et al., 2007]. While Cdc42 seems to be largely independent of signalling from the SC-surrounding basal lamina, FAK activity is dependent on the β1-integrin subunit. Through the interaction with laminins the β1-integrin subunit and dystroglycan are critical for radial sorting [Feltri and Wrabetz, 2005, Berti et al., 2011, Feltri et al., 2002, Yang et al., 2005]. Intracellular effectors of β1-integrin include Rac1 and ILK (integrin-linked kinase), both of which promote the extension of radial lamellipodia that are considered to be important for radial sorting [Benninger et al., 2007, Pereira et al., 2009]. The timed activity of Wnt/β-catenin was also shown to promote radial sorting through the promotion of process extension, although in this case most likely independently of the basal lamina [Grigoryan et al., 2013].

Upon reaching the pro-myelinating stage, SCs exit the cell cycle and activate myelin gene expression which is mainly orchestrated through the transcription factor Krox20 [Pereira et al., 2012]. The major driver of Krox20 expression is Nrg1. The thickness of the myelin produced is directly proportional to the calibre of the axon and is thought to be largely dependent on the amount of Nrg1 presented on the surface of the axon [Michailov et al., 2004].

A remarkable feature of SCs is their plasticity, which upon injury enables them to reverse their commitment towards the myelinated state and re-enter the cell cycle to orchestrate regrowth of axons and remyelination [Pereira et al., 2012]. During this process they transiently acquire characteristics broadly similar to those of the immature SC stage. However transitions between both SC states need to be precisely controlled and a failure to do so is linked to various pathologies [Niemann et al., 2006]. The plasticity of SCs is linked to the balance of negative and positive regulators of myelination [Jessen and Mirsky, 2008]. These are largely responsible for either the maintenance of the immature SC-like state *vs* the myelinating SC fate (Fig. 1.2). Characteristics of negative regulators of myelination involve (1) their inactivation prior to myelination, (2) interference with myelination if aberrantly expressed during myelination, (3) their activation upon injury and (4) their ability to drive SC dedifferentiation.

A well-described example of this type of these negative regulators is Notch1 [Woodhoo et al., 2009]. Notch signalling is critical for the formation of immature SCs and their proliferation. However its enforced activation was shown to delay the onset of myelination by interfering with Krox20 expression. Furthermore its activation

is a critical driver of dedifferentiation after PNS injury. Other negative regulators of myelination include Sox2 and c-Jun [Pereira et al., 2012, Parkinson et al., 2008].

Prominent positive regulators of myelination promote myelination and often counteract directly or indirectly the negative regulators [Jessen and Mirsky, 2008]. Many of the physiologically relevant positive regulators of myelination in SCs act as downstream effectors of Nrg1 to synergise in the activation Krox20 expression, and include Erk1/2, YY1 and Nfatc4 [Newbern et al., 2011, He et al., 2010, Kao et al., 2009, Pereira et al., 2012]. Nrg1, in particular the membrane-bound form Nrg1 type-III, acts by activating ErbB2-ErbB3 receptor tyrosine kinases in SCs [Pereira et al., 2012]. The three major signalling cascades downstream of activated ErbB2-ErbB3 complexes in SCs are the PI3K (Phosphatidylinositol-4,5-bisphosphate 3-kinase)-Akt, PLCγ (Phospholipase Cγ) and MEK pathway [Pereira et al., 2012]. While

Figure 1.2 | Positive and negative regulators of myelination. Green arrow indicates factors positive regulators of myelination and red arrow indicates negative regulators of myelination. Adapted from Jessen and Mirsky (2005).

PLCγ and MEK pathway activities have been mainly linked to the activation of Krox20, the PI3K-Akt pathway is suggested to support myelination mainly through the induction of lipid and cholesterol biosynthesis.

In addition to transcriptional and metabolic regulation, myelination also involves the establishment of cell polarity [Pereira et al., 2012]. Many of the proteins involved in this process are already well-described in the concept of mesenchymal-to-epithelial transition [Lamouille et al., 2014]. Among them is Par3, which is asymmetrically located at the SC-axon junction and its co-localisation with the p75 neurotrophin receptor (also known as Ngfr) is crucial for the onset of myelination [Chan et al., 2006].

Given the importance of the process of myelination, malfunctions of this system are naturally associated with severe diseases. In the PNS these peripheral neuropathies, the most common being Charcot-Marie-Tooth disease, are often associated with mutations in key proteins involved in myelination [Niemann et al., 2006].

1.2 Biogenesis and function of microRNAs

miRNAs are small non-coding RNAs that have ubiquitous evolutionary conserved gene regulatory functions in nearly all eukaryotes [Berezikov, 2011]. The first miRNA, *lin-4*, was discovered in *C. elegans* in a screen for genes important for development [Lee et al., 1993]. Since then a plethora of regulatory functions of miRNAs in eukaryotes has been described at the post-transcriptional level in physiological and pathological scenarios [Ambros, 2004, Mendell and Olson, 2012, Ameres and Zamore, 2013,
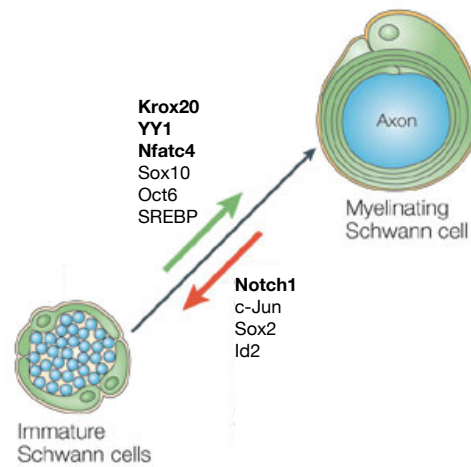
Berezikov, 2011]. Genes encoding miRNAs constitute one of the largest family of genes and currently involves 1920 mature miRNAs in mice (see www.mirbase.org), although many of these still lack functional validation [Kozomara and Griffiths-Jones, 2014]. Many of these miRNA genes share sequence homologies and are likely the product of gene duplications [Hertel et al., 2006]. Based on these homologies 'miRNA-families' are generally defined as miRNAs that have identical sequences for nucleotides 2-8 [Bartel, 2009]. The number of miRNA families has continuously expanded during metazoan evolution and most of them largely remain phylogenetically conserved [Wheeler et al., 2009]. The currently most commonly used nomenclature (see www.mirbase.org) names miRNAs with numerical names (for example miR-338, miR-16). miRNAs within the same family are usually distinguished by letters (such as miR-27a and miR-27b). Exceptions to these rules are the first miRNAs discovered which were named at that time by the obtained phenotype after their deletion (for example let-7). As each miRNA locus generates two mature miRNA strands out of the precursor, the miRNA derived from the 5′- and 3′-strand of the precursor are indicated '-5p' and '-3p', respectively (for example miR-338-5p and miR-338-3p). At the genomic level, miRNA genes can be located in various regions. The majority was found to be located in defined transcriptional units out of which most are encoded within introns [Rodriguez et al., 2004]. Several miRNA genes are found in close proximity (called 'miRNA clusters') and cotranscribed as polycistronic units, such as the miR-100~let-7~miR-125 cluster [Roush and Slack, 2008].

The primary transcript of a miRNA (pri-miRNA) can be generated through activation of the host gene promoters or by independent transcriptional start sites [Ozsolak et al., 2008]. Transcription of endogenous pri-miRNAs is generally carried out by Pol II, and the transcripts are capped and polyadenylated [Cai et al., 2004, Lee et al., 2004]. Certain miRNAs show tissue- and developmental stage-specific expression which is often connected to their critical functions in that tissue's homeostasis and in cell fate decisions [Landgraf et al., 2007, Wienholds et al., 2005, Ambros, 2004]. Pri-miRNAs contain a local hairpin secondary structure that is recognised and processed by the microprocessor complex [Lee et al., 2003, Ha and Kim, 2014]. This complex consists of the RNA-binding protein DGCR8 (also known as Pasha in *Drosophila melanogaster*) and the RNAse III Drosha (Fig. 1.3). DGCR8 is a ∼90 kDa protein mainly localised to the nucleus [Shiohama et al., 2007, Yeom et al., 2006]. It recognises pri-miRNAs through its two double-strand RNA binding domains (dsRBDs) and interacts with Drosha through its C-terminal domain [Han et al., 2006, Yeom et al., 2006]. This interaction primes Drosha, a ∼160 kDa protein, to cut the pri-miRNA approximately 11 bp from the 'basal' region of the hairpin [Han et al., 2006]. The cut is performed through tandem RNAse III domains located within Drosha's C-terminal domain [Han et al., 2004].

The processing of pri-miRNAs is subject to complex modulation through auxiliary factors of diverse nature linking the microprocessor to various cell context-dependent stimuli. Apart from secondary structure elements, primary sequence elements were shown to enhance pri-miRNA processing [Auyeung et al., 2013]. These elements are located in the basal (UG and CNNC motif) and terminal loop region of pri-miRNAs and at least one of these motifs is present in 79% of human miRNAs. Under con-

ditions of high cell density Hippo-mediated cytoplasmic retention of YAP facilitates p72 association with the CNNC motif, which results in increased microprocessor activity [Mori et al., 2014]. The activity of the microprocessor is also modulated by post-translational modifications of DGCR8 or Drosha through phosphorylation and acetylation which were shown to affect protein stability, nuclear localisation and substrate affinity [Wada et al., 2012, Tang et al., 2013, Herbert et al., 2013, Tang et al., 2011]. Furthermore microprocessor activity was shown to be affected through secondary protein-protein interactions. Phosphorylated methyl-CpG binding protein 2 (MeCP2) was shown to bind DGCR8 and interfere with the assembly of Drosha and DGCR8, thereby suppressing miRNA biogenesis and dendritic growth in neurons [Cheng et al., 2014]. Upon neuronal activity MeCP2 gets dephosphorylates and pri-miRNA processing is reestablished. The processing of a subset of pri-miRNAs can also be specifically regulated at the level of the microprocessor. DEAD-box RNA helicase subunits p68 and p72 are part of a high molecular weight microprocessor and promote Drosha processing of certain miRNAs [Fukuda et al., 2007]. Furthermore p53 and TGFβ-dependent SMAD proteins were shown to promote microprocessor activity through interaction with p68 [Suzuki et al., 2009, Davis et al., 2008, Davis et al., 2010]. In a distinct manner RNA-binding protein hnRNP A1 was also shown to promote the processing of miR-18a through interaction with its pri-miRNA [Guil and Caceres, 2007]. Similarly during DNA damage, ATM-mediated phosphorylation of DDX1 was shown to enhance processing of DNA damage-induced miRNAs [Han et al., 2014]. Another major way to affect processing of a subset of miRNAs is through the interaction with the loop region of specific pri-miRNA hairpins (see 1.4).

Following microprocessor catalysis, the produced $\sim$70 nt long hairpin (pre-miRNA) is translocated to the cytoplasm via exportin 5 [Yi et al., 2003, Lund et al., 2004, Bohnsack et al., 2004]. In the cytoplasm, the hairpin is further processed by the RNAse III Dicer [Hutvagner et al., 2001, Ha and Kim, 2014]. Dicer is a $\sim$200 kDa protein harbouring besides tandem RNAse III domains a PAZ domain that is necessary for the interaction with the termini of the pre-miRNA [Macrae et al., 2006]. The location of the cleavage site is suggested to be defined by the distance between the PAZ and the RNAse III domains acting as a 'molecular ruler' [Zhang et al., 2004, Macrae et al., 2006]. Dicer can also associate with RNA binding proteins which modulate Dicer processing. Binding of TAR RNA-binding protein (TRBP) leads to altered processing efficiency of certain pre-miRNAs and modified length of mature miRNAs [Fukunaga et al., 2012, Chakravarthy et al., 2010].

Cleavage of the pre-miRNA releases a $\sim$22 bp mature miRNA duplex which is loaded into AGO protein [Tabara et al., 1999, Hammond et al., 2001]. During this process one of the strands (called the 'guide' strand) remains bound to the AGO protein to form the miRNA-induced silencing complex (miRISC) while the other strand (called the 'passenger' strand) is released and rapidly degraded. Strand selection is mainly determined through the thermodynamic stability of the two ends of the duplex [Khvorova et al., 2003]. The strand with the less stable 5′ end is usually selected as the 'guide' strand. The miRISC interacts with target mRNAs through imperfect base pairing leading to translational repression and/or 3′–5′ accelerated decay of target

mRNAs [Ha and Kim, 2014]. The miRISC components locate to defined cytoplasmic foci named P-bodies which are believed to be active sites of miRNA-target repression [Liu et al., 2005].

The majority of target interactions happen through Watson-Crick pairing of 6-8 nucleotides at the $5'$ end of the miRNA (called 'seed' sequence) [Lim et al., 2005, Krutzfeldt et al., 2005, Bazzini et al., 2012, Rodriguez et al., 2007]. These canonical 'seed' sequences usually start with the second nucleotide of the miRNA unless the first nucleotide is an adenine [Lewis et al., 2005]. 'Seed' matches involving 8mers are generally more efficient in inducing target repression than 7mers, while 6mers often do not lead to significant effects [Grimson et al., 2007]. Another important characteristic of miRNA-targeting is reflected by the degree of conservation of the interaction. More than half of the human genes show strong evidence for evolutionary selection to maintain $3'$-UTR pairing to miRNAs [Friedman et al., 2009]. Based on that, conserved motifs within $3'$-UTR can largely be explained by miRNA targeting [Xie et al., 2005]. Nonconserved seed matches, although functional, are often *in vivo* not coexpressed with their targeting miRNAs as a consequence of evolutionary avoidance [Farh et al., 2005]. The minority of nonconserved targets expressed still constitute a significant fraction of all targets therefore making non-conserved targeting widespread [Krutzfeldt et al., 2005, Bazzini et al., 2012]. Most of the commonly used algorithms employ the determinants for conserved seed matching to predict miRNA targets [Bartel, 2009]. However, recently performed global biochemical screens of miRNA-mRNA interactions revealed that a sizeable fraction (6 to 60% of detected targets) of identified miRNA binding sites does not show canonical seed matching [Helwak et al., 2013, Zisoulis et al., 2010, Khorshid et al., 2013, Chi et al., 2009, Skalsky et al., 2012, Gottwein et al., 2011, Loeb et al., 2012, Hafner et al., 2010, Betel et al., 2010]. The function of such non-canonical sites was demonstrated in various physiological scenarios [Vo et al., 2010, Didiano and Hobert, 2006, Chi et al., 2012, Tay et al., 2008, Brennecke et al., 2005, Vella et al., 2004, Shin et al., 2010, Lal et al., 2009, Lu et al., 2010]. These non-canonical target sites can involve mismatches, guanine bulges (G-bulge) and G·U Wobble pairs within the 'seed' sequence. Furthermore centered pairing has been observed in which the 11-12 nucleotides in the centre of the miRNA form Watson-Crick pairs with their targets [Shin et al., 2010]. In fact, the targeting of lin-41 by let-7, one of the first identified miRNA-mRNA interactions, happens through two non-canonical sites within the lin-41 $3'$-UTR involving extensive $3'$ pairing [Vella et al., 2004]. Additional determinants affecting the efficiency of target repression involve the location of the target site [Grimson et al., 2007]. Sites within the $3'$-UTR typically result in more efficient repression than sites located in the open reading frame or the $5'$-UTR. Within the $3'$-UTR sites close to the stop codon or the poly(A)-tail are generally less efficient that the ones located in the centre of the $3'$-UTR. Even more important that the location of the site is composition of the nucleotides surrounding the site, with AU-rich context being preferable. Furthermore $3'$ pairing of the miRNA, in particular with miRNA nucleotides 13-16, can also enhance miRNA function and partially compensate for imperfect seed matches [Brennecke et al., 2005].

The detailed mechanism of how AGO-loaded miRNAs silence gene expression is still controversial, as evidence exists for mechanisms ranging from repression of translational initiation or elongation to accelerated miRNA decay [Ameres and Zamore, 2013]. Through association with GW182 proteins the miRISC can recruit the CCR4-NOT complex to induce deadenylation [Braun et al., 2011, Chekulaeva et al., 2011, Fabian et al., 2011]. However these studies have also shown that the CCR4-NOT complex can induce translational repression. To assess the relative importance of translational repression *vs* mRNA decay as effects of miRISC-mRNA association global proteomics coupled with transcriptomics approaches were performed. Such studies have shown that the majority of changes in protein abundance due to miRNAs are coupled to mRNA decay [Selbach et al., 2008, Baek et al., 2008, Guo et al., 2010]. However there is still a noteworthy fraction (11-16%) of miRNA targets that seems to be regulated through a block in translation. Although it seems logical that accelerated decay is naturally coupled with less translation of that message, studies for example in zebrafish suggest that translational repression can precede mRNA decay [Bazzini et al., 2012]. Although the major consequence of miRISC targeting is the silencing of gene expression, there are exceptions that show the opposite. Neuronal miR-128 for example targets the machinery of nonsense-mediated decay to induce a global increase of gene expression [Bruno et al., 2011]. This mechanism is important for neuronal differentiation as it leads to the overrepresentation of genes associated with neurogenesis. Association of miRNAs with their targets also seems to protect them from degradation [Chatterjee and Grosshans, 2009]. In *C. elegans* it was shown that AGO-bound miRNAs are protected from XRN-2 mediated exonuclease suggesting a role of active turnover in the efficient control of the pool of active miRNAs.

Given the short length of the 'seed' sequence more than half of protein-coding genes in mammals are subject to miRNA regulation [Friedman et al., 2009]. Thereby miRNAs constitute a powerful mechanism to shape gene expression. The essential role of the miRNA pathway in development is well reflected by the early embryonic lethality of *Dicer1*, *Dgcr8* or *Drosha* germline-deficient mice [Bernstein et al., 2003, Wang et al., 2007, Chong et al., 2010]. It is noteworthy that the majority of single miRNA knockout mice did not produce major defects in embryonic development [Mendell and Olson, 2012]. As most of these miRNAs do not share family members intrafamily redundancy is not the likely explanation. However redundancy due to miRNAs targeting an overlapping set of targets could explain for the lack of defects in these mouse mutants. Another explanation comes from stress conditions that could sensitise the system to the lack of miRNAs. In fact there are multiple cases in which a miRNA knockout does not show developmental defects but exhibits profound defects in response to certain stress conditions [Mendell and Olson, 2012]. For example, miR-375 knockout mice develop a functional endocrinic pancreas but under conditions of obesity-induced insulin resistance they fail to expand β-cell mass resulting in a severe diabetic state [Poy et al., 2009].

Certain miRNAs (known as non-canonical miRNAs) are generated through alternative pathways that are either microprocessor- or Dicer-independent [Ameres and Zamore, 2013]. These pathways include the formation of certain

intron-derived miRNAs as products of alternative splicing where the debranched lariat refolds into a pre-miRNA that is further processed by Dicer [Berezikov et al., 2007]. Furthermore tRNA maturation and snoRNAs can yield miRNAs in a microprocessor-independent Dicer-dependent manner [Babiarz et al., 2008, Ender et al., 2008]. Interestingly, pre-miRNA-like structures can also be generates directly by Pol II transcription, like in the case of microprocessor-independent miR-320 [Xie et al., 2013]. The Dicer-independent pre-miRNA-451 is generated by Drosha processing with a stem too short for Dicer processing [Cheloufi et al., 2010]. Thus it is directly matured through AGO2 endonuclease activity after loading. Additionally microprocessor-independent miRNAs derived from transcriptional start sites (TSS-miRNAs) were recently introduced as another functional class of non-canonical miRNAs with potential broad physiological functions [Zamudio et al., 2014].

The machinery involved in the biogenesis of miRNAs is also involved in the biogenesis of other small RNAs including endogenous siRNAs. In mouse oocytes these Dicer-dependent small RNAs are together with piRNAs necessary to suppress retrotransposition [Watanabe et al., 2008]. Another unexpected role of Drosha and Dicer-dependent small RNAs has been described during the DNA damage response [Francia et al., 2012]. These small RNAs are derived from the DNA damage site and necessary for the activation of the DNA damage response.

1.3 miRNA-independent functions of the microprocessor

Besides its critical role during canonical miRNA biogenesis the microprocessor is also associated with additional miRNA-independent regulatory functions (Fig. 1.3). Apart from pri-miRNAs it was shown that the microprocessor interacts with several other RNA substrates [Macias et al., 2012]. Among them are mRNAs, long non-coding RNAs, snoRNAs and transposable elements all of which are predicted to harbour pri-miRNA-like hairpin structures. A global transcriptomics analysis in *Drosophila* cells could also identify multiple RNA species distinct from miRNAs as potential substrates of the microprocessor [Kadener et al., 2009]. A notable example is the autoregulation of DGCR8 and Drosha, where DGCR8 stabilises Drosha through protein-protein interactions whereas Drosha cleaves a conserved hairpin within the DGCR8 mRNA [Han et al., 2009]. In a similar manner the microprocessor was shown *in vitro* to counteract retrotransposition of LINE-1 and Alu elements by binding to hairpin structures within their RNA transcripts [Heras et al., 2013]. During neurogenesis the microprocessor-dependent regulation of neurogenin 2 mRNA was shown to prevent premature neuronal differentiation [Knuckles et al., 2012]. This regulation is based on Drosha-dependent destabilisation of neurogenin 2 mRNA through binding of a local predicted conserved pri-miRNA-like hairpin. In a similar manner the microprocessor was shown to regulate Aurora kinase B mRNA stability together with p67 (DDX4 in humans) during cell-cycle progression [Jung et al., 2014].

Another study has discovered that the microprocessor is involved in the regulation of Pol II processivity at HIV-1 promoter through the recruitment of Setx, Xrn2 and
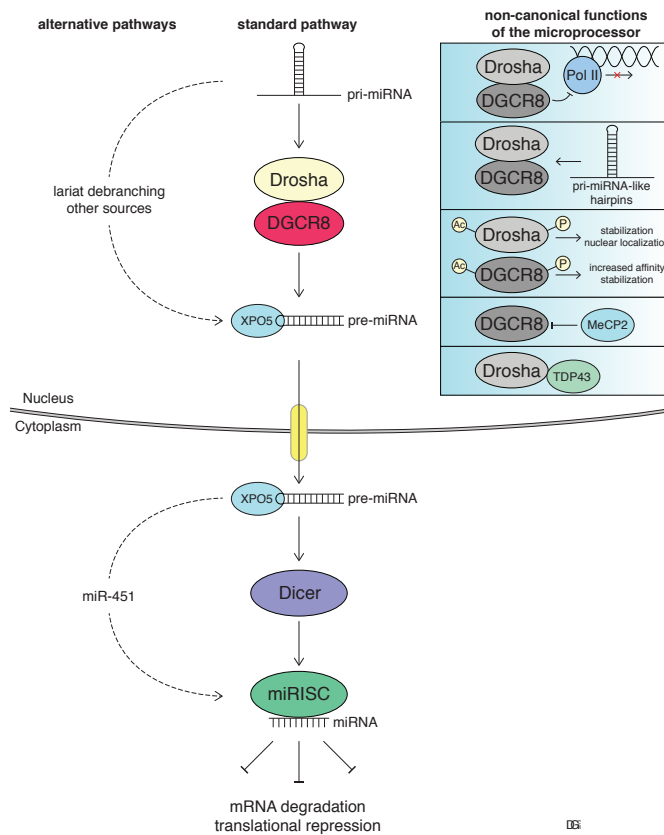
Figure 1.3 | Biogenesis of miRNAs and non-canonical functions of the microprocessor. Scheme illustrates the biogenesis of miRNAs through sequential processing of a Pol II-dependent pri-miRNA. First the microprocessor, consisting of DGCR8 and Drosha, cleaves a hairpin structure releasing the pre-miRNA which after export to the cytoplasm is subject to processing through Dicer. Dicer generates the mature miRNA duplex, of which one strand is bound by AGO forming the miRISC. The miRISC can target RNAs through interactions with a seed sequence in the miRNA for translational repression and/or 3′–5′ accelerated decay. Non-canonical miRNA biogenesis pathways are indicated by dashed arrows. Apart from catalysing the generation of pre-miRNAs the microprocessor members DGCR8 and Drosha were attributed with non-canonical functions. Drosha and DGCR8 were involved in the repression of certain gene loci by inducing pausing of Pol II. Other RNA species apart from pri-miRNA harbouring pri-miRNA-like hairpin structures were shown to be substrates of the microprocessor. Drosha and DGCR8 were shown to be subject to post-translational modifications affecting their function as indicated. Methyl CpG binding protein 2 (MeCP2) was shown to bind DGCR8 and thereby prevent its association with Drosha. Drosha was shown to bind TAR DNA-binding protein 43 (TDP43) leading to stabilisation and increased microprocessor activity.

Rrp6 [Wagschal et al., 2012]. This study has also demonstrated that the microprocessor directly associates with other cellular targets including 461 human genes leading to their transcriptional repression. Whole genome analysis of Drosha-bound chromatin regions came to a similar conclusion identifying regions upstream of transcriptional start sites of multiple human genes [Gromak et al., 2013]. This cleavage-independent function of Drosha enhances gene expression at these loci through binding of the nascent RNA and through interaction with Pol II and CBP80.

The microprocessor has also been implicated in the processing of ribosomal RNAs (rRNA). DGCR8 and Drosha were both shown to localize to nucleoli and through interaction with p67 and p72 promote biogenesis of 5.8S rRNA [Wu et al., 2000, Shiohama et al., 2007, Fukuda et al., 2007]. The nucleolar localization of DGCR8 could be mediated through its interaction with nucleolin [Shiohama et al., 2007].

Given the interaction of the microprocessor with several splicing factors including hnRNPA1, SF2/ASF, U5 and U6 it would be tempting to assess if alternative splicing could be regulated by miRNA-independent functions of the microprocessor in addition to the splicing-independent functions of these interactions in the control of pri-miRNA processing efficiency [Guil and Caceres, 2007, Wu et al., 2010, Kataoka et al., 2009]. In fact analysis of splicing and pre-miRNA production of the miR-106b~25 cluster revealed evidence of competition of the splicing and the microprocessor machinery within the supraspliceosome [Agranat-Tamir et al., 2014]. Furthermore in the case of the *eIFH4* gene Drosha, most likely together with DGCR8, was shown to promote exon inclusion of exon 5 through binding of a local conserved hairpin structure thereby acting as a splicing enhancer [Havens et al., 2014]. Whether this function is also true for other genes harbouring conserved hairpin structures possibly on a whole-genome level needs further investigated.

Patients of Fragile X-associated tremor/ataxia syndrome (FXTAS) suffer from a neurodegenerative disorder caused by the inherited expansion of CGG repeats in the *FMR1* gene. A recent study has shown that DGCR8 can bind to these repeat elements on the RNA level leading to its sequestration together with Drosha [Sellier et al., 2013]. This sequestration is associated with reduced miRNA biogenesis and is linked to neuronal degeneration. Whether such a sequestration model by CGG repeat-like motifs could also be involved in a physiological context remains unclear and needs to be addressed.

Global analysis of DGCR8-interacting RNA species also revealed a significant fraction of small nucleolar RNAs (snoRNAs) [Macias et al., 2012]. This study demonstrated a Drosha-independent function of DGCR8 in the maturation of these snoRNAs. A recent study has also described a physiological Drosha- and miRNA-independent function of DGCR8 in the control of fly neuronal morphogenesis, however whether this is mechanistically linked to snoRNA biogenesis is unclear [Luhur et al., 2014].

DGCR8 was recently identified as a target gene of ΔNp63 [Chakravarti et al., 2014]. By this mechanism both proteins are essential for terminal differentiation of epidermal cells, as loss of ΔNp63 and DGCR8 leads to induced multipotency. However it was not entirely clear whether this function is dependent on miRNAs or on miRNA-independent functions of DGCR8.

It seems that the general paradigm of RNA-binding proteins pairing with RNAse

enzymes to gain different specificity and catalytic activities observed across several species holds also true for members of the miRNA biogenesis pathway [Ameres and Zamore, 2013]. A more detailed description of the molecular mechanisms of these non-canonical functions requires rigorous comparative characterisation of the individual components of the miRNA processing machinery on a global and subcellular level.

1.4 The Lin28 – let-7 pathway

The family of let-7 miRNAs is one of the most conserved across species and has crucial functions in development and disease [Thornton and Gregory, 2012]. It comprises 10 different mature miRNAs originating from 13 different genetic loci
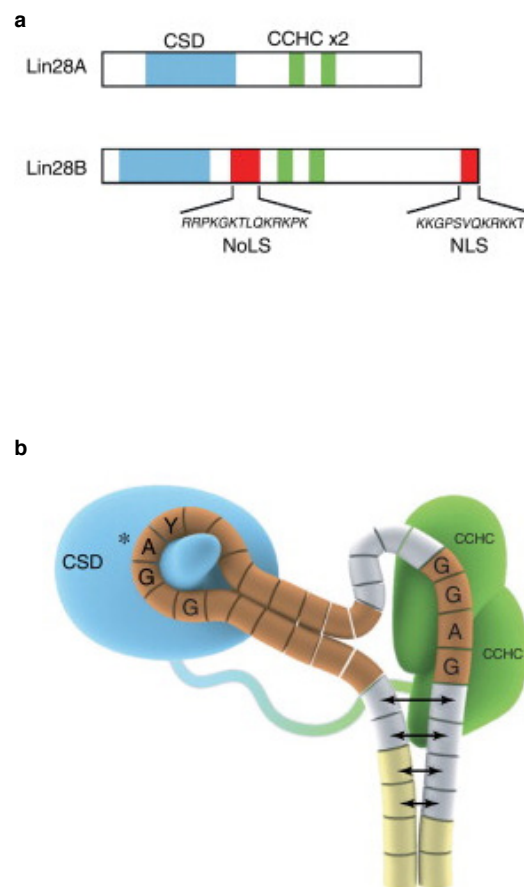

Figure 1.4 | Lin28 structure and function. (**a**) Primary structure of Lin28A and Lin28B highlighting CSD and CCHC-type zinc finger domains. Nucleolar (NoLS) and nuclear localisation domains (NLS) are highlighted in red. (**b**) Model of the interaction of CSD and CCHC-type zing fingers with preE. Adapted from Thornton et al (2012).

[Griffiths-Jones et al., 2006]. Let-7 miRNAs remain repressed in embryonic stem cells which is mainly attributed to the function of the RNA binding protein Lin28 [Thornton and Gregory, 2012]. Lin28A and its paralogue Lin28B are $<$30 kDa proteins containing a Cold-Shock Domain (CSD) and two CCHC-type zinc fingers (Fig. 1.4). Repression of let-7 occurs through binding to the terminal loop or pre-element (preE) of pre- and pri-let-7 [Piskounova et al., 2008], thereby preventing their processing by the microprocessor and Dicer. Binding of preE occurs through both (i) the CSD binding to the apical part of the loop and (ii) the CCHC-type zinc fingers binding to a GGAG motif adjacent to the Dicer cleavage site [Piskounova et al., 2008, Heo et al., 2009, Nam et al., 2011]. A flexible linker between both domains allows Lin28 to recognise any let-7 isoform despite differences in their loop sequence and length [Thornton and Gregory, 2012]. The CCHC-type zinc fingers inhibit Dicer cleavage by partially melting the double strand near the base of the loop. In addition Lin28 proteins recruit terminal uridyl transferase TUT4 (also known as Zcchc11) to induce 3′-oligouridylation of pre-let-7, resulting in facilitated 3′–5′ degradation [Hagan et al., 2009, Heo et al., 2009]. In turn, let-7 miRNAs can repress Lin28A and Lin28B by targeting their mRNAs [Ha and Kim, 2014]. Therefore the Lin28 – let-7 pathway works as a bistable switch favouring either the presence of Lin28 or of let-7. During development these two states are associated with various cell fate decisions; let-7 usually induces differentiation while Lin28 promotes maintenance of preceding developmental stages [Thornton and Gregory, 2012]. Apart from their important functions in physiology, Lin28 proteins also function as oncogenes in 15% of all cancers analysed, and this largely through the targeting of let-7 miRNAs [Viswanathan et al., 2009].

1.5 The Hedgehog pathway

Hedgehog (Hh) proteins act in an evolutionary conserved pathway with crucial functions in patterning and organogenesis during development (Fig. 1.5) [Amakye et al., 2013]. In adulthood the pathway is largely inactive except in cases of tissue repair or disease. The pathway is activated by the secreted ligands Sonic Hedgehog (Shh), Desert Hedgehog (Dhh) and Indian Hedgehog (Ihh) which bind to the negative regulatory transmembrane receptor Patched (Ptch) [Varjosalo and Taipale, 2008]. Without the presence of ligands, Ptch inhibits another membrane protein named Smoothened (Smo). This inhibition is reversed upon ligand binding, which enables Smo to activate a signalling cascade that eventually can result in the release and activation of GLI transcription factors. The precise mechanism of this cascade is still not fully understood. Although GLI target genes including Gli1 mRNA are widely accepted as a readout of this pathway [Scales and de Sauvage, 2009], evi-
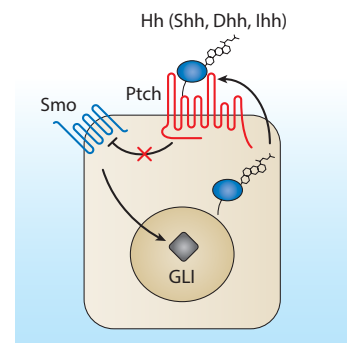

Figure 1.5 | The Hedgehog pathway. Simplified scheme of the Hedgehog pathway showing the ligand-dependent activation of Smo via Ptch. Adapted from Amakye et al (2005).

dence exists that there can be cross-talk with other critical signalling pathways including the PI3K-Akt pathway, the RAF-MEK-MAPK cascade and the TGFβ-Smad pathway [Riobo et al., 2006, Ji et al., 2007, Dennler et al., 2007].

In the PNS the Hh pathway activated through SC-secreted Dhh is crucial for the formation and organisation of the perineurial fibroblast layer surrounding the axons peripheral nerves [Parmantier et al., 1999]. Furthermore, Shh was shown to be up-regulated in SCs after PNS injury and suggested to carry out neuroprotective functions through induction of brain-derived neurotrophic factor (BDNF) [Hashimoto et al., 2008].

1.6 Outline of thesis

Dicer catalysis was shown to be indispensable for PNS myelination [Pereira et al., 2010, Bremer et al., 2010, Yun et al., 2010, Verrier et al., 2010]. This thesis aims to follow up these findings by addressing the nature of RNA species involved and their mechanistic function. Through the combined analysis of various genetically engineered mouse models and RNA sequencing data at multiple stages during myelination the following sections demonstrate that SC survival during radial sorting is promoted through regulation of Shh by the microprocessor. Furthermore Lin28B-dependent let-7 miRNAs emerge as the major regulatory miRNAs during myelination and promote Krox20 expression through suppression of Notch1 signalling.

1 Introduction

2 Materials and Methods

2.1 Materials

2.1.1 Antibodies

anti-mouse IgG	315-001-008	Jackson
anti-Notch1	MAB5352	Millipore
anti-Olig2	AF2418	R&D
anti-Hes1	ab71559	Abcam
anti-Egr2	13491-1-AP	Proteintech Europe
anti-E-cadherin	ALX-804-202-C100	Enzo Lifesciences
anti-Hmga2	#8179	Cell Signaling
anti-β-actin	A5316	Sigma
anti-MBP	MCA409s	Serotec
anti-Neurofilament	N5264	Sigma
anti-FLAG M2 magnetic beads	M8823	Sigma

2.1.2 Buffers

1. Basic AG buffer

   10 mM Tris base

   1 mM EDTA

   0.05% Tween 20

   in H_2O.

2. Blocking Buffer I for Immunoblots

   5% BSA

   in 1× PBS.

3. Blocking Buffer II for Immunoblots

   5% Dry milk

   in 1× PBS.

4. Blocking Buffer for Immunostainings

   0.1% Triton X100

   5% Normal Goat Serum

   in $1\times$ PBS.

5. C Medium

   $4\,\mathrm{mg/mL}$ D-glucose

   $2\,\mathrm{mM}$ L-glutamine

   10% FBS

   $50\,\mathrm{ng/mL}$ NGF

   in MEM.

6. IP Lysis Buffer

   $50\,\mathrm{mM}$ HEPES (pH 7.5)

   $0.4\,\mathrm{M}$ NaCl

   $1\,\mathrm{mM}$ EDTA

   0.5% Triton X-100

   10% glycerol

   $1\,\mathrm{mM}$ DTT

   in DEPC-treated H_2O.

7. NB Medium

   $1\times$ B27 supplement

   $4\,\mathrm{mg/mL}$ D-glucose

   $2\,\mathrm{mM}$ L-glutamine

   $50\,\mathrm{ng/mL}$ NGF

   in Neurobasal medium.

8. RIP Buffer

   $50\,\mathrm{mM}$ HEPES (pH 7.5)

   $0.1\,\mathrm{M}$ NaCl

   $5\,\mathrm{mM}$ EDTA

   0.5% Triton X-100

   10% glycerol

   1% SDS

   $10\,\mathrm{mM}$ DTT

   in DEPC-treated H_2O.

9. SDS Lysis Buffer

    2% SDS

    10 mM NaCl

    25 mM Tris-HCl (pH 7.4)

    1× protease inhibitor cocktail

    1× phosphatase inhibitor cocktail

10. Sample Buffer

    6.2 mM Tris

    1% β-mercaptoethanol

    2% glycerol

11. TBST

    20 mM Tris (pH 7.5)

    150 mM NaCl

    0.1% Tween 20

    in H_2O.

12. Transfer buffer

    20% methanol

    190 mM glycine

    25 mM Tris base

    in H_2O.

2.1.3 Devices and consumables

3 cm, 10 cm and 15 cm dishes	Thermo Fisher Scientific
3.5 mL centrifuge tube	Thermo Fisher Scientific
8-well cell culture slides	SPL Life Sciences
38.5 mL centrifuge tube	Thermo Fisher Scientific
AH-650 rotor	Thermo Fisher Scientific
Bioanalyzer 2100	Agilent
Conical adapeters for AH-650 rotor	Thermo Fisher Scientific
Cryotome	Thermo Fisher Scientific
Fusion detector	Enzo Life Sciences
Glass needle for microinjection	Harvard Apparatus
Light microscopes	Axio Imager M2/Axio Observer D1, Zeiss
Micromanipulator	Sutter Instruments
Nitrogen pulse generator	Picospritzer, Parker
Pestle for 1.5 mL tubes	VWR
Plastic molds	Electron Microscopy Sciences
PVDF membrane	Millipore
Real-time PCR machine	Roche Lightcycler 480 II
Syringe filter .45 µm	Sarstedt
SW28 rotor	Thermo Fisher Scientific
Thermocycler	Professional TRIO, Biometra
Thermomixer	Eppendorf
Western blot detection	Vilber Lourmat Fusion FX7
Wet blot module	Hoefer

2.1.4 Primers

All primers below are listed from 5′- to 3′-end and supplied by Microsynth AG, Balgach.

Egr2 forward, mouse and rat	ACAGCCTCTACCCGGTGGAAGAC
Egr2 reverse, mouse and rat	CAGAGATGGGAGCGAAGCTACTCGGATA
Gapdh forward, mouse and rat	GGTGAAGGTCGGTGTGAACGGATTTGG
Gapdh reverse, mouse and rat	GGTCAATGAAGGGGTCGTTGATGGCAAC
Hes1 forward, mouse	CTACCCCAGCCAGTGTCAACACGAC
Hes1 reverse, mouse	AGCTTGGAATGCCGGGAGCTATCTTTC
Hmga2 forward, mouse	TGATGTCCACTGCTCGACCC
Hmga2 reverse, mouse	CGACTTGTTGTGGCCATTTCC
Hmga2 forward, rat	CCCAAAGGCAGCAAGAACAAG
Hmga2 reverse, rat	GGTAGAAATTGAATGTCGGCGC
Lin28a forward, mouse	GGCATCTGTAAGTGGTTCAACG
Lin28a reverse, mouse	GCCAGTGACACGGATGGATT
Lin28b forward, mouse	AACGTGCGCATGGGATTCGG
Lin28b reverse, mouse	TGACTCAAGGCCTTTGGGGGAT
Notch1 forward, mouse and rat	TCCCACAGGCTGGCAAGGTCAAAC

Notch1 reverse, mouse and rat	AGCGGTAGCTGCCATTGGTGTTCTG
Shh forward, mouse	GAGCAGACCGGCTGATGACT
Shh reverse, mouse	TGATGTCCACTGCTCGACCC
dhhCre (genotyping) forward	ATACCGGAGATCATGCAAGC
dhhCre (genotyping) reverse	GGTGGTGTGGTAGAGCAGGT
Dgcr8 (genotyping) forward	CAAATCCTGAGTGCTTCATGG
Dgcr8 (genotyping) reverse	TGTGCCACTCTGCACATCTC
Dicer (genotyping) forward	ATTGTTACCAGCGCTTAGAATTCC
Dicer (genotyping) reverse	GTACGTCTACAATTGTCTATG
Drosha (genotyping) forward	GCAGAAAGTCTCCCACTCCTAACCTTC
Drosha (genotyping) reverse	CCAGGGGAAATTAAACGAGACTCC
let7f-TuD-forward	TGACGGCGCTAGGATCATCAACAACTATACAAT-CATCTTACTACCTCACAAGTATTCTGGTCACAG-AATACAACAACTATACAATCATCTTACTACCTCA-CAAGATGATCCTAGCGCCGTCTTTTTTC
let7f-TuD-reverse	TCGAGAAAAAAGACGGCGCTAGGATCATCTTG-TGAGGTAGTAAGATGATTGTATAGTTGTTGTAT-TCTGTGACCAGAATACTTGTGAGGTAGTAAGAT-GATTGTATAGTTGTTGATGATCCTAGCGCCGTCA
Notch1 3′-UTR forward	TTATTTCAGTGCTGGGTGGCCC
Notch1 3′-UTR reverse	CGTCCCAGATCACCCACATTCC

2.1.5 Reagents

0.25% Trypsin-EDTA	Life Technologies
2-hydroxypropyl-β-cyclodextrin	Sigma
AP substrate	CDP-Star, Roche
Aqua-Poly/Mount	Polysciences
B27 supplement	Life Technologies
β-mercaptoethanol	Sigma
Buprenorphine	Reckitt Benckiser
BSA	Applichem
Control antagomir	Kind gift from M. Stoffel
DEPC	Sigma
DMEM	Life Technologies
DMEM-F12	Life Technologies
DNAse I	Roche
Fast Green	Sigma
FBS	Life Technologies
Forskolin	Sigma
Glutardialdehyde	Merck
Glycogen (RNAse-free)	Thermo Fisher Scientific
H_2O (RNAse-free)	Qiagen

HBSS medium	Life Technologies
HRP substrate	ECL Prime, GE Health Care
Human heregulin β1	Peprotech
Isoflurane	Baxter
ITO coverslips	Optic Balzers
KAAD-cyclopamine	Calbiochem
L-15 medium	Life Technologies
Lead citrate	Electron Microscopy Sciences
let-7f antagomir	Kind gift from M. Stoffel
Lipofectamine 2000	Life Technologies
Matrigel (growth factor reduced)	BD Biosciences (no. 356230)
Maxima First Strand cDNA Synthesis Kit	Thermo Fisher Scientific
MEM	Life Technologies
miRIDIAN mimics	Thermo
N2 supplement	Life Technologies
Neurobasal medium	Life Technologies
NGF	Life Technologies
Non-fat dry milk	Life Technologies
OCT compound	Sakura
Osmium tetroxide	EMS
Tamoxifen	Sigma
PBS	Life Technologies
Phusion polymerase	Thermo Fisher Scientific
Penicillin/streptomycin	Life Technologies
Pentobarbital	Pfizer Animal Health S.A.
Phosphatase inhibitor cocktail	Roche
Precast polyacrylamide gels	Bio-Rad (no. 456_1083)
Protease inhibitor cocktail	Sigma
PFA	Electron Microscopy Sciences
Poly-D-Lysine	Sigma
Polyacrylamide gels	Biorad
Purmorphamine	Calbiochem
Qiazol	Qiagen
RNAse inhibitor	Life Technologies
Spurr resin	EMS
Sucrose	Sigma
VET seal	Braun
Toluidine blue	Sigma
Uranyl acetate	Electron Microscopy Sciences

2.1.6 Vectors

pMD2.G	Addgene Plasmid #12259
pSPAX2	Addgene Plasmid #12260
pMSCV-mLin28A	Addgene Plasmid #26357
pmirGLO	Promega
pFLAG/HA-DGCR8	Addgene Plasmid #10921
pSicoR	Addgene Plasmid #11579
pSicoR-Δ3loxP	based on pSicoR, 3′-loxP site removed

2.2 Methods

2.2.1 Cloning

To generate pmirGLO-Notch1-UTR, the 3′-UTR of Notch1 was amplified by PCR from genomic DNA using Phusion polymerase and ligated into pmirGLO (see 2.1.6). For expression of let-7 tough decoys (TuD), the let-7f-TuD-forward and let-7f-TuD-reverse primers (see 2.1.4) were annealed and cloned into pSicoR-Δ3loxP (see 2.1.6).

2.2.2 Dorsal root ganglion cultures

Dorsal root ganglion cultures (DRG explants) are a suitable system to analyse myelination *ex vivo* with the advantage of having a convenient access for experimental perturbations.

To obtain cultures, C57BL6 mice were time-mated by putting male and female together for one night, after which pregnant females were euthanised at E13.5 by exposure to CO_2. The embryos were collected in cold L-15 medium and separated from their red organs and the head. Next, the spinal cord was dissected starting from the ventral side. Using scissors the vertebral arches were removed and the spinal cord carefully removed and placed into a dish with L-15 medium. For each embryo, 40 dorsal root ganglia (DRG) were collected and digested in a 3 cm dish containing 0.25% Trypsin-EDTA solution for 1 h at 37 °C and 5% CO_2. In the mean time, 8-well cell culture slides were coated with Matrigel diluted 1:10 in DMEM by pipetting 200 µL per well and leaving it for 1 min. Afterwards, the matrigel can be used to coat further uncoated wells. After the digestion, 800 µL of DMEM containing 10% FBS was added and the whole solution transferred to a 2 mL tube. After centrifugation at $500 \times$ g for 5 min the supernatant was removed and the pellet was resuspended in C medium containing 0.2% penicillin/streptomycin, using 200 µL per 3 DRG, by pipetting 20 times up and down. Next, 200 µL of cell suspension is added per matrigel-coated well and incubated at at 37 °C and 5% CO_2. The next day, the medium is replaced by NB medium and the cultures are grown in that medium for another 6-7 day, changing the medium every 2-3 d. To induce myelination, NB medium was exchanged by C medium containing 50 µg/mL ascorbic acid and then the cultures were kept in that medium for another 6-7 d with medium change every 2-3 d.

Scrambled control and let-7f antagomir were cholesterol-conjugated and had the same terminal phosphothioate and 2-O-Methyl modifications as

described [Krutzfeldt et al., 2005] and were used at a final concentration of $5\,\mathrm{\mu g/mL}$. Antagomirs were added to the medium 3 d prior to the induction of myelination.

2.2.3 Electron microscopy

Electron microscopy is a suitable technique for the initial morphological description of phenotypes in the peripheral nervous system. Based on the observations made with this technique a more detailed mechanistic hypothesis about the system can be proposed.

Mice were euthanised with a single injection of Pentobarbital ($150\,\mathrm{mg/kg}$ intraperitoneal). Tissue was subsequently fixed with 3% glutardialdehyde and 4% paraformaldehyde in 0.1 M phosphate buffer. The tissue was further treated with 2% osmium tetroxide, dehydrated over a series of acetone gradients and embedded in Spurr resin. Semithin sections were stained with a 1% toluidine blue solution for light microscope analysis. Ultrathin sections (65 nm) were imaged with a FEI Morgagni 268 TEM for high resolution micrographs. Additional sections (99 nm) were used to perform morphological quantifications. The sections were harvested on ITO coverslips and the entire surface of the nerve section was imaged with either a Zeiss Gemini Leo 1530 FEG or Zeiss Merlin FEG scanning electron microscopes attached to Zeiss ATLAS modules, which allows imaging of large areas at very high resolution.

2.2.4 Image analysis

For an unbiased quantification of myelination of DRG explants, 10 random images were taken at $10\times$ magnification for each condition and the area positively stained for myelin basic protein (MBP) and neurofilament (NF) was analysed using the CellProfiler software. Briefly, for each channel the background was subtracted resulting in binary images. At first the illumination was separately corrected for all images of each channel. Large objects such as cell bodies of neurons were excluded during this step. For each condition, the ratio of MBP-positive area divided by NF-positive area was calculated.

2.2.5 Immunostaining

Immunostainings are a suitable method to identify cell markers and morphology in order to integrate structure and function.

For tissue sections animals were either perfused with 4% PFA in PBS or in the case of the sciatic nerve (SN) fixed by local immersion of the nerve in 4% PFA for 10 min. After extraction the nerves were fixed for another hour in 4% PFA in PBS and then incubated successively in 10%, 20% and 30% sucrose in PBS, at each step for 20 min. The nerves then were transferred into plastic molds filled with OCT compound and frozen on dry ice. The frozen blocks were stored at -80 °C until further use. The blocks were cut with the use of a cryotome into 10 µm thick sections. The sections were kept at RT for 30 min to 2 h and then frozen at -80 °C until further use. For immunostainings, first the samples were fixed another time in 4% PFA for 10 min at RT and then washed with PBS. Explant cultures were fixed for another 20 min in methanol at -20 °C. For tissue sections, antigen retrieval was performed in basic AG buffer at 95 °C for 15 min. After equilibration to

RT and washing with PBS, the samples were submitted to blocking buffer for 1 h at RT. Next, the primary antibody was diluted in blocking buffer (1:200 - 1:300) and incubated with the samples overnight at 4 ℃. The next day, the samples were washed with PBS and then incubated with the secondary antibody diluted in blocking buffer (1:300) for 1 h at RT. Then, the samples were washed with PBS, incubated with 0.2 mg/mL DAPI diluted 1:1500 in PBS for 10 min at RT and washed another time in PBS. Finally, the samples were mounted on slides or coverslips using Aquamount.

2.2.6 Immunoblotting

Immunoblots serve as a semi-quantitative method to determine the level of expression of proteins of interest.

Proteins were extracted directly by resuspension of samples in SDS sample buffer. For SNs, after removal of the perineurial layer the tissue was first ground in 1.5 mL tubes using a plastic pestle and then suspended in SDS lysis buffer. Afterwards, the samples were supplemented with Sample buffer and boiled for 5 min at 95 ℃ and then either stored at -20 ℃ or further analysed.

For immunoblots, the samples were loaded on precast polyacrylamide gels and then separated by gel electrophoresis at 150 V. Next, the proteins in the gel were transferred in transfer buffer on a PVDF membrane using a wet blot module at 25 V for 2 h. The membrane then was incubated in TBST for 10 min and then incubated in 5% non-fat dry milk in TBST for 1 h at RT. Afterwards, it was incubated with the primary antibody diluted in blocking buffer I (1:1000) overnight at 4 ℃. The next day, the membrane was washed three times in PBS for 10 min and then incubated with the secondary antibody diluted in blocking buffer II (1:10,000) for 1 h at RT. After 3 washes in PBS for 10 min each, the membrane was incubated with either AP or HRP substrate and then analysed using a Fusion detector.

2.2.7 *In silico* analysis

Target mRNAS of let-7 were predicted using established algorithms including RNAhybrid, TargetScan and miRWalk [Rehmsmeier et al., 2004, Miranda et al., 2006, Dweep et al., 2011]. Seed matches within the mouse Notch1 3′-UTR were predicted using RNAhybrid. Level of conservation was manually checked for each seed match using the conservation track in the UCSC genome browser (mm10).

2.2.8 *In vivo* injections

For Shh antagonist treatments, KAAD-cyclopamine was dissolved in DMSO at a concentration of 0.7 mg/mL. Injections were performed to a bodyweight ratio of 0.5 mg/kg by diluting KAAD-CPA in 45% 2-hydroxypropyl-β-cyclodextrin/PBS up to a total volume of 10 µL. For Shh agonist treatments, purmorphamine was dissolved in DMSO at a concentration of 5.2 mg/mL. Injections were performed to a bodyweight ratio of 5.2 mg/kg by diluting purmorphamine in 45% 2-hydroxypropyl-β-cyclodextrin/PBS up to a total volume of 10 µL. A submuscular injection was performed in DGCR8 mutant animals

in the region of the *gluteus superficialis* and *biceps femoris* muscles. The sciatic nerve is located in this area, and therefore comes in contact with the injected solution. We performed one daily injection over 2 consecutive days, and the tissue was harvested the following day.

For the delivery lentiviral particles (see 2.2.15) into SNs of P1-P3 pups first the animals were injected with analgesic (0.05 $^{mg}/_{kg}$ buprenorphine) and then anaesthetised by continuous inhalation of 1.5-2 $^{L}/_{min}$ 5% isoflurane for induction, 3% during anaesthesia and 0% for the wake up phase. After successful induction of anaesthesia monitored by the respiration rate and toe pinch reflex the SN was elevated out the region between the *gluteus superficialis* and *biceps femoris* muscles using a blunt needle, and flooded with 0.9% saline. Next, 5 µL of concentrated lentivirus was transferred into a glass needle. After mounting the needle onto the micromanipulator the tip of the needle was broken until it became permeable and then inserted longitudinally into the SN. Immediately after penetration of the nerve the injection was started using a nitrogen pulse generator at a frequency of 0.9 Hz and a pressure between 6 to 12 psi depending on the flow rate through the needle. After delivery of the virus the SN was carefully placed back into the tissue and the wound was closed using VET seal. The post-operative pain and possible infections was addressed pro-actively by injection of 0.05 $^{mg}/_{kg}$ buprenorphine every 12 h for 2 d starting after the surgery.

2.2.9 Mice

The use of all mice (*Mus musculus*) was approved by the veterinary office of the Canton of Zurich. Mice heterozygous for a *Lin28b* transgene expressed upon Cre-recombination [Molenaar et al., 2012] were crossed with transgenic mice expressing Cre recombinase under the *Dhh* regulatory elements [Jaegle et al., 2003] to obtain mice expressing Lin28B specifically in SCs. Deletion of Dicer, DGCR8 and Drosha during development was achieved by crossing Dicer$^{fl/fl}$ [Murchison et al., 2005], DGCR8$^{fl/fl}$ [Wang et al., 2007] or Drosha$^{fl/fl}$ mice [Chong et al., 2008] with *Dhh*Cre-Dicer$^{fl/wt}$, -DGCR8$^{fl/wt}$ or -Drosha$^{fl/wt}$ mice (Fig. 2.1). *Dhh*-Cre is expressed in SCs from E12/E13 onwards. Experimental animals were of both sexes. Genotypes were determined by genomic PCR (primers see 2.1.4). Animals were euthanised using either exposure to CO_2 or lethal *intraperitoneal* injection of Pentobarbital (150 $^{mg}/_{kg}$).

2.2.10 RNA purification

Total RNA from tissue and cells was extracted using Qiazol™. Tissue was ground in 1.5 mL tubes using a plastic pestle and then suspended in 500 µL of Qiazol™. Cells in culture were immediately lysed in 500 µL of Qiazol™. Next, 100 µL of chloroform was added, after which the samples were mixed for 10 sec and then incubated at RT for 2 min. After two phases became visible, the samples were centrifuged at 17000 × g for 15 min at 4 ℃. The upper aqueous phase was carefully transferred into new 1.5 mL tubes. Next, 1 µL of Glycogen (RNAse-free) was added followed by the addition of 1 equivalent of isopropanol. The samples then are mixed for 10 sec and centrifuged
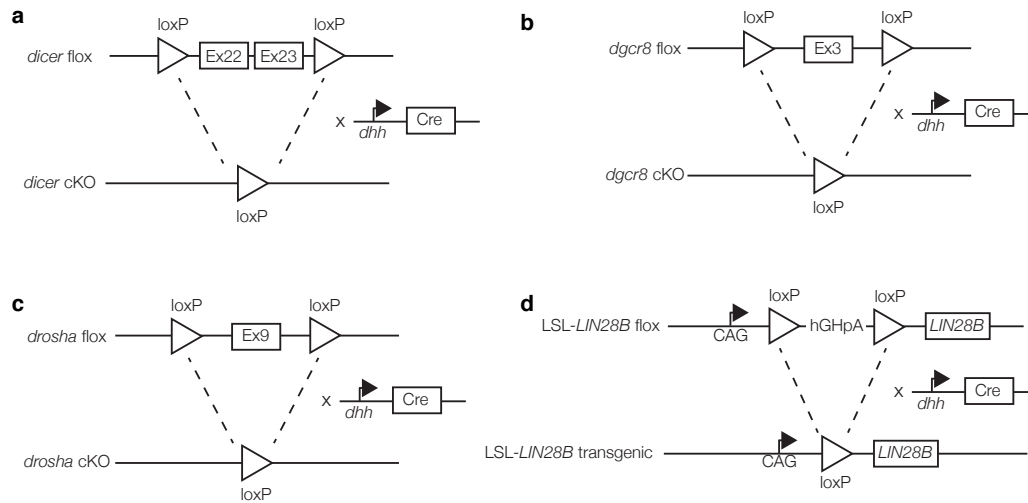
Figure 2.1 | Schematic representation of the generation of Dicer, DGCR8, Drosha and Lin28b mutant mice. (**a-c**) Dicer (**a**), DGCR8 (**b**) and Drosha (**c**) were conditionally depleted in SCs through recombination of the depicted floxed coding exons (Ex) with Cre recombinase (Cre) expressed under control of the Dhh promoter (dhh). (**d**) Transgenic Lin28b expression under the chicken actin gene promoter (CAG) in SCs was obtained by recombination of a floxed human growth hormone termination signal (hGHpA) with Cre recombinase expressed under control of the Dhh promoter.

at $17000 \times$ g for 15 min at 4 ℃. The supernatant is discarded and the pellet washed twice with 70% ethanol by centrifugation at $11000 \times$ g for 5 min at 4 ℃. Finally, the supernatant is completely removed, after which the pellet is dried for 5 min at RT and then resuspended in 20 µL H_2O (RNAse-free).

2.2.11 Reverse transcription

For the preparation of total cDNA libraries, 100 ng of total RNA was used for reverse transcription with the Maxima First Strand cDNA Synthesis Kit by mixing the following components:

5× Maxima reaction mix	4 µL
Enzyme mix	2 µL
total RNA	100 ng
H_2O	to 20 µL.

The reaction was performed in a thermocycler with the following program:

Step	Temperature	Time
1	25 ℃	10 min
2	50 ℃	15 min
3	85 ℃	5 min
4	6 ℃	∞

For qPCR the obtained cDNA was diluted 1:10 in H_2O.

To obtain cDNA from mature miRNAs, 2 ng of total RNA was used in a reverse transcription reaction for each target miRNA as follows:

100 mM dNTPs	0.15 µL
MultiScribe Reverse Transcriptase	1 µL
10× RT buffer	1.5 µL
RNAse Inhibitor	0.18 µL
5× Taqman micro RNA RT Primer	3 µL
total RNA	2 ng
H_2O	to 15 µL.

The reaction was performed in a thermocycler with the following steps:

Step	Temperature	Time
1	16 °C	30 min
2	42 °C	30 min
3	85 °C	5 min
4	6 °C	∞

2.2.12 Quantitative real-time PCR

For the quantitative analysis of target mRNAs, cDNA obtained from total RNA (see 2.2.11) was mixed such that each well of a 384 well plate contained the following:

2× FastGreen Essential Master Mix	5 µL
5 µM Forward Primer (see 2.1.4)	0.5 µL
5 µM Reverse Primer (see 2.1.4)	0.5 µL
cDNA	2 µL
H_2O	2 µL

Quantitative real-time PCR was performed using the following settings:

Cycles	Temperature	Time
1	94 °C	45 s
45	94 °C	45 s
	60 °C	45 s
	72 °C	1 $^{min}/_{kb}$
1	72 °C	10 min

For the detection of mature miRNAs reverse transcribed mature miRNAs (see 2.2.11) were diluted 1:3 and mixed so that each well of a 384 well plate contained the following:

TaqMan 2× Universal PCR Master Mix	5 µL
TaqMan MicroRNA Assays 20× TaqMan Assay	0.5 µL
RT product	2 µL
H_2O	2.5 µL

Quantitative real-time PCR was performed using the following settings:

Cycles	Temperature	Time
1	94 °C	45 s
45	94 °C	45 s
	60 °C	45 s
	72 °C	1 min/kb
1	72 °C	10 min

2.2.13 RNA sequencing

RNA sequencing was chosen as a method to quantify the differential expression of RNAs in the PNS. Main advantages compared to microarrays included its annotation independent coverage and higher accuracy [Wang et al., 2009]. Nevertheless RNA sequencing data were validated for selected candidates by quantitative PCR.

For small RNA sequencing, RNA from E17.5, P1, P4, P10, P30 and P60 SNs of C57bl6 animals was extracted with Qiazol according to as described above (see 2.2.10). Additionally, RNA from cultured primary rat SCs induced to differentiate by incubation for 56 h with dibutyl-cAMP, and RNA from P4 Dicer KO SN, was included to help account for which miRNAs are SC-derived and which are not. Library preparation and sequencing was performed with Fasteris SA. Briefly, after RNA quality assessment with a Bioanalyzer 2100 the fraction of 15-35 nt was purified using gel electrophoresis and linked to Illumina TruSeq adapters. For multiplexing, barcodes were introduced during PCR amplification. Sequencing was performed using the Illumina HiSeq 2000 platform with a read length of 50 bp. The ncPRO pipeline was used to map the reads against the mouse genome (version mm9) and the rat genome (version rn4) [Chen et al., 2012]. We used Bowtie with default options (but -m 5000 and -e 50). The miRNA quantities were normalised by the number of mapped reads from the corresponding library and then multiplied by 1000000 to obtain the unit in reads per million (RPM). The R software package DESeq R (Version 1.14.0) [Anders and Huber, 2010] was used to assess the statistical significance of differences in gene expression. Genes showing altered expression with adjusted P-value < 0.05 (Benjamini and Hochberg method) were considered as differentially expressed. All data have been deposited in the NCBI GEO database (GSE64562).

For RNA sequencing, total RNA from SN of P1 Lin28 tg, Dicer KO and controls was extracted using Qiazol (Qiagen) according to as described above (see 2.2.10). Library preparation, sequencing and mapping of reads was performed at the Functional Genomics Centre in Zurich (FGCZ). The quality of the isolated RNA was determined with a Bioanalyzer 2100 (Agilent). Only those samples with a 260 nm/280 nm ratio between

1.8–2.1 and a 28S/18S ratio within 1.5–2 were further processed. The TruSeq RNA Sample Prep Kit v2 (Illumina, Inc.) was used in the following steps. Briefly, total RNA samples (100-1000 ng) were depleted of ribosomal RNA using Ribo Zero Gold (Epicentre) and then reverse-transcribed into double-stranded cDNA. The cDNA samples then were fragmented, end-repaired and polyadenylated before ligation of TruSeq adapters containing the index for multiplexing fragments containing TruSeq adapters on both ends were selectively enriched with PCR. The quality and quantity of the enriched libraries were validated using Qubit®(1.0) Fluorometer and the Caliper GX LabChip®GX (Caliper Life Sciences, Inc.). The product was a smear with an average fragment size of approximately 260 bp. The libraries were normalized to 10 nM in Tris-HCl 10 mM (pH 8.5) with 0.1% Tween 20. The TruSeq PE Cluster Kit v3-cBot-HS or TruSeq SR Cluster Kit v3-cBot-HS (Illumina, Inc.) was used for cluster generation using 10 pM of pooled normalized libraries on the cBOT. Sequencing was performed on the Illumina HiSeq 2000 paired end at $2\times$ 101 bp using the TruSeq SBS Kit v3-HS (Illumina, Inc.). *In silico*, the obtained raw reads were first cleaned by removing adapter sequences and trimming of low quality ends. Sequence alignment of the resulting reads to the mouse reference genome (mm10) and quantification of gene level expression was carried out using RSEM (Version 1.2.12) [Li and Dewey, 2011]. The R software package from Bioconductor, DESeq2 (Version 1.4.5) [Anders and Huber, 2010], was used to determine the statistical significance of differences in gene expression. Genes showing altered expression with adjusted p-value < 0.05 (Benjamini and Hochberg method) were considered as differentially expressed. All data have been deposited in the NCBI GEO database (GSE64562).

2.2.14 Schwann cell cultures

Primary rat Schwann cells (rSCs) were used as a model system to analyse Nrg1-dependent Krox20 expression under control and experimentally perturbed conditions.

In the course of the primary rSC purification, two 10 cm dishes were incubated overnight at 4 ℃ with 50 µg/mL rabbit anti-mouse IgG diluted in 50 mM Tris-HCl buffer (pH 9.5). The next morning the dishes were washed three times with PBS and then incubated with 7 mL OX-7 cell supernatant (containing anti-Thy1.1 antibodies) for 1 to 3 h. Afterwards, the dishes were washed three times with PBS and then immediately used for Schwann cell purification. For PDL coating, dishes were incubated with PDL solution (100 µL of 2 mg/mL PDL diluted in 40 mL PBS) for 5 to 10 min and washed twice with H_2O.

Primary rSCs were isolated from P2 to P3 rat SNs obtained from two pregnant females. After extraction the nerves were placed in L-15 medium and separated from the epi- and perineurial layers. The remaining nerve was cut into smaller pieces and digested for 1 h in HBSS containing 1.25 mg/mL trypsin and 2 mg/mL collagenase at 37 ℃ and 5% CO_2. Afterwards, the cells were centrifuged at 1000 rpm and then resuspended in DMEM containing 10% FBS, 0.2% penicillin/streptomycin and 10 µM Ara-C. The cells were then plated on a 10 cm dish coated with PDL and incubated for 24 h at 37 ℃ and 5% CO_2. After 24 h, the medium was replaced by DMEM containing 10% FBS, 0.2% penicillin/streptomycin and 4 µg/mL bovine pituitary extract (SC growth medium).

Furthermore, Forskolin was freshly added to the medium to a final concentration of $2\,\mu M$. The cells were incubated until they reach 80 to 90% confluency whilst replacing the medium every 2 to 3 d. Next, the cells were washed with PBS and detached by brief incubation with 0.25% Trypsin-EDTA solution. After inactivation of trypsin by dilution in 10 mL SC growth medium the cells were centrifuged for 5 min at $300 \times$ g. The pellet were resuspended in 7 mL of SC growth medium and then seeded on the dish coated with Thy1.1 antibodies. After incubating for 10 min at $37\,°C$ in 5% CO_2, the dish was shaken carefully and incubated for another 10 min. The suspension was transferred to the second dish coated with Thy1.1 antibodies and the incubation procedure repeated. Afterwards, the cells remaining in suspension were seeded on a dish coated with PDL and grown until they were confluent. Cells were expanded to three 15 cm dishes and then frozen in 10% DMSO in FBS using a freezing rack bathed in isopropanol at -80 °C. For long-term storage the cells were transferred to liquid nitrogen.

For experiments rSCs were cultured for at least one week in SC growth medium, after which differentiation was induced by 18 h incubation in DMEM containing $1\times$ N2 supplement followed by addition of 25 ng/mL Nrg1 (human heregulin beta1). Primary rat Schwann cells were transfected with pmirGLO (Promega) or pmirGLO-Notch1-3-UTR for 48 h. As mimics, hsa-let-7f-5p and control miRIDIAN mimics were used at a final concentration of 10 nM. Luciferase assays were performed with the Promega Luciferase Assay System according to the manufacturers instructions.

SpL201 cells were grown in DMEM containing 10% FBS and 10 ng/mL EGF [Lobsiger et al., 2001]. For differentiation, medium was changed to DMEM containing 10% FBS and 20 mM Forskolin.

2.2.15 Virus production

Concentrated lentivirus was prepared by transfection of a confluent 15 cm PDL-coated dish of HEK cells with 27 μg transfer vector, 9 μg pMD2.G and 13.5 μg pSPAX2 using Lipofectamine 2000™. 48 h and 72 h after transfection supernatants were collected and centrifuged for 5 min at $500 \times$ g. Next, the supernatant was filtered through a 0.45 μm syringe filter collected in 38.5 mL centrifuge tubes and centrifuged in a SW28 rotor at 21000 rpm for 2 h at 11 °C. After discarding the supernatant the pellet was resuspended in 3.4 mL of DMEM with 10% FBS and transferred to a 3.5 mL centrifuge tube. With the help of conical adapters the tubes were placed into a AH-650 rotor and centrifuged at 17000 rpm for 1 h at 4 °C. After removing the supernatant, the pellet was resuspended in 40 μL of PBS with 62.5 ppm Fast Green. The so obtained virus was aliquoted, frozen in liquid nitrogen and stored at -80 °C until further use.

2.2.16 Statistics

The two-tailed Student's t-test was chosen as an appropriate test to determine statistical significance within our sample sizes and was applied unless stated otherwise. Detailed information about error bars and sample sizes are included in all figure legends (see Chapter 3) and further specifications can be found in the respective Methods sectionss.

3 Results

3.1 Manuscript A — The microprocessor regulates Shh to protect Schwann cell survival during radial sorting

Authors: Deniz Gökbuget[1,3], Jorge A Pereira[1,3], Antonin Marchais[2], Markus Stoffel[1], Olivier Voinnet[2], Ueli Suter[1]

Affiliations:
1: ETH Zurich, Department of Biology, Institute of Molecular Health Sciences, Otto-Stern-Weg 7, 8093 Zurich, Switzerland.
2: ETH Zurich, Department of Biology, Institute of Agricultural Sciences, Universitätsstrasse 2, 8092 Zurich, Switzerland.
3: These authors contributed equally to this work.

Contributions:
D.G., J.A.P. and U.S. designed the study. D.G. and J.A.P. performed most of the experiments and data analysis. A.M. conducted analysis of raw sequencing data and helped with bioinformatic analysis. D.G. wrote the manuscript (revised by J.A.P.). D.G. and J.A.P. prepared the figures.

(Manuscript in preparation.)

Myelination by Schwann cells (SCs) is fundamental for appropriate function of the nervous system. SC myelination is preceded by radial sorting, during which the immature SC population expands to match numbers of available axons and establish 1:1 SC-axon relations. The microRNA (miRNA) pathway is necessary for SC myelination, but the entities directly responsible remain largely unknown. Through comparative analysis of mice with conditional ablation of Dicer, DGCR8 and Drosha in SCs we observed that the microprocessor protects SC survival in a miRNA-independent manner. RNA sequencing revealed sonic hedgehog (Shh) as the most prominently upregulated transcript in DGCR8 mutants, while almost absent in Dicer mutants and control animals. We found a detrimental role of Shh signalling in SC survival during radial sorting of wildtype mice, whereas its suppression in DGCR8 mutants protects SCs from ongoing apoptosis and restores radial sorting.

MicroRNAs (miRNAs) are a crucial part of the endogenous RNA interference pathway, and allow the cell to fine-tune changes in gene expression [Ebert and Sharp, 2012, Mendell and Olson, 2012]. Biogenesis of most miRNAs requires cleavage of the primiRNA hairpin by the microprocessor complex, consisting of the RNA binding protein DiGeorge syndrome critical region gene 8 (DGCR8) and the ribonuclease type III Drosha [Ha and Kim, 2014]. The resulting precursor (pre)-miRNA product is further processed by Dicer to generate a mature miRNA duplex. One strand of the duplex is then incorporated into the RNA-induced silencing complex (RISC), and serves as a probe to identify RNA targets for silencing.

Besides the canonical miRNA biogenesis outlined above, some miRNA precursors do not arise through processing by the microprocessor complex and can be directly cleaved by Dicer [Ameres and Zamore, 2013, Kim et al., 2009]. The precursor form of such miRNAs is generated as a product of alternative splicing or of short hairpin RNA transcription, or as a by-product of tRNA production. These are collectively referred to as non-canonical miRNAs [Miyoshi et al., 2010]. Comparative analysis of animals containing cells lacking Dicer and the microprocessor complex members DGCR8 or Drosha allows the evaluation of the relative physiological relevance of canonical and non-canonical miRNAs [Yang and Lai, 2011]. Studies of skin development found very similar phenotypes in epithelial and hair follicle cells of Dicer compared to DGCR8 mutants [Teta et al., 2012, Yi et al., 2009]. Additional work on regulatory T cells and natural killer cells also revealed a high degree of overlap in DGCR8 and Dicer mutant phenotypes [Bezman et al., 2010, Chong et al., 2008]. These similarities most likely stem from the loss of canonical miRNAs. However, in embryonic stem (ES) cells, deletion of Dicer leads to a more severe phenotype than is observed upon deletion of DGCR8 [Babiarz et al., 2008, Chong et al., 2010, Kanellopoulou et al., 2005, Murchison et al., 2005, Wang et al., 2007]. Further sequencing experiments in ES cells revealed a poor correlation in mRNAs altered upon Dicer or DGCR8 deletion, and furthermore confirmed the presence of non-canonical miRNAs in DGCR8 mutants [Babiarz et al., 2008]. Additional studies on postmitotic brain neurons [Babiarz et al., 2011] and on T cell progenitors [Chong et al., 2010] of Dicer and microprocessor knockout mice also encountered a more severe phenotype upon Dicer deletion. These observations argue in favour of important roles being played by non-canonical miRNAs.

In addition to the changes in miRNA fractions, comparison of Dicer and microprocessor mutants also highlighted transcriptome changes arising specifically upon microprocessor deletion [Chong et al., 2010]. Interestingly, numerous upregulated mRNAs contained hairpins resembling pri-miRNA structures [Chong et al., 2010]. In fact, the microprocessor has been shown to bind and cleave pri-miRNA-like hairpin structures present in the 5′-UTR of the DGCR8 mRNA [Han et al., 2009, Triboulet et al., 2009]. This feature is evolutionarily conserved, since it is also observed in *Drosophila melanogaster* [Kadener et al., 2009]. These observations provide proof-of-principle evidence that the microprocessor complex can target and silence mRNA expression independently of its

function in miRNA biogenesis. To systematically explore the dimension of miRNA-independent functions of the microprocessor complex, Macias and colleagues performed cross-linked immunoprecipitation of DGCR8 and associated RNAs, followed by high throughput sequencing (HITS-CLIP) [Macias et al., 2012]. The HITS-CLIP data revealed that DGCR8 can bind several RNA species including mRNAs, long-non-coding (lnc) RNAs, small nucleolar (sno) RNAs and even retrotransposons, all of which contain pri-miRNA-like hairpin structures [Heras et al., 2013, Macias et al., 2012]. Furthermore, pri-miRNAs did not represent the dominant fraction of all detected RNA species. These observations open a new perspective in considering microprocessor functions in the cell. The physiological relevance of miRNA-independent microprocessor functions is now beginning to emerge [Macias et al., 2013]. In the mammalian central nervous system (CNS), the microprocessor directly suppresses neurogenin 2 mRNA, thereby contributing to stem cell maintenance [Knuckles et al., 2012]. Deletion of the microprocessor but not of Dicer leads to precocious neuronal differentiation coupled to a reduction of the stem cell pool.

In the peripheral nervous system (PNS), analyses of Dicer mutant mice performed by our lab and others revealed a clear dependence of SC differentiation on the miRNA biogenesis pathway [Pereira et al., 2010, Bremer et al., 2010, Yun et al., 2010, Verrier et al., 2010]. SCs are the myelinating glia of the PNS, and are responsible for electrical insulation and providing trophic support to peripheral axons [Quintes et al., 2010]. SC precursors are derived from neural crest stem cells and are able to differentiate into immature SCs [Jessen and Mirsky, 2005]. These surround groups of axons forming bundles, and gradually expand their population as they engage and sort out a single axonal segment from the bundle, a process termed radial sorting [Pereira et al., 2012]. The expansion of the immature SC pool is achieved through a balance of proliferation [Benninger et al., 2007, Grove et al., 2007] and survival [D'Antonio et al., 2006, Nakao et al., 1997, Yu et al., 2005]. It is crucial that the expansion of SC numbers properly takes place during radial sorting, since immature SCs are originally outnumbered by the axonal segments that they must sort and myelinate [Peters and Muir, 1959, Webster et al., 1973]. In the final stage of differentiation, SCs activate myelination-associated genes and produce the concentric lipid-rich spiral membrane that provides the electrical insulation to the axon [Jessen and Mirsky, 2005]. Myelination is of crucial importance, as reflected by the devastating effects of demyelinating pathologies in humans [Berger et al., 2006]. However, it cannot properly take place if the preceding step of radial sorting fails [Benninger et al., 2007, Berti et al., 2011, Feltri and Wrabetz, 2005, Grigoryan et al., 2013, Grove et al., 2007, Montani et al., 2014, Nodari et al., 2007, Pereira et al., 2009, Yu et al., 2005]. Not all axons in the adult PNS are myelinated. Axons under approximately 1 µm in diameter will not undergo radial sorting and instead will remain engaged by non-myelinating SCs in a Remak bundle [Salzer, 2012]. In Remak bundles, non-myelinating SCs extend processes that surround every axon they engage. In contrast, immature bundles are surrounded by the immature SCs but the axons within are not isolated from each other [Beirowski, 2013]. Among the multiple stages of SC differentiation, miRNAs seem to play the most prominent role at the onset of myelination, immediately after radial sorting.

Signalling by Shh has been most extensively studied during early stages of embryogenesis [Matise and Wang, 2011]. Apart from its vital role in patterning and organogenesis, Shh also promotes survival of neural crest stem cells prior to SC generation [Delloye-Bourgeois et al., 2014]. Expression of Shh by SCs has a neuroprotective effect on spinal motor neurons following SN injury [Hashimoto et al., 2008]. However the response to this powerful morphogen is strongly dependent on the physiological context of its target cell. In neural crest-derived dorsal root ganglion neurons, Shh induces programmed cell death and dorsal-ventral patterning of the ganglia [Guan et al., 2008]. In the extensive differentiation events that occur from immature SC stage up to the fully myelinated stage, the importance of Shh signalling remains currently unexplored.

In the present study, we aimed to understand which mechanisms associated with miRNA biogenesis are physiologically relevant for SC differentiation. We address the relative importance of canonical and non-canonical miRNAs during SC development, and we investigate miRNA-independent functions of the microprocessor complex. Through comparison of SC-specific mutants for Dicer and DGCR8 we can relate similar phenotypes to loss of canonical miRNA functions. Likewise, different phenotypes can either be related to loss of non-canonical miRNAs or to loss of miRNA-independent functions of the microprocessor complex. Our findings reveal that canonical miRNAs are primarily necessary for the onset of SC-myelination, and are also crucial for the maturation of Remak bundles. Non-canonical miRNAs are expressed at very low levels and seem not to play a relevant role during these stages of SC maturation. We show that the microprocessor complex is necessary at an earlier stage, in which it drives radial sorting in a miRNA-independent manner by suppressing Shh signalling. This study is the first to reveal a detrimental physiological role of Shh in SC survival during radial sorting. When provided to developing wildtype SNs, Shh agonist leads to a significant reduction in the number of cells in the nerve. Finally, suppression of Shh signalling in DGCR8 knockout mice increases the number of cells in the SN and allows them to resume the radial sorting program.

Results

Conditional deletion of DGCR8 leads to severe impairment of radial sorting by SCs.

In order to evaluate the relative physiological importance of miRNA biogenesis pathways in SCs, we analysed animals with conditional SC-specific deletion of DGCR8 (DGCR8 KO) in comparison to SC-specific Dicer deletion (Dicer KO) (Figures 3.2A-B). These animals were generated by crossing mice with floxed *Dgcr8* and *Dicer1* alleles [Bernstein et al., 2003, Yi et al., 2009] with mice expressing Cre recombinase (Cre) under the control of the desert hedgehog (dhh) promoter [Lindeboom et al., 2003]. We observed a prominent reduction of several miRNAs in SN lysates at P1 (Figure 3.1) but not yet at E17.5 (Figure 3.2D) in both mutant mice. Analysis of SNs at P24 (Figures 3.1A-C) revealed in DGCR8 KO a surprisingly widespread presence of large axonal bundles (asterisk, Figure 3.1C), which are characteristic features of early development when radial sorting is ongoing (quantification in Figures 3.1D-E). In addition,

SNs of DGCR8 KO presented fewer 1:1 not-myelinated SC-axon profiles than Dicer KOs, and an almost complete absence of myelin. As previously reported by our lab and others [Pereira et al., 2010, Bremer et al., 2010, Yun et al., 2010, Verrier et al., 2010], Dicer KO SNs are strongly enriched in 1:1 SC-axon relations at the pro-myelinating stage (white arrowheads, Figure 3.1B). There are also sporadic axonal bundles (asterisk, Figure 3.1B), coupled with a complete absence of Remak bundles. The features of both mutant mice are pathological, since SNs of P24 control animals are thoroughly myelinated and the only axons lacking myelin are those below 1 µm in diameter, which remain engaged in Remak bundles (Figure 3.1A). Analysis of different regions of the PNS, including dorsal (sensory nerve) and ventral (motor nerve) roots, reveals a consistent aggravation of the phenotype in DGCR8 versus Dicer KO (Figures 3.2E-F). CNS glia are present in both dorsal and ventral roots, as illustrated by the presence of Olig2-positive oligodendrocytes that produce myelin without the PNS marker myelin protein zero (P0), and of astrocytes strongly expressing glial fibrillary acidic protein (GFAP) (Figures 3.2G-H). The myelin produced by oligodendrocytes was confirmed in electron micrographs of DGCR8 KO roots which, unlike myelin of SCs, lacks a surrounding extracellular basal lamina (Figure 3.2J, magnification boxes). In addition, dorsal roots display sporadic large holes (Figure 3.2E) at the cross section level from around P14 onwards, sometimes containing axonal debris or surrounded by oligodendrocyte myelin residues (data not shown), suggesting these might be derived from degenerating axons. Overall, dorsal and ventral roots of DGCR8 KO are populated by unusual large groups of axons (Figures 3.2E,I) and show near complete absence of 1:1 SC-axon profiles or SC myelin (Figure 3.2F). Similar to our observations in SNs, Dicer KO roots show predominantly an arrest at the pro-myelinating stage (Figures 3.2E,I). Taken together our data reveal that DGCR8 KO have a strong impairment of radial sorting, in contrast to Dicer KO which arrest development at the later 1:1 pro-myelinating stage.

Analyses of DGCR8 – Dicer double mutants argue against non-canonical miRNAs as the cause of the radial sorting defects in DGCR8 mutants.

A possible reason for the earlier developmental arrest of DGCR8 KO is linked to microprocessor-independent miRNAs. To address whether the sole presence of these miRNAs is actively aggravating the defect in SC differentiation in DGCR8 KO, we generated SC-specific conditional mutants for DGCR8 and Dicer (double KO) by breeding both alleles together and crossing them with Dhh-Cre mice. Even though double KO also lack microprocessor-independent miRNAs, the phenotypic hallmarks displayed both in SNs (Figures 3.3A,C) and PNS roots (Figures 3.4A-B) match the ones observed in DGCR8 KO. This result argues against a detrimental role of microprocessor-independent miRNAs and suggests that the earlier developmental arrest of DGCR8 KO is promoted by miRNA-independent functions of DGCR8. The breedings to generate double KO also gave rise to DGCR8 KO carrying one functional *Dicer1* allele, and Dicer KO carrying one functional *Dgcr8* allele. These mutants displayed, despite half the gene dose and the equalised genetic background, the respective phenotypic hallmarks of single DGCR8 KO and Dicer KO in P24 SNs and roots (Figure 3.4D). This observation is based on multiple
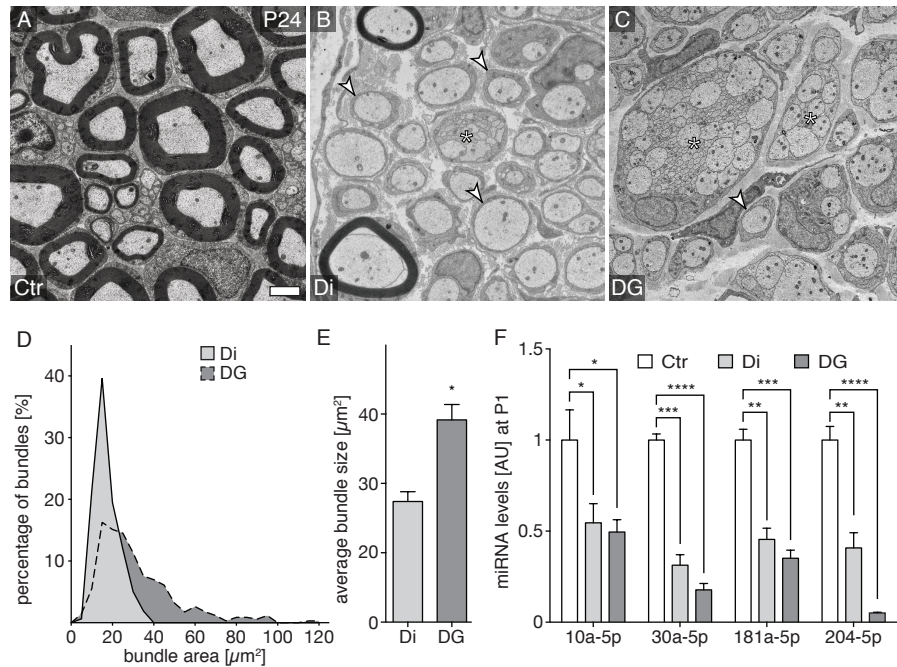
Figure 3.1 | DGCR8-depleted SCs show an exclusive arrest at the radial sorting stage when compared to Dicer-depleted SCs. (**A-C**) Electron micrographs of SN of control (Ctr), Dicer KO (Di) and DGCR8 KO (DG) at P24. SNs from DGCR8 KO display large bundles of unsorted axons (**C**, asterisks) and sporadic axons engaged by SCs in a 1:1 not-myelinated relation (**C**, white arrowhead). In contrast, Dicer KO SNs display small bundles (**B**, asterisk) and abundant 1:1 pro-myelinating SC-axon relations (**B**, white arrowheads). At this age, control SNs have completed radial sorting and are already thoroughly myelinated, and the only axons lacking myelin are those contained in Remak bundles. (**D**) Frequency distribution of bundle sizes of Di and DG at P24 per cross-section (n = 3 for each genotype). Most bundles present in Dicer KO SNs are smaller than 20 µm², whereas in DGCR8 KO there are more of larger bundles measuring up to 100 µm². (**E**) Average bundle size per cross-section in P24 Di and DG (n = 3 for each genotype) showing significantly smaller bundles on Dicer KO compared to DGCR8 KO. (**F**) Levels of selected miRNAs (miR-10a-5p, miR-30a-5p, miR-181a-5p and miR-204-5p) in Ctr, Di and DG at P1 (n = 3 for each genotype) normalised on snoRNA-202. The levels of all 4 mature miRNAs are significantly reduced in SN lysates of both KO animals compared to controls confirming the functional loss of the miRNA biogenesis machinery in both mutants. Scale bar equals 2 µm (**A-C**). Error bars represent standard error of the mean. Two-tailed Student's t-test * $P < 0.05$, ** $P < 0.01$, *** $P < 0.001$, **** $P < 0.0001$ (**E,F**). See also Figure 3.2.

littermate mice from various breedings, and argues strongly against genetic background variations as a meaningful component in the differences observed between the two single KOs.

Analysis of Drosha KO mice suggests that the DGCR8 KO phenotype is microprocessor-dependent.

DGCR8 and Drosha form the core components of the microprocessor complex. Besides their roles within the microprocessor, recent studies suggest additional functions for DGCR8 and Drosha independently of one another [Macias et al., 2013]. To address whether the defects in radial sorting present in DGCR8 KO are associated with microprocessor function, we generated SC-specific conditional mutants for Drosha using dhh-Cre (Figure 3.2C-D) [Chong et al., 2008], from here onwards referred to as Drosha KO. Analyses of SNs of Drosha KO at P24 revealed the same phenotypic hallmarks of DGCR8 KO and double KO (Figures 3.3B-D; Figure 3.4C). This observation could be confirmed analysing PNS roots at P24 (Figures 3.4A-B). The striking similarities between the DGCR8 KO and Drosha KO phenotypes are consistent with Drosha and DGCR8 acting together as the microprocessor complex to promote developmental radial sorting in SCs.

Maturation of Remak bundles is dependent on canonical miRNAs.

In the adult PNS axons smaller than 1 µm are not myelinated. Instead they are engaged in groups by non-myelinating SCs, which extend protrusions around every individual axon, thereby forming a mature Remak bundle. The absence of mature Remak bundles in SNs of Dicer and DGCR8 KO suggests that the maturation of these specialised non-myelinating SCs might depend on miRNAs. To address this hypothesis we analysed peripheral nerves from the sympathetic trunk, which are mainly composed of Remak bundles and contain very few myelinated axons [Frank et al., 2000]. Our analysis revealed that maturation of Remak bundles is impaired in DGCR8, Dicer and double KO (Figure 3.4E), since the axons are not individually encircled and isolated from each other by the non-myelinating SC (Figure 3.4E, false-coloured processes). Our observations support a prominent role of SC-derived canonical miRNAs in Remak bundle maturation.

The microprocessor promotes SC survival during radial sorting.

Successful radial sorting depends, among other factors, on the correct matching of SC numbers to the available axons [Jessen and Mirsky, 2005]. To address whether there are sufficient SCs, we quantified the number of cells in SNs of DGCR8 KO, Dicer KO, and control animals (Figures 3.5A-J). Analysis at P1 and P5 revealed a striking deficit in the number of cells in DGCR8 but not in Dicer KO (Figures 3.5D-J). At E17.5, which marks early stages of radial sorting, the number of cells was still the same in every animal (Figures 3.5A-C,J). The deficit in cell numbers in DGCR8 KO starting from P1 could be confirmed in Drosha KO (Figure 3.6C) and double KO (data not
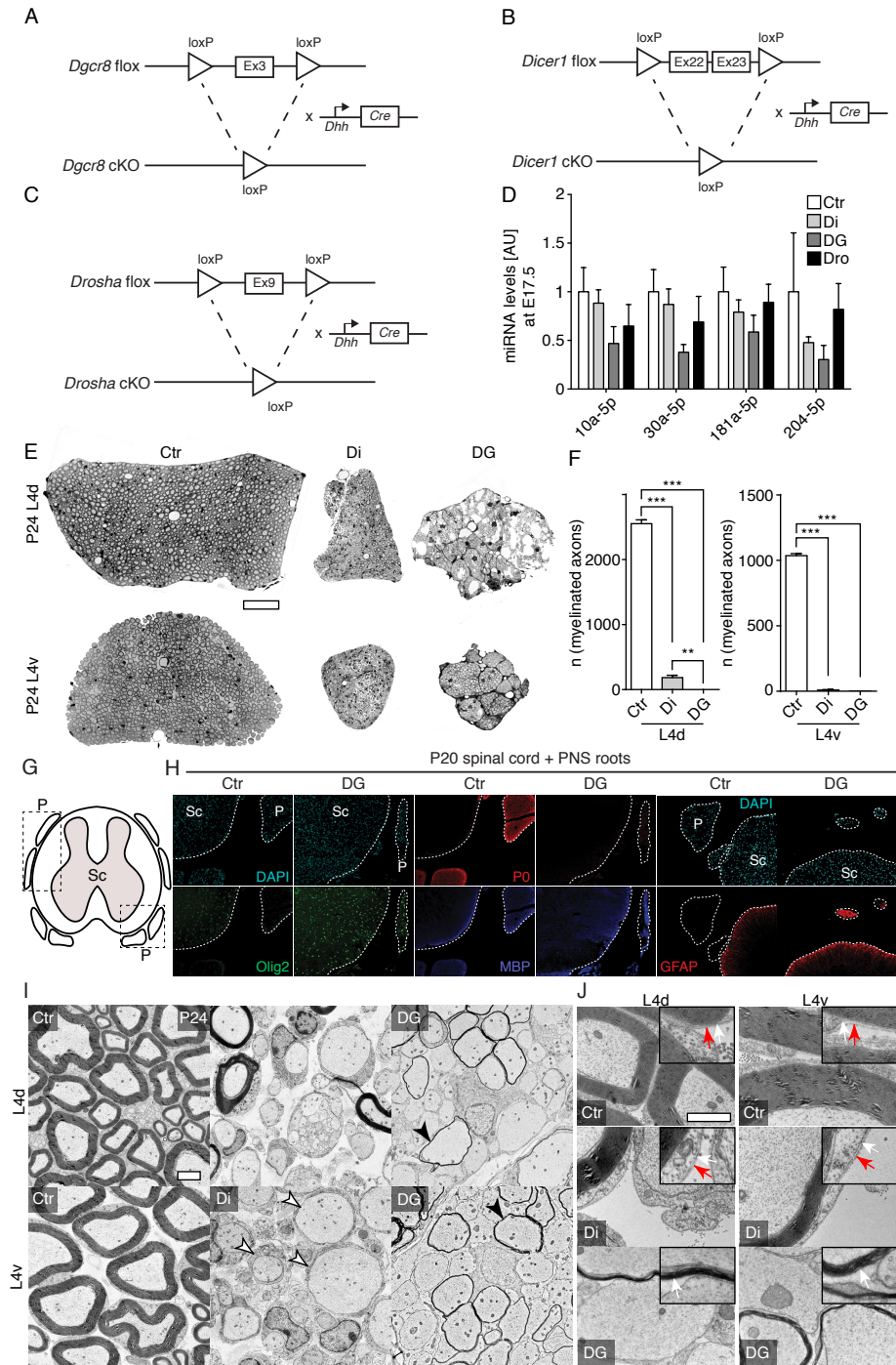
shown). These data support a role of DGCR8 and Drosha in the regulation of SC numbers. Matching the number of SCs to axons is achieved through a fine balance between proliferation and apoptosis of SCs [Jessen and Mirsky, 2005, Nakao et al., 1997, Peters and Muir, 1959, Webster et al., 1973]. To address if these processes are disturbed, we analysed apoptosis through TUNEL assays in DGCR8 and Dicer KO at E17.5, P1 and P5 (Figure 3.5K). At E17.5 both mutants showed unchanged numbers of TUNEL-positive cells when compared to controls, whereas at P1 DGCR8 KO showed a striking increase in TUNEL-positive cells, which was sustained at P5. Analysis of double KO corroborated these observations (data not shown). In contrast, SNs of Dicer KO showed no increase in apoptosis at P1 and presented significantly less apoptosis compared to DGCR8 KO at P5. Analysis of proliferation revealed no significant changes in DGCR8 KO, Dicer KO (Figure 3.6A) and double KO (Figure 3.6B), which argues

---

Figure 3.2 *(preceding page)* | Conditional depletion of Dgcr8, Dicer1 and Drosha and resulting phenotypic hallmarks in PNS roots. (**A-C**) Conditional targeting for ablation of Dgcr8, Dicer1 and Drosha in SC using dhhCre. (**D**) Levels of selected miRNAs (miR-10a-5p, miR-30a-5p, miR-181a-5p and miR-204-5p) in controls (Ctr), Dicer KO (Di), DGCR8 KO (DG) and Drosha KO (Dro) at E17.5 (n = 3 for each genotype). None of the miRNAs is significantly changed at this age in the mutant mice. (**E**) Toluidine blue-stained semithin sections of dorsal (L4d) and ventral L4 roots (L4v) of Ctr, Di and DG at P24. DG animals show pathological organisation of the endoneurium into large fascicles on both dorsal and ventral roots, in addition to sporadic holes only obvious on the dorsal roots. These features are not visible on Di or Ctr roots. Both DG and Di mice show smaller roots than Ctr, which evidently lack myelin. (**F**) Number of myelinated fibres by SCs in L4d and L4v of Ctr, Di and DG at P24 (n = 3 for each genotype). Both Di and DG roots show drastically reduced numbers of SC-myelinated fibres compared to controls, and DG dorsal roots also show significantly less compared to Di. (**G**) Schematic representation of the area of immunohistochemical analysis. Spinal cord (Sc) and dorsal and ventral roots (both marked with P). Both dorsal and ventral roots were analysed. (**H**) Immunohistochemical analysis of Ctr, Di and DG PNS root sections using antibodies against Olig2 (green), P0 (red), MBP (blue) and GFAP (red). Nuclei were counterstained with DAPI. Spinal cord (SC) and PNS roots (P) are highlighted with dashed lines. Olig2 is expressed by oligodendrocytes, but not SCs. Unlike Ctr, DG animals contain Olig2$^+$ cells in the roots, indicating the present of oligodendrocytes in the PNS of these mice. Ctr mice present MBP+ and P0+ myelin on the PNS roots, as expected. However, DG mice show MBP$^+$ and P0$^-$ myelin, similar to the one visible within the spinal cord. GFAP is strongly expressed by astrocytes in the CNS, and is also clearly labelling PNS roots of DG but not Ctr mice. Our observations reveal presence of CNS glia in PNS roots of DG animals, and suggest ongoing oligodendrocyte myelination in PNS roots. Our observations were the same on dorsal and ventral roots, therefore representative images of either roots were included. (**I**) Electron micrographs of L4d and L4v of Ctr, Di and DG at P24. Ctr are thoroughly myelinated on both roots, whereas Di roots contain axons mostly arrested at the 1:1 stage (white arrowheads) as in the SN. Some small axon bundles can also be found in dorsal roots of Di mice. However, DG mice show very large areas of axons bundled together in fascicles, and the images depicted only represent a small fraction of one such fascicle. Interestingly, there is very thin myelin associated with some axons within these fascicles (black arrowheads). (**J**) High-magnification electron micrographs of myelinated axons of Ctr, Di and DG in L4 roots. In both Ctr and Di roots the axons are myelinated by cells which contain a basal lamina characteristic of SCs (red arrows) surrounding the myelinating cell plasma membrane (white arrows). In contrast, the thinly myelinated axons detected in dorsal and ventral roots of DG mice display no basal lamina surrounding the myelinating cell membrane (white arrows). This is consistent with myelination by oligodendrocytes since these cells produce no basal lamina. Scale bar equals 50 μm (**E**), 2 μm (**I**, left side) and 1 μm (**I**, right side). Error bars represent standard error of the mean. Two-tailed Student's t-test * $P < 0.05$, ** $P < 0.01$, *** $P < 0.001$ (**D,F**).
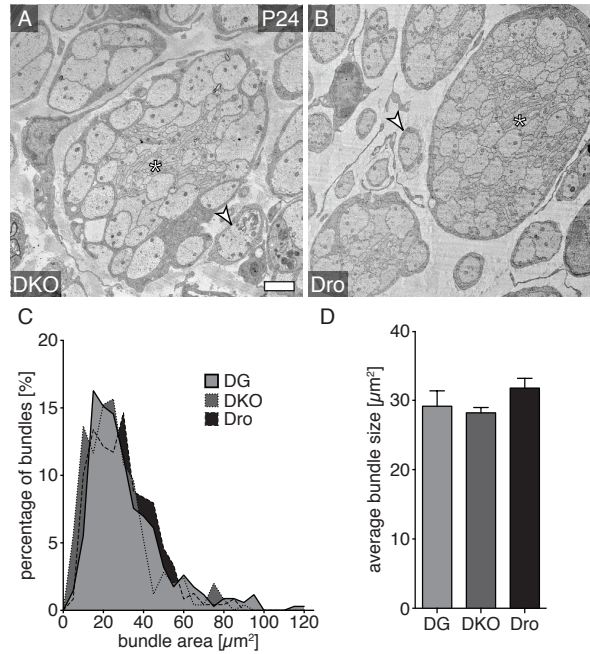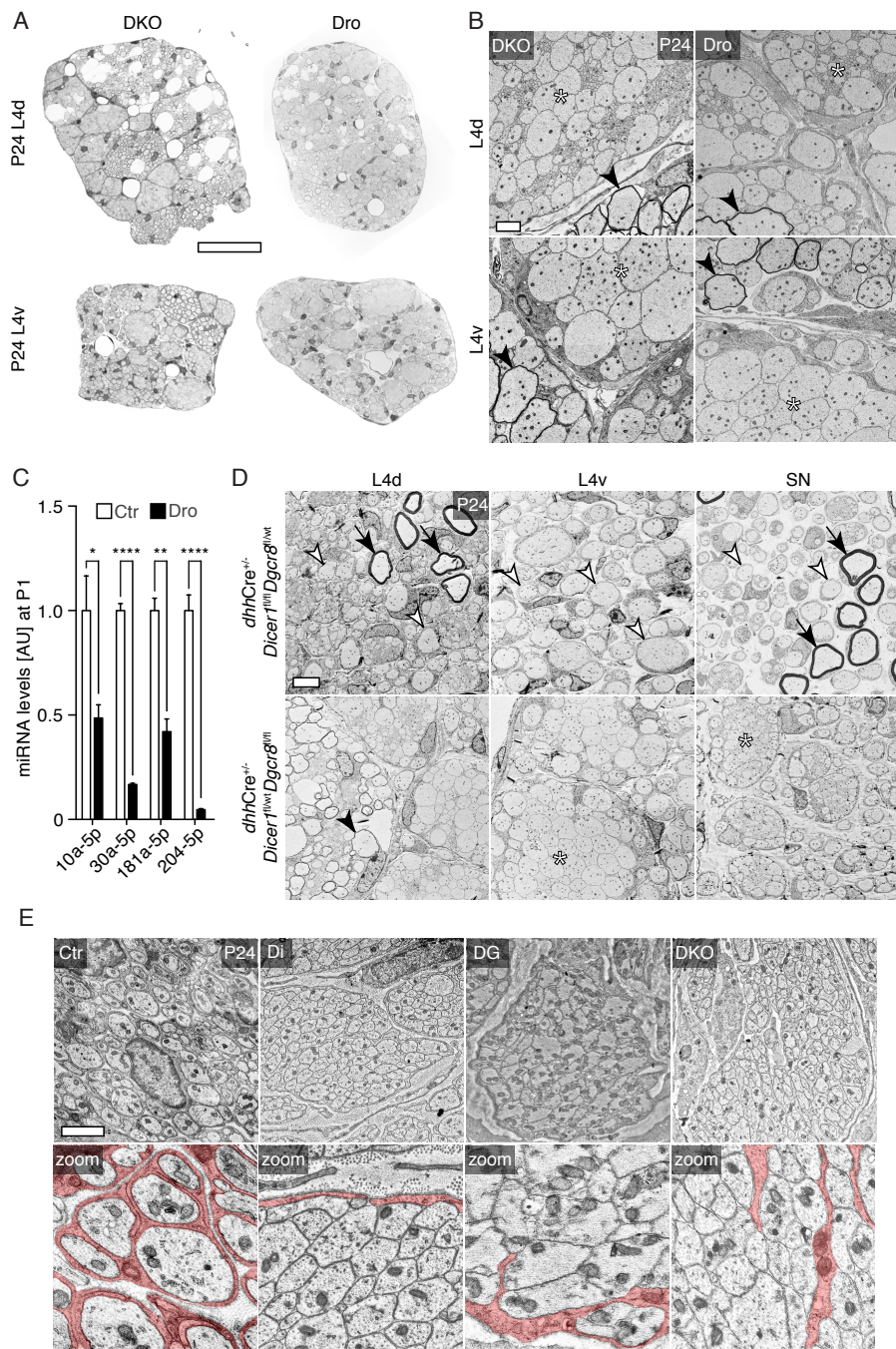
Figure 3.3 | The microprocessor regulates radial sorting in a miRNA-independent manner. (**A-B**) Electron micrographs of Dicer-DGCR8 double KO (DKO) and Drosha KO (Dro) SNs at P24. Both mutants display the same phenotypic hallmarks as DGCR8 KO (see Figure 3.1), with the immature bundles of axons (asterisks) and 1:1 not-myelinated profiles (white arrowheads). (**C**) Frequency distribution of bundle sizes of DG, DKO and Dro SNs at P24 per cross-section (n = 3 per genotype). The three mutants display the same distribution pattern of bundle sizes supporting their shared phenotypic hallmarks. (**D**) Average bundle size per cross-section in P24 DG, DKO and Dro SNs. (n = 3 per genotype). There are no significant differences in the average bundle size between the DKO and the Dro when compared to DG mice. Scale bar equals 2 μm (**A-B**). Error bars represent standard error of the mean. Two-tailed Student's t-test reveals no significant changes $P > 0.05$ (**D**). See also Figure 3.4.

against a significant contribution of proliferation towards the reduced number of cells in SNs of the microprocessor mutant mice. Taken together our results support a role of the microprocessor in promoting SC survival, which allows a progressive buildup of SCs necessary for appropriate radial sorting.

Deep sequencing reveals that Shh is upregulated in DGCR8 KO but not Dicer KO animals.

Besides its crucial function during canonical miRNA biogenesis the microprocessor was shown to have miRNA-independent cellular functions. These include the binding and cleaving of other RNA species through the recognition of pri-miRNA-like hairpin structures [Heras et al., 2013, Knuckles et al., 2012, Macias et al., 2013] and the association with certain gene loci to suppress their transcription [Wagschal et al., 2012]. Given the phenotypic differences of DGCR8 and Dicer KO, we hypothesised that such miRNA-independent functions of the microprocessor underlie the earlier developmental arrest observed in DGCR8 KO. To obtain an unbiased collection of possibly derepressed tran-

scripts which could be subject of miRNA-independent microprocessor regulation we performed deep sequencing of RNA extracted from SNs of DGCR8 KO, Dicer KO and control animals at P1 (Figure 3.7). Our data reveal numerous mRNAs exclusively regulated in DGCR8 KO in comparison to Dicer KO and control SNs (Figures 3.7A-C). In addition, hierarchical cluster analysis of differentially expressed genes reveals less similarities between DGCR8 KO and Dicer KO than between Dicer KO and control mice (Figure 3.7B). This is in line with our morphological analysis, and reveals that the strong differences between DGCR8 KO and Dicer KO are reflected at the transcriptome level as well. Among all the upregulated transcripts, we surprisingly found that Shh is the most upregulated mRNA in DGCR8 KO (Figure 3.7D, arrow), while remaining almost undetectable in controls and Dicer KO. This specific upregulation in DGCR8 KO could be validated by qRT-PCR analysis (Figure 3.7E). Taken together, our data reveal that deletion of DGCR8 in SCs leads to specific upregulation of genes when compared to Dicer KO, with Shh being the most prominently upregulated.

Shh signalling hinders radial sorting and SC survival in wildtype mice.

Shh is a powerful morphogen but its function during radial sorting is unknown. Given the strong upregulation of Shh mRNA specifically in SNs of DGCR8 KO, we sought to explore the impact of active Shh signalling during radial sorting in wildtype mice. To address this, we provided the Shh agonist purmorphamine (PMA) [Chechneva et al., 2014] to SNs of wildtype animals, for 2 consecutive days starting at P0, and compared the SNs to those of vehicle-treated controls. Morphological analysis at P2 revealed a significant

---

Figure 3.4 *(preceding page)* | Radial sorting defects in DGCR8 KO are due to loss of microprocessor miRNA-independent functions, whereas maturation of Remak bundles is dependent on canonical miRNAs. (**A**) Toluidine blue-stained semithin sections of dorsal (L4d) and ventral L4 roots (L4v) of DGCR8-Dicer double KO (DKO) and Drosha KO (Dro) at P24. The phenotypic hallmarks visible in the roots of these animals are consistent with the ones of DGCR8 KO (see Figure 3.2E). They contain large fascicles of bundled axons, almost complete absence of SC myelin and sporadic holes in the dorsal roots. (**B**) Electron micrographs of L4d and L4v of DGCR8-Dicer double KO (DKO) and Drosha KO (Dro) in at P24. Fascicles of axon bundles (asterisks) are highlighted. The roots of both mutants also contain thinly myelinated axons which resemble the oligodendrocyte myelin present in DG animals (black arrowheads). (**C**) Levels of selected miRNAs (miR-10a-5p, miR-30a-5p, miR-181a-5p and miR-204-5p) in Ctr and Dro at P1 (n = 3 for each genotype). The reduction of all mature miRNAs confirms the loss of miRNA biogenesis due to Drosha depletion. (**D**) Electron micrographs of L4d, L4v and SN of littermate (*dhh*Cre$^{+/-}$*Dicer1*$^{fl/wt}$*Dgcr8*$^{fl/fl}$) and *dhh*Cre$^{+/-}$*Dicer1*$^{fl/fl}$*Dgcr8*$^{fl/wt}$ at P24. Animals depleted of DGCR8 and with half the gene-dose of Dicer (*dhh*Cre$^{+/-}$*Dicer1*$^{fl/wt}$*Dgcr8*$^{fl/fl}$) show phenotypic hallmarks of DGCR8 KO including abundant large bundles in the SNs and PNS roots (asterisks) coupled to almost no SC myelin. In addition, the roots contain thinly myelinated axons (black arrowheads) similar to oligodendrocyte myelinated structures present in DGCR8 KO (see Figures 3.2I,J). In contrast littermate mice with half the gene-dose of DGCR8 and depleted of Dicer (*dhh*Cre$^{+/-}$*Dicer1*$^{fl/fl}$*Dgcr8*$^{fl/wt}$) contain few myelinated axons (black arrows) and numerous 1:1 pro-myelinating profiles (white arrowheads), similar to our observations in Dicer KO. (**E**) Electron micrographs of the sympathetic trunk of Ctr, Di, DG and DKO at P24. Zoomed images in second row show SC cytoplasm false-coloured in red. SCs in Ctr mice encircle every axon they engage individually, whereas Di, DG and DKO SCs do not. Scale bar equals 50 µm (**A**) and 2 µm (**B,D,E**). Error bars represent standard error of the mean. Two-tailed Student's t-test * $P < 0.05$, ** $P < 0.01$, *** $P < 0.001$ **** $P < 0.0001$ (**C**).
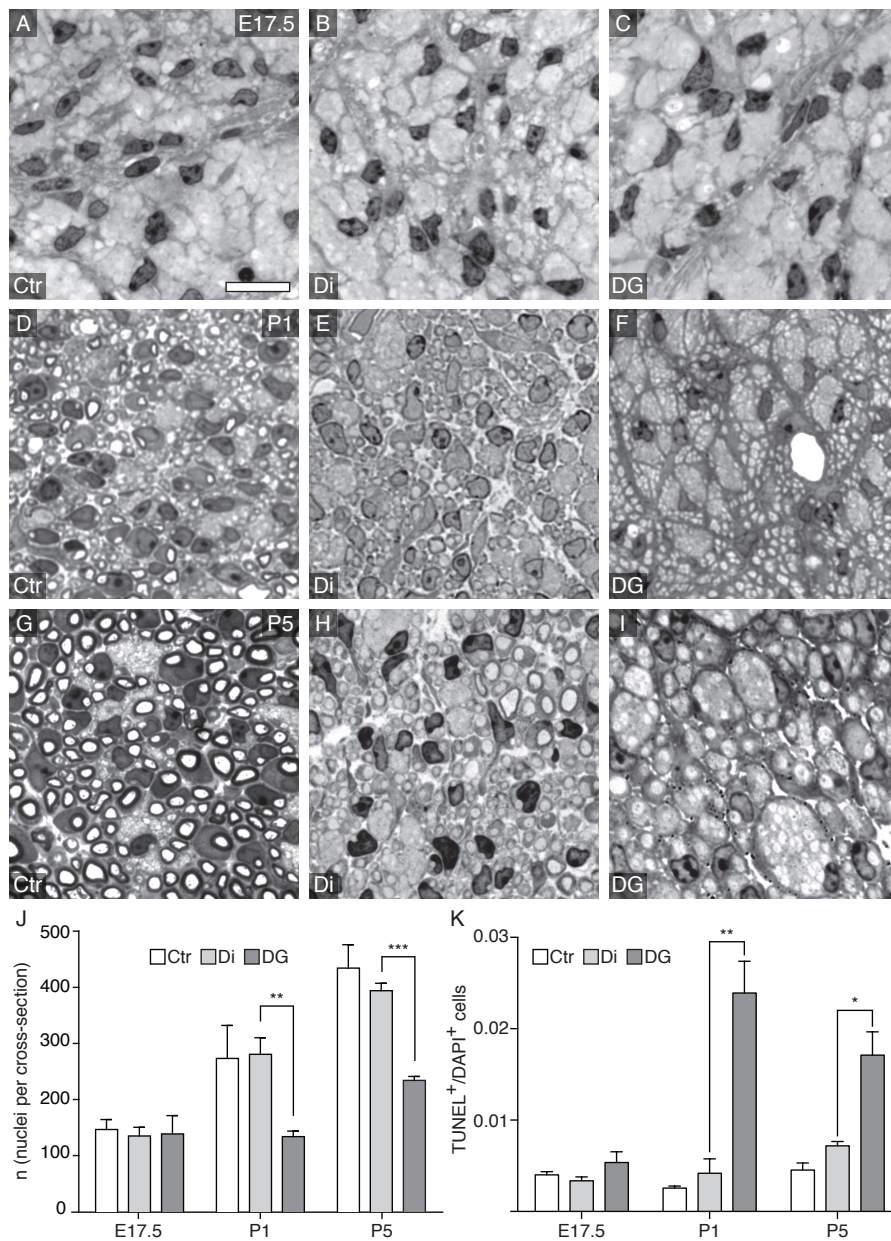
Figure 3.5 | SN of DGCR8 KO, but not of Dicer KO, show reduced cell numbers and increased cell death starting at P1. (**A-I**) Toluidine blue-stained semithin sections of control (Ctr), Dicer KO (Di) and DGCR8 KO (DG) at E17.5, P1 and P5. From P1 onwards there is a striking decrease in the number of nuclei visible in DG SNs exclusively, and at P5 the bundles are also notoriously larger in DG animals. (**J**) Number of nuclei per SN cross-section in Ctr, Di and DG at E17.5, P1 and P5 (n = 3 for each time-point and genotype). At E17.5 there are no differences between DG when compared to Di animals. At P1 and P5, there is a significant decrease in the number of nuclei present in DG animals exclusively. Di animals do not differ from controls. (**K**) Number of TUNEL$^+$ cells per DAPI$^+$ cells in SN of Ctr, Di and DG at E17.5, P1 and P5 (n = 3 for each time-point and genotype). At E17.5 there are no significant differences between the animals. At P1 there is a significant increase in apoptosis in DG compared to Di and Ctr animals, which is consistent at P5. Dicer animals do not differ from controls at P1 and have only a minor increase in apoptosis at P5 ($P = 0.041$, *). Scale bar equals 10 µm (**A-I**). Error bars represent standard error of the mean. Two-tailed Student's t-test * $P < 0.05$, ** $P < 0.01$, *** $P < 0.001$ (**J,K**). See also Figure 3.6.
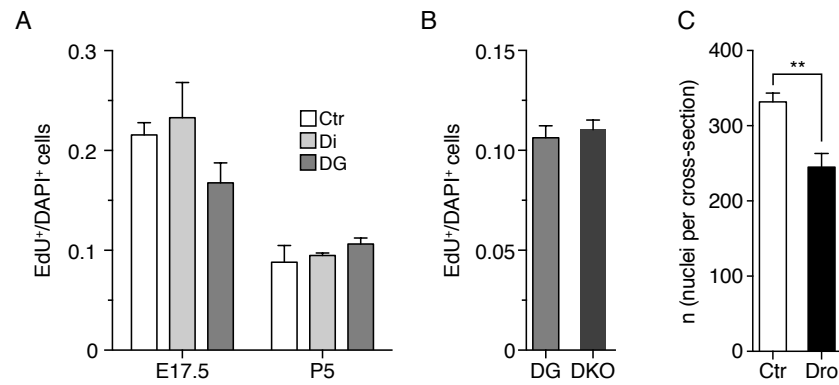
43

Figure 3.6 | Proliferation is not altered in DGCR8 or Dicer-depleted SCs, and Drosha-depleted SCs show compromised survival at P1. (**A**) Number of EdU$^+$ per DAPI$^+$ cells in SN of control (Ctr), Dicer KO (Di) and DGCR8 KO (DG) at E17.5 and P5 (n = 3 per genotype). We observed no significant changes in proliferation at any of the time points analysed. (**B**) Number of EdU$^+$ per DAPI$^+$ cells in SN of DG and double KO (DKO) at P5 (n = 3 per genotype). The DG and DKO SNs have the same levels of proliferation when compared to each other, and these also do not differ from Ctr SNs. (**C**) Number of nuclei per SN cross-section in controls (Ctr) and Drosha KO (Dro) at P1 (n = 3 per genotype). Dro animals show significantly less cells per cross-section, similar the results obtained from DGCR8 KO (see Figure 3.5). Error bars represent standard error of the mean. Two-tailed Student's t-test * $P < 0.05$, ** $P < 0.01$, *** $P < 0.001$ **** $P < 0.0001$ (**A-C**).

reduction in cell numbers in PMA-treated SNs compared to controls (Figures 3.8A-C), which is constistent with the observed reduced cell numbers and increased apoptosis in SNs of DGCR8 KO. In addition, we could observe a significant decrease in the number of sorted but not-myelinated SC-axon profiles (Figure 3.8D), but no change in the number of myelinated axons (Figure 3.8E). Taken together, these results illustrate a detrimental role of Shh signalling in SC survival during radial sorting.

Inhibition of Shh signalling rescues DGCR8 KO phenotype *in vivo.*

Based on the impairments observed in response to activation of Shh signalling in wild-type mice, we asked whether the decreased SC survival and impaired radial sorting observed in DGCR8 KO is a consequence of active Shh signalling. To address this, we inhibited Shh signalling in DGCR8 KO by treating SNs with cyclopamine (KAAD-CPA) [Ecke et al., 2008, Mahindroo et al., 2009], and compared them to those of DGCR8 KO treated with vehicle only. To evaluate the state of radial sorting, we analysed P5 SNs for the number of cells, the area occupied by bundles of unsorted axons, and the number of 1:1 SC-axon relations. We found a significant increase in the number of cells, a decrease in the overall area occupied by bundles of unsorted axons, and an increase in the number of axons engaged by SCs in a 1:1 relation specifically in the KAAD-CPA-treated SNs (Figures 3.8F-J). In conclusion, our data reveal that suppression of Shh signalling rescues the DGCR8 KO phenotype and supports a model in which the microprocessor is necessary to protect SC survival and promote radial sorting by suppressing Shh.

The present study highlights a hitherto unknown physiological role of the micropro-
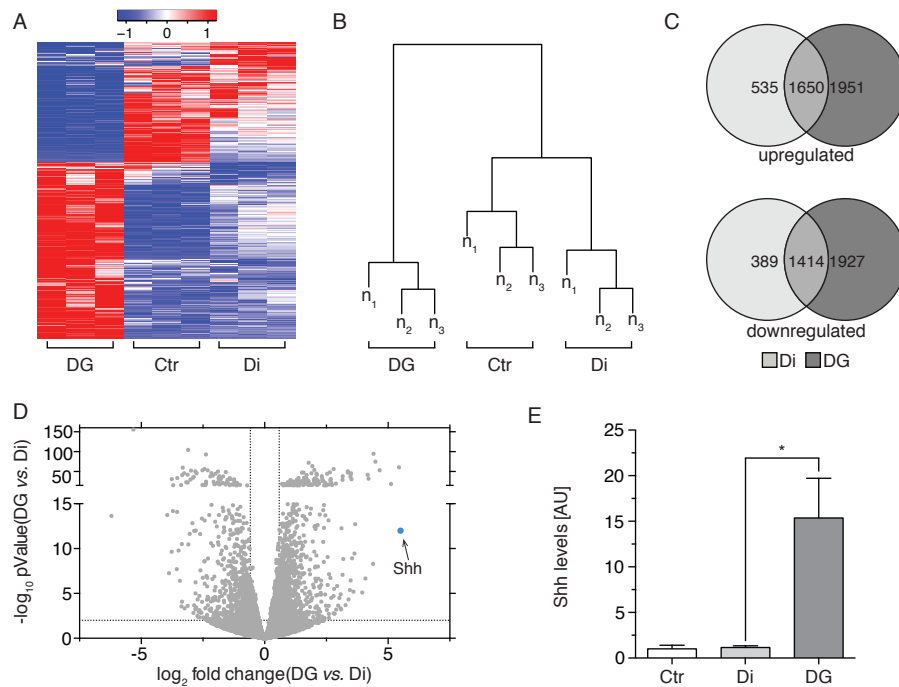
Figure 3.7 | Shh mRNA is strongly upregulated exclusively in DGCR8 KO. (**A**) Heatmap diagram (Z-score per row) of differentially expressed genes in DGCR8 KO (DG), Ctr and Dicer KO (Di) with a P value < 0.01 and $\log_2$ ratio > 0.5 (n = 3 for each genotype). (**B**) Hierarchical cluster analysis of differentially expressed genes of DG, Di and Ctr, indicating substantial differences of DGCR8 KO when compared to Dicer KO and controls (n = 3 for each genotype). (**C**) Venn diagrams showing significantly upregulated (linear fold change > 1.2, $P < 0.05$) and downregulated (linear fold change < 0.8, $P < 0.05$) transcripts in Di and DG at P1 when compared to Ctr. The diagram highlights numerous genes exclusively regulated upon DGCR8 deletion (n = 3 for each genotype). (**D**) Volcano plot highlighting Shh (blue, see arrow) strongly upregulated in DG compared to Di at P1 (n=3 for each genotype). (**E**) Real-time PCR analysis of Shh in Ctr, Di and DG SNs at P1 normalised to GAPDH (n = 3 for each genotype). Shh is exclusively upregulated in DG animals compared to Di and control animals. Error bars represent standard error of the mean. Two-tailed Student's t-test * $P < 0.05$, ** $P < 0.01$, *** $P < 0.001$ (**E**).
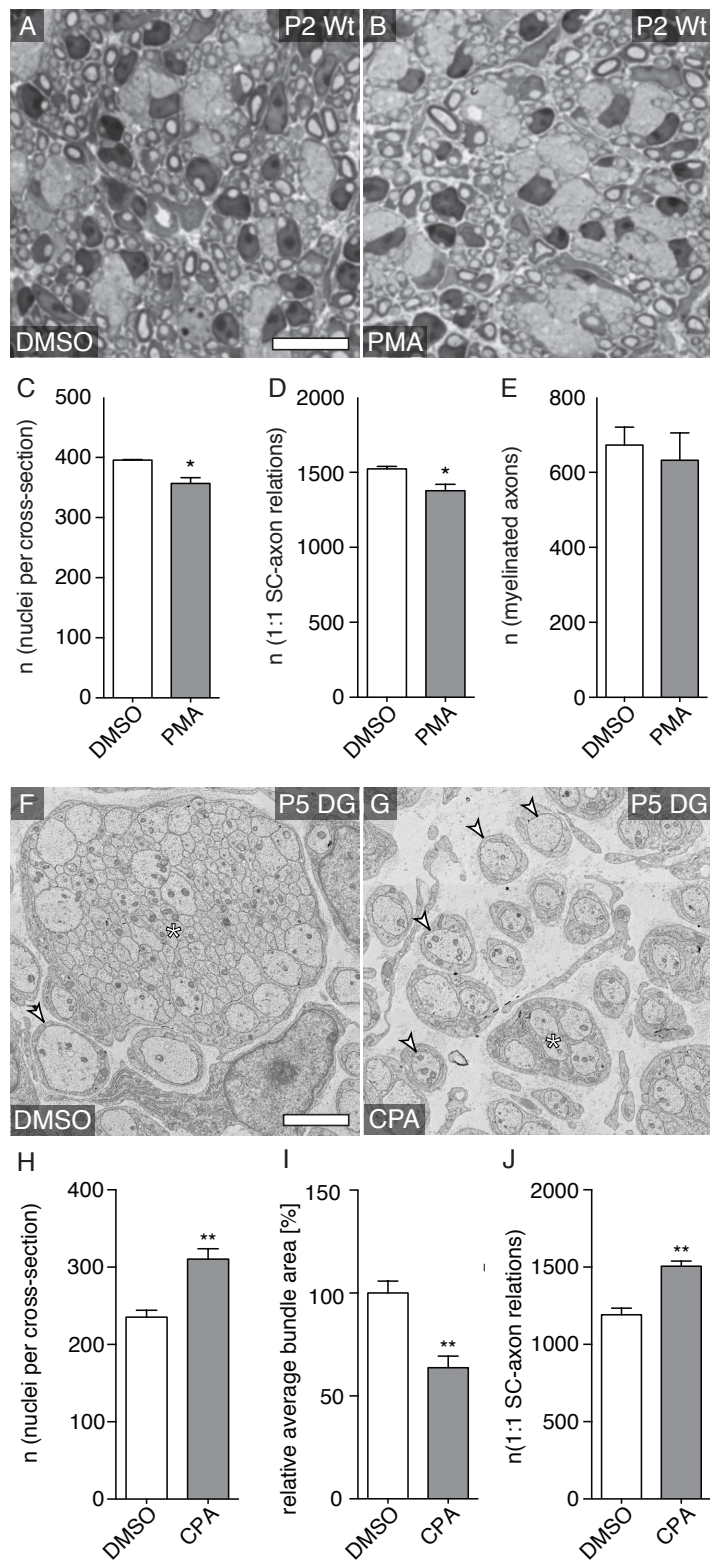
cessor during a major developmental process. We identify Shh signalling as a powerful pathway that needs to be kept suppressed by the microprocessor during early events of radial sorting. Failure to do so compromises SC survival and impairs radial sorting (Figure 3.9).

Discussion

Our study has uncovered a hitherto unknown regulatory axis in which the microprocessor suppresses Shh signalling to promote SC survival during radial sorting. This conclusion is firstly based on phenotypic hallmarks specific to conditional mouse mutants with loss of DGCR8 or Drosha, which are not shared by Dicer mutants. Second, activation of Shh signalling in wild-type mice mimics the phenotypic hallmarks of DGCR8 and Drosha KO whereas inhibition of Shh signalling rescues the phenotype of DGCR8 KO. The comparative analysis of DGCR8 and Dicer KO mice also revealed a common impairment at the onset of myelination, which is most likely mediated by canonical miRNAs. In fact, our sequencing experiments revealed numerous canonical miRNAs abundantly expressed through the onset of myelination. Non-canonical miRNAs have also been shown to play important roles in various tissues [Macias et al., 2013, Yang and Lai, 2011]. In these situations, the comparison of loss of Dicer and loss of microprocessor mutants revealed a more severe phenotype upon Dicer deletion. However, our data do not point to a beneficial role for non-canonical miRNAs in SCs, since Dicer KO show a milder impairment than that seen in DGCR8 and Drosha KO. It is worth noting that the presence of non-canonical miRNAs in the absence of the canonical miRNAs is a non-

---

Figure 3.8 *(preceding page)* | Activation of Shh signalling hinders radial sorting and SC survival in wildtype mice, whereas its inhibition rescues the DGCR8 KO phenotype in vivo. (**A-B**) Toluidine blue-stained semithin sections of SNs from wildtype C57bl6 animals treated with the Shh signalling agonist purmorphamine (PMA) or with DMSO for two consecutive days at P0 and P1, analysed at P2. (**C**) Number of nuclei per SN cross-section of DMSO vehicle-treated and PMA-treated littermates C57bl6 wild-type mice at P2 (n = 3 per condition). PMA treatment leads to a reduction in the number of cells. (**D**) Number of 1:1 SC-axon pro-myelinating relations per SN cross-section of DMSO-treated and PMA-treated littermates C57bl6 wild-type mice at P2 (n = 3 per condition). PMA treatment leads to a reduction in the number of sorted axons, indicating impairment of radial sorting. (**E**) Number of myelinated axons per SN cross-section of DMSO control-treated and PMA-treated littermates C57bl6 wild-type mice at P2 (n = 3 per condition). PMA treatment does not alter myelination. (**F-G**) Electron micrographs of SNs from DG animals treated with the Shh signalling antagonist KAAD-CPA (CPA) or with DMSO for two consecutive days at P3 and P4, analysed at P5. Animals treated with DMSO vehicle still show large immature axon bundles (asterisk), whereas CPA-treated mice show smaller bundles (asterisk) and more 1:1 SC-axon not-myelinated profiles (white arrowheads). (**H**) Number of nuclei per SN cross-section of DMSO-treated and KAAD-CPA-treated (CPA) DG mice at P5 (n = 3 per condition) reveals a significant increase in the number of nuclei upon CPA treatment. (**I**) Comparative average bundle area (in %) per SN cross-section of DMSO-treated and KAAD-CPA-treated (CPA) DG mice at P5 (n = 3 per condition). Inhibition of Shh signalling leads to a decrease in the size of immature axon bundles. (**J**) Number of 1:1 SC-axon relations per SN cross-section of DMSO-treated and KAAD-CPA-treated (CPA) DG mice at P5 (n = 3 per condition). The increase in the number of sorted axons engaged in a 1:1 relation by SCs indicates that radial sorting has been restored in CPA-treated DG animals. Scale bar equals 2 µm (**A,B,F,G**). Error bars represent standard error of the mean. Two-tailed Student's t-test * $P < 0.05$, ** $P < 0.01$ (**C-E,H-J**).

physiological situation in SCs. We considered the possibility that these might further destabilise the system to have an overall detrimental effect. Our analysis of Dicer and DGCR8 double KO animals does not support this hypothesis, as even in the absence of non-canonical miRNAs the double KO mice phenocopy DGCR8 and Drosha KO mice. In line with this we detected non-canonical miRNAs only in low abundances in mouse SNs and differentiated primary SCs using small RNA sequencing (data not shown).

We also found no Remak bundles in SNs of the various KO mice analysed in this study. The literature that describes mechanisms regulating Remak bundle maturation is fragmentary, and this path of differentiation is not well understood in comparison to its myelination counterpart. SCs rely on cues derived from the axons [Faroni et al., 2014, Orita et al., 2013, Shin et al., 2014] and from the extracellular matrix [Salzer, 2012, Yu et al., 2009] to drive Remak bundle maturation, but SC-intrinsic factors that regulate this
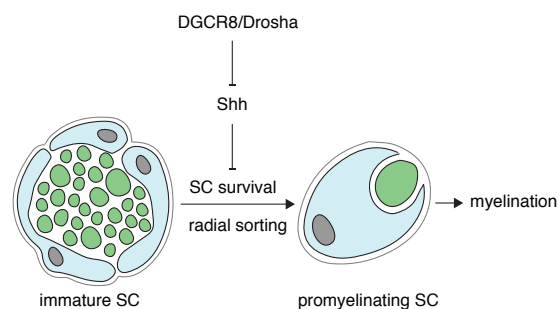

Figure 3.9 | Model of microprocessor-mediated regulation of SC survival and radial sorting through suppression of Shh. Axons are illustrated in green, SC cytoplasm in blue and SC nuclei in gray.

fate remain largely obscure. Here we report for the first time, according to the best of our knowledge, that maturation of Remak bundles is positively regulated by canonical miRNAs. Given that we could not find mature Remak bundles in SNs of Dicer KO at P24, it is likely that most bundled axons in Dicer KO were actually meant to be engaged by mature non-myelinating SCs in Remak bundles. This is in sharp contrast to the much larger immature bundles present in SNs of DGCR8 and Drosha mutant mice, which indicates a major impairment in the process of developmental radial sorting on top of impaired Remak bundle maturation.

At the onset of radial sorting, immature SCs are greatly outnumbered by the axon segments they need to myelinate [Peters and Muir, 1959, Webster et al., 1973]. The selection of axons to myelinate and the expansion of the immature SC pool occur simultaneously throughout radial sorting. Since the period of neuronal death is completed at the radial sorting stage, matching the numbers of SCs to the axonal segments to be myelinated is achieved through a combination of SC proliferation and apoptosis [Jessen and Mirsky, 2005, Nakao et al., 1997]. Work from various labs has reported radial sorting defects coupled to a strong decrease in SC numbers in various mutant lines [Benninger et al., 2007, Berti et al., 2011, Chen and Strickland, 2003, Grove et al., 2007]. To the best of our knowledge there are no published developmental studies showing a prominent reduction in the number of immature SCs yet success in radial sorting. This process, in addition to others [Norrmen et al., 2014] such as process extension [Benninger et al., 2007, Montani et al., 2014, Nodari et al., 2007, Pellegatta et al., 2013, Pereira et al., 2009, Pereira et al., 2012], is absolutely required for proper PNS development.

Radial sorting defects with persistent axonal bundles in adulthood have also been reported in mouse model studies for human pathologies, such as congenital muscular dystrophy 1A (MDC1A) [Miyagoe-Suzuki et al., 2000]. The disease is associated with deficient laminin signalling towards SCs. Studies in mouse models revealed a reduction in the number of SCs in peripheral nerves, coupled to reduced proliferation and increased apoptosis [Feltri and Wrabetz, 2005]. In addition to the pathways promoting survival in SCs, other pathways actively promote apoptosis [D'Antonio et al., 2006, Jacob et al., 2011, Syroid et al., 2000]. In one example, histone deacetylase 1 (HDAC1) suppresses the levels of active β-catenin (ABC), which would otherwise promote SC apoptosis during radial sorting [Jacob et al., 2011]. The temporal regulation and the SC response to ABC is highly specific, since the level of ABC naturally increases at the onset of myelination where it then acts as a signal to promote further differentiation [Jacob et al., 2011]. In SCs, as in many other systems, the cellular response to specific signals is frequently strictly restricted to particular differentiation stage(s) within the physiological context of peripheral nerves, and cannot be generalised. In SNs of DGCR8 and Drosha mutants we observed a decrease in the number of cells which is in agreement with increased SC apoptosis in SNs of DGCR8 mutants when compared to controls and Dicer KOs. The deficiency in the number of SCs due to excessive death is therefore the most logical explanation for the strong radial sorting defects. As we could not detect a deficit in SC numbers in Dicer KO, loss of miRNAs is unlikely to be the cause for the radial sorting and SC survival defects observed in DGCR8, Drosha and double KO, however we cannot fully exclude a contribution.

We hypothesised that miRNA-independent functions of the microprocessor are necessary to protect SC survival during radial sorting. This concept has been recently brought up in the literature and our work is one of the first studies implicating it in a neurophysiologically relevant scenario. Assuming the microprocessor directly suppresses gene expression either through the recognition of pri-miRNA-like hairpin structures within mRNAs or through direct binding at the level of the genomic DNA, these genes should be upregulated after microprocessor depletion. Our deep sequencing data has revealed 1951 genes specifically upregulated in DGCR8 KO which would qualify as potential subjects to miRNA-independent microprocessor suppression. Among these Shh mRNA was the most prominently upregulated transcript. Previous research on Shh has focused mostly on early embryogenesis, where it frequently promotes survival and tissue morphogenesis [Delloye-Bourgeois et al., 2014, Matise and Wang, 2011]. However, Shh also promotes apoptosis in specific sensory neuron subtypes derived from neural crest stem cells in dorsal root ganglia [Guan et al., 2008]. These cells only respond with apoptosis at a very specific stage of differentiation. A similar pro-apoptotic role of Shh has been reported for several other neural crest-derived and other cells, usually associated with morphogenesis and always at very specific developmental stages [Oppenheim et al., 1999, Panman and Zeller, 2003, Sanz-Ezquerro and Tickle, 2000, Siggins et al., 2009, Zuzarte-Luis and Hurle, 2005]. Early in development, Shh promotes survival of neural crest stem cells, prior to the generation of SC precursors [Delloye-Bourgeois et al., 2014]. In adult SCs, Shh is expressed following PNS injury and has been reported to promote survival of motor

neurons [Hashimoto et al., 2008]. However, in the period between early development and adult injury the role of Shh in SCs remained unexplored and we therefore focussed on exploring the consequences of active Shh signalling during early events of myelination. We hypothesised that the microprocessor is necessary to suppress Shh signalling during radial sorting to promote SC survival and safeguard appropriate matching of SC to axon numbers. In support of this hypothesis, when we provided Shh agonist to SNs of wild-type animals during radial sorting we observed a consistent decrease in the number of cells compared to vehicle-treated syblings. This observation is consistent with increased apoptosis and decreased cell numbers in SNs of DGCR8 KO mice. Furthermore, animals treated with Shh agonist also displayed significantly less sorted but not-yet myelinated axons. Conversely, silencing of Shh signalling in SNs of DGCR8 KO resulted in an increased number of cells and rescue of radial sorting, as determined through a decrease in the area occupied by bundles of unsorted axons and a concomitant increase in the number of 1:1 SC-axon relations. In summary these data reveal that suppression of Shh signalling by the microprocessor is necessary to protect SC survival during radial sorting. This function of the microprocessor seems to be largely independent of miRNAs as Dicer KO neither show compromised SC survival nor increased Shh expression. Failure to repress Shh as a result of microprocessor depletion in SCs therefore largely accounts for the compromised SC survival, however we cannot exclude a contribution of additional RNA species dependent on the microprocessor. Additional studies will be needed to address whether this suppression of Shh happens in a direct manner such as interaction of the microprocessor with the Shh mRNA or with the *Shh* gene, or by an indirect mechanism. Regarding the regulation of the onset of myelination in SCs it is important to note that despite an increase in sorted axons, the number of myelinated axons remained the same in Shh antagonist-treated DGCR8 KO when compared to vehicle-treated SNs. This is in agreement with our data and previously published results implicating miRNAs to be crucial for the onset of myelination but not during the stage of radial sorting [Pereira et al., 2010, Bremer et al., 2010, Yun et al., 2010, Verrier et al., 2010].

Through the comparative analysis of multiple SC-specific conditional mutant mice for various components of the miRNA biogenesis pathway, we unveiled a hitherto unknown and physiologically relevant miRNA-independent mechanism of the microprocessor, which suppresses Shh signalling during radial sorting to protect SC survival and ensures appropriate matching of SC to axon numbers. Our data support a detrimental role of Shh in SC survival, but this response and the requirement for suppression by the microprocessor is likely to be restricted to the radial sorting time frame and the physiological context of peripheral nerves at this stage. The logic of this timing may derive from the fact that it is during radial sorting where the number of SCs needs to be matched to the number of axons. We are confident that our study provides a significant advance to our current understanding of the physiological relevance of the miRNA biogenesis pathway in the PNS, and we believe it will motivate new projects to explore similar regulatory circuits in various developmental and pathological paradigms.

3.2 Manuscript B — The Lin28 – let-7 axis is critical for myelination in the peripheral nervous system

Authors: Deniz Gökbuget[1,4], Jorge A Pereira[1,4], Sven Bachofner[1], Antonin Marchais[2], Constance Ciaudo[1], Markus Stoffel[1], Olivier Voinnet[2], Johannes H Schulte[3], Ueli Suter[1]

Affiliations:
1: ETH Zurich, Institute of Molecular Health Sciences, Otto-Stern-Weg 7, 8093 Zurich, Switzerland.
2: ETH Zurich, Department of Biology, Institute of Agricultural Sciences, Universitäts-strasse 2, 8092 Zurich, Switzerland.
3: Children's Hospital Essen, Department of Pediatric Oncology and Haematology, Essen, Germany.
4: These authors contributed equally to this work.

Myelination is a remarkable example of cell differentiation that ensures fast signal propagation in the vertebrate nervous system. The process is tightly controlled by the balance of negative and positive regulators, and in the PNS requires the integration of axonal and Schwann cell (SC)-derived signals. miRNAs are crucial regulators of myelination. However, the miRNAs species required and the underlying mechanisms are largely unknown. We found that let-7 miRNAs are highly abundant during PNS myelination and that their levels are inversely correlated to the expression of Lin28B, an antagonist of let-7 accumulation. Sustained expression of Lin28B and consequently reduced levels of let-7 miRNAs resulted in a failure of SC myelination in transgenic mouse models and in cell culture. Subsequent analyses revealed that let-7 miRNAs promote expression of the myelination-driving master transcription factor Krox20 through suppression of the myelination inhibitory Notch signalling. We conclude that the Lin28B – let-7 axis acts as a critical driver of PNS myelination, identifying this pathway also as a potential therapeutic target in demyelinating diseases.

Posttranscriptional regulation by miRNAs is ubiquitously important in cell differentiation and tumorigenesis [Mendell and Olson, 2012]. Typically, the biogenesis of

miRNAs involves sequential processing of the primary miRNA transcript by the RNAse III family enzymes Drosha and Dicer to yield a 22-nucleotide duplex. One strand of the mature miRNA duplex is loaded into the miRNA-induced silencing complex (miRISC) which targets mRNAs for translational repression and/or accelerated decay [Ameres and Zamore, 2013].

The let-7 family comprises one of the evolutionary most conserved families of miRNAs, and multiple let-7 isoforms have crucial functions in development, homeostasis and tumour suppression [Thornton and Gregory, 2012]. Key regulators of let-7 expression are the RNA-binding proteins Lin28A and Lin28B. Both block specifically let-7 biogenesis, and in turn, are targeted by let-7. Thus, the Lin28 - let-7 system is able to act as a bi-stable switch that regulates the transition of opposing differentiation states with let-7 usually promoting this process and Lin28 opposing it [Thornton and Gregory, 2012].

Dicer-mediated miRNA biogenesis is indispensable for myelination in the PNS [Pereira et al., 2010, Bremer et al., 2010, Yun et al., 2010, Verrier et al., 2010]. Dicer-deficient SCs arrest their development when they engage with axons in a 1:1 relationship, known as the pro-myelinating stage. Such mutant SCs fail to activate the correct myelination program and are unable to repress negative regulators of myelination, including Notch1 and Sox2. However, the physiologically relevant regulatory miRNA species involved have yet to be identified in this context.

Given the importance of miRNAs during PNS myelination, we quantitatively assessed miRNA expression during sciatic nerve (SN) development by small RNA sequencing. We found that let-7 family members are particularly strongly expressed in Schwann cells during myelination (Fig. 3.10a,b; Fig. 3.11a). Analysis at earlier developmental time points revealed that let-7 isoforms are induced prior to myelination onset, and that their levels are inversely correlated to those of Lin28B (Fig. 3.10c). Lin28A was not detectable at the time points examined (data not shown). Next, as a broad readout of let-7 function, we analysed differential expression of predicted let-7 targets in P4 SN of mice lacking Dicer in SCs (Dicer KO) compared to control mice, using RNA sequencing. We found globally increased levels of let-7 targets in Dicer KO (Fig. 3.10d). In addition, analysis of developmental expression of Hmga2, a well-described let-7 target, revealed a prominent decline upon let-7 induction in SN (Fig. 3.10e). Consistently, Hmga2 protein levels were strongly elevated in SN of Dicer KO (Fig. 3.11c,d). Taken together, our data demonstrate that the let-7 family is functionally enriched during PNS myelination and suggest that the decline of Lin28B expression before myelination might be causal in this context.

To test if Lin28B repression and subsequently increased let-7 biogenesis is functionally required for PNS myelination, we employed conditionally inducible transgenic Lin28B mice [Molenaar et al., 2012] and crossed them with Dhh-Cre mice [Jaegle et al., 2003] to obtain animals with sustained SC-specific expression of Lin28B (Lin28 tg). Expression analysis confirmed that let-7 isoforms are depleted in SN of these mice (Fig. 3.12d). Morphologically, at P5, SN of Lin28 tg showed an almost complete lack of myelinated axons and were developmentally arrested at the pro-myelinating stage, comparable to P5 SN with a Dicer KO background (Fig. 3.12a-c,e). Furthermore, the very few myelinated axons present in Lin28 tg had thinner myelin compared to control axons with the same
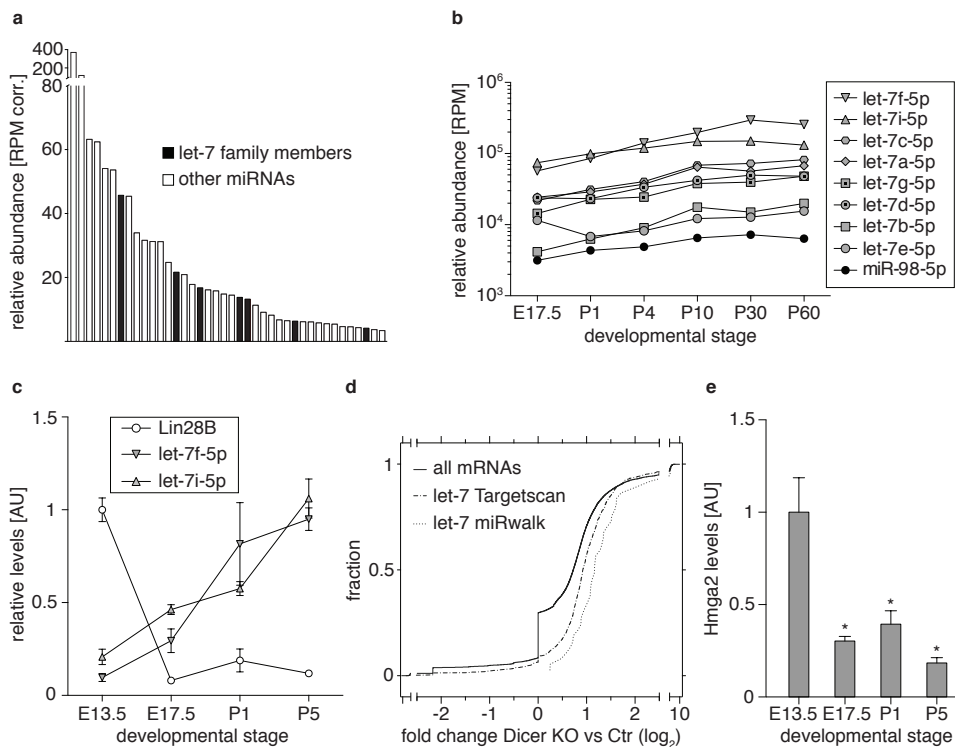
Figure 3.10 | Let-7 miRNAs are highly expressed during myelination and inversely correlated to Lin28B expression. (**a**) Forty most abundant miRNAs in the SN of wild-type mice at P4 corrected for values in SN of P4 mice with SC-specific deletion of Dicer (Dicer KO; see Methods section). (**b**) Levels of abundant let-7 isoforms and the Lin28-dependent miR-98-5p at embryonic day (E) 17.5, P1, P4, P10, P30 and P60 in SN of wild-type mice. (**c**) Levels of Lin28B mRNA and of mature let-7f-5p and let-7i-5p during development in wild-type mice, normalised to GAPDH for Lin28B and to snoRNA-202 for let-7 miRNAs (n = 3). (**d**) Cumulative distribution of differential expression of all mRNAs and predicted let-7 targets in Dicer KO vs. control SN at P1. The rightward shifts in the curves for targets indicate enrichment compared to all mRNAs. (**e**) Hmga2 mRNA levels during SN development (n = 3); n: Number of biological replicates used per condition or time point (**a,b,c,e**); Error bars indicate standard error of the mean (**c,e**); *$P < 0.05$, two-tailed Student's t-test (**e**).
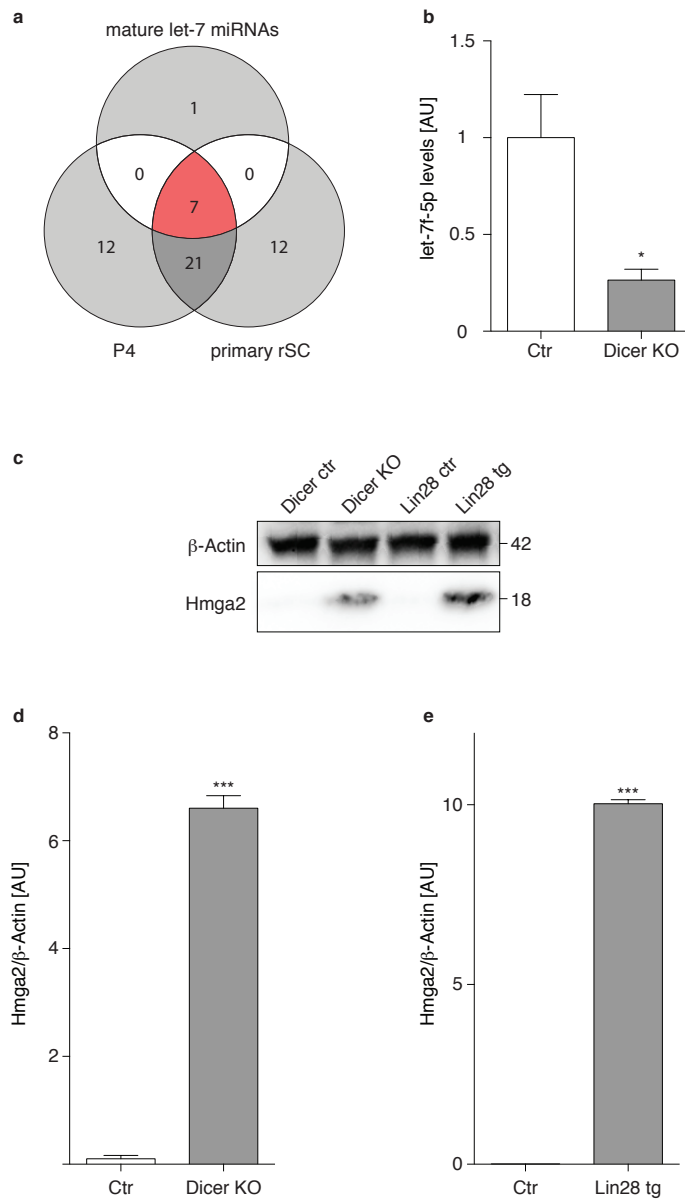
Figure 3.11 | **Small RNA sequencing of differentiated SC and Hmga2 protein expression analysis. (a)** Venn diagram showing the common presence of most let-7 family members (annotated in mm9) among the 40 most enriched miRNAs in P4 wild-type (corrected for P4 Dicer expressed miRNAs) and in differentiated SC. **(b)** Levels of mature let-7f-5p in P4 Dicer KO at P5, normalised to snoRNA-202 (n = 3). **(c)** Immunoblot of Hmga2 from P1 SN of Dicer KO, Lin28 tg and their respective controls. ?-Actin serves as control. **(d,e)** Quantification of protein levels of Hmga2 in Dicer KO and Lin28 tg normalised to β-Actin levels (n = 3); n: Number of biological replicates used per condition. Error bars indicate standard error of the mean. Two-tailed Student's t-test $*P < 0.05$, $**P < 0.01$, $***P < 0.001$ **(b,d,e)**.

calibre (Fig. 3.12f). At P14, SN of Lin28 tg and Dicer KO still had drastic deficits with regard to the onset of myelination (Fig. 3.13m-o). To determine whether the impairments due to sustained Lin28B expression were consistent in other PNS regions, we analysed dorsal (sensory nerve) and ventral (motor nerve) roots of Lin28 tg and Dicer KO mice (Fig. 3.13). Morphological analysis revealed the same defective hallmarks as in SN, confirming the spatiotemporal consistency of the phenotype. To support the morphological observations at the molecular level, we examined expression of marker proteins associated with on-going myelination. Immunoblots of SN lysates from P5 Lin28 tg and Dicer KO revealed strongly decreased levels of Krox20, E-cadherin and MBP compared to controls (Fig. 3.12g; Fig. 3.17a-f). We conclude that sustained Lin28B expression leads to impaired onset of PNS myelination, pointing to a crucial regulatory role of the Lin28B – let-7 pathway in this process.

Given the defects observed in response to sustained Lin28B overexpression, we asked if loss of let-7 miRNAs is the principal reason for the impaired myelination onset by targeting let-7 activity in myelinating ex vivo dorsal root ganglion cultures (DRG explants) using antagomirs [Krutzfeldt et al., 2005]. Strongly diminished myelination was found in such anti-let-7-treated cultures (Fig. 3.15a-g) and similarly observed with DRG explants derived from Lin28 tg cultured under myelination-competent conditions (Fig. 3.14a-i). In vivo, we sought to rescue the myelination deficits in Lin28 tg using the validated let-7S21L chimera that bypasses Lin28 binding and thus allows let-7 maturation despite Lin28 expression [Piskounova et al., 2008]. To achieve this, we generated lentiviral particles encoding let-7S21L followed by injection into neonatal Lin28 tg SN under conditions targeting SCs only (Fig. 3.14j) [Cotter et al., 2010, Ozcelik et al., 2010]. Seven days later, the number of myelinated axons was significantly increased compared to control virus-injected Lin28 tg (Fig. 3.15h-j). Taken together, these results indicate that Lin28B-regulated let-7 isoforms are required for myelination.

Krox20 is the master regulator of PNS myelin gene expression and mice lacking its expression in SCs fail to start myelination, reminiscent of the Lin28 tg phenotype [Ozcelik et al., 2010, Pereira et al., 2012]. Since Krox20 was strongly reduced in Lin28 tg and Dicer KO, we investigated the role of Lin28B and let-7 in the regulation of Nrg1-dependent Krox20 expression. We transfected primary SCs with Lin28B or with let-7 targeting tough decoy expression vectors (let-7 TuD) prior to a 1h Nrg1-stimulation [Haraguchi et al., 2009]. Nrg1-induced Krox20 expression was decreased both in Lin28B- and let-7 TuD-transfected cells (Fig. 3.15k) suggesting that Lin28B-dependent let-7 expression can directly affect Nrg1-induced Krox20 expression. To express Krox20 and to start myelination, SCs need to shift their balance of negative to positive regulators of myelination [Pereira et al., 2012]. We hypothesised that let-7 isoforms might promote this shift by down-regulating negative regulators of myelination. To obtain an unbiased collection of possible candidate targets, we compared P1 SN of Lin28 tg, Dicer KO and controls by RNA sequencing. A MetaCore™ pathway analysis of transcripts that were upregulated in both mutants and carrying predicted let-7 sites in their 3′-UTRs, identified Notch signalling as the most affected pathway. We found significantly increased RNA reads for Jag1, Notch1, Hes1, Hey1, Hey2, Tle3 and Tle4 in Lin28 tg and Dicer KO (Fig. 3.16a). Quantitative RT-PCR measurements confirmed increased Notch1 ex-
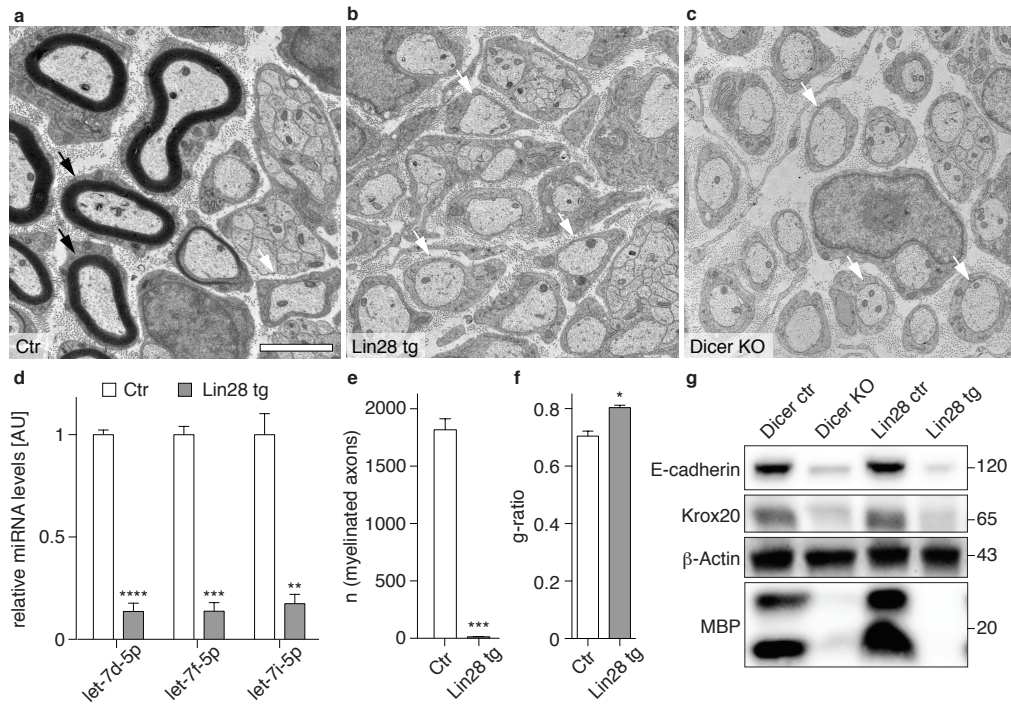
Figure 3.12 | Sustained expression of Lin28B in SC causes impaired onset of myelination. (**a-c**) Electron micrographs of SN of Ctr, Lin28 tg and Dicer KO at P5. Examples of myelinated axons (black arrows) and 1:1 SC-axon relations (white arrows) are highlighted. (**d**) Levels of mature let-7f-5p, let-7i-5p and let-7d-5p in SN of Ctr and Lin28 tg at P14, normalised to snoRNA-202 (n = 3). (**e,f**) Quantification of myelinated axons per cross-sections (**e**) and g-ratios (ratio of the inner axonal diameter to the total outer nerve fibre diameter) (**f**), determined on SN electron micrographs at P5 (n = 3). (**g**) Immunoblots of E-cadherin, Krox20, MBP and β-Actin as control, from P5 SN of Lin28 tg, Dicer KO and their respective controls. Numbers refer to molecular weight [kDa]. For quantifications of three biological replicates, see Fig. 3.17a-f; n: Number of biological replicates used per condition (**d-f**); Scale bar equals 2 µm (**a-c**); Error bars indicate standard error of the mean; Two-tailed Student's t-test *$P < 0.05$, **$P < 0.01$, ***$P < 0.001$, ****$P < 0.0001$ (**d-f**).
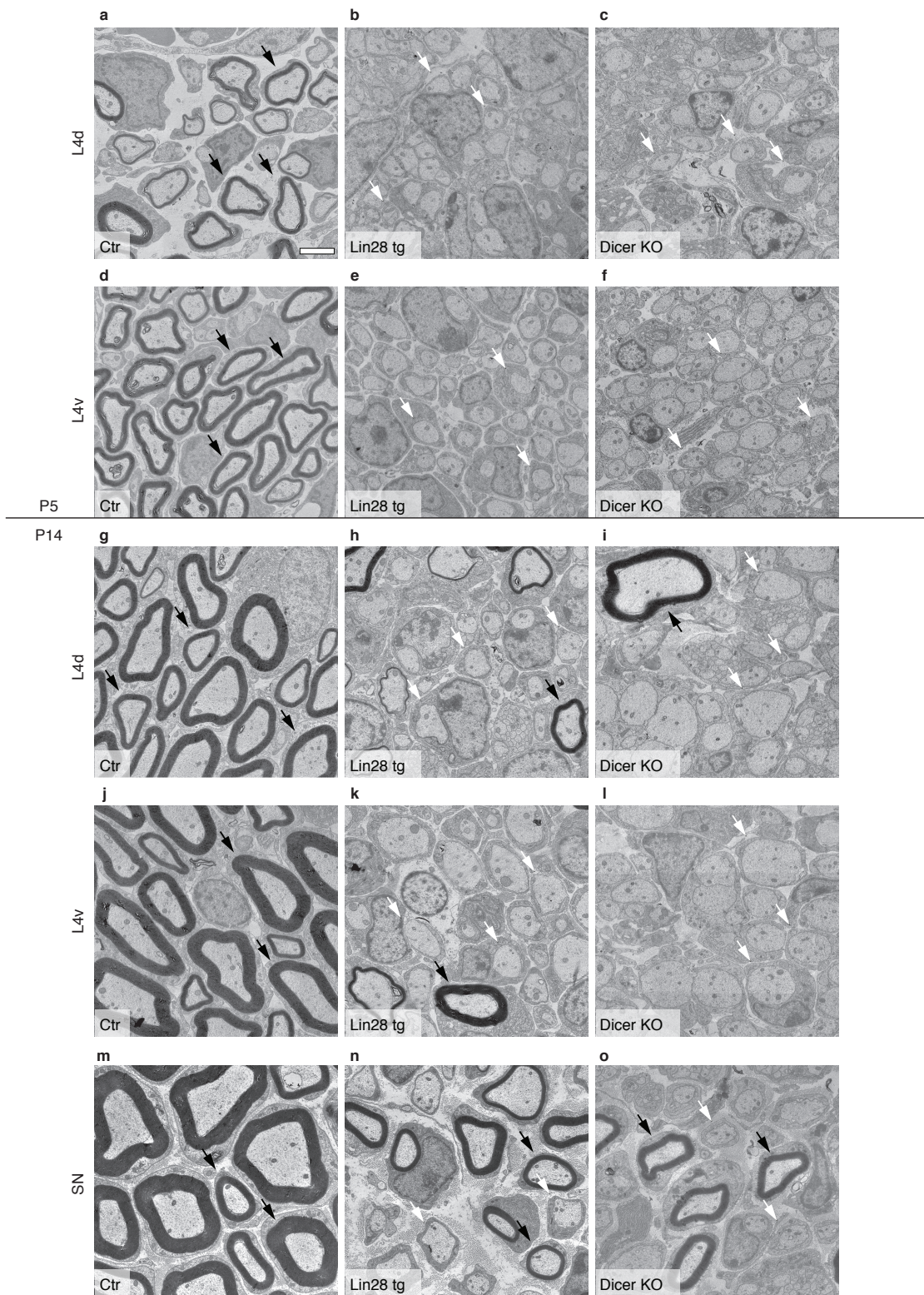
pression in both mutants (Fig. 3.16b,c). Next, we assessed Notch pathway activity in SN of Lin28 tg and Dicer KO by measuring protein levels of the intracellular domain of Notch1 (NICD) and its downstream target, Hes1. Both were increased compared to controls (Fig. 3.16d; Fig. 3.17g-j). These results identify let-7 as a critical regulator of the Notch pathway during myelination.

Notch1 is a well-known negative regulator of myelination. Sustained Notch1 expression interferes with PNS myelination by opposing the forward driver Krox20 [Woodhoo et al., 2009]. Thus, we further investigated the interplay between let-7 and the Notch pathway. To test if aberrantly increased Notch signalling interferes with myelination in Lin28 tg, we aimed at rescuing myelination in Lin28 tg with the Notch signalling inhibitor LY411575, a γ-secretase blocker. Consistent with our hypothesis, treatment with LY411575 caused a prominent increase in the number of myelinated axons (Fig. 3.18a-c). Furthermore, LY411575 treatment prevented the decrease of Krox20 expression in primary SCs expressing let-7-TuD (Fig. 3.18d). To examine if Notch1 levels are dependent on let-7, we analysed Notch1 expression in differentiated cells of the SC precursor line SpL201, 48h after transfection with Lin28 or treatment with anti-let-7 antagomirs. Both conditions led to increased Notch1 levels compared to controls (Fig. 3.18e). These combined results concord with our in vivo observations, and suggest that let-7 isoforms positively affect Krox20 expression by downregulating Notch1 expression. To address if this regulation occurs directly through let-7 binding, we searched for predicted let-7 seed matches in the Notch1 3′-UTR. In silico analysis revealed multiple conserved seed matches (Fig. 3.18f,g; Fig. 3.19). To biochemically validate these seed matches as *bona fide* let-7 target sites, the Notch1 3′-UTR was cloned into a luciferase reporter construct and luciferase activity was assayed in the presence or absence of let-7 mimics after transfection of primary SCs. Let-7 mimics caused decreased luciferase activity compared to scrambled controls or the empty vector (Fig. 3.18h,i). We conclude that let-7 isoforms promote Krox20 expression at least partly via targeting the Notch1 3′-UTR and suppression of Notch signalling in SCs.

In our studies, we have discovered a hitherto unknown, physiologically critical function of the Lin28 - let-7 pathway during terminal cell differentiation. First, we identified let-7 isoforms as the main class of regulatory miRNAs that promote PNS myelination. Through targeting and reducing Notch signalling, let-7 miRNAs inhibit a central pathway opposing myelination. Second, we found that Lin28B is a fundamental negative regulator of PNS myelination since Lin28B repression is necessary to enable let-7 biogenesis. Based on these findings, we propose a model in which Lin28B repression and concomitant let-7 induction drives myelination through inhibition of the Notch pathway (Fig. 3.18j).

Figure 3.13 *(preceding page)* | Morphological analysis of Lin28 tg at P5 and P14. (**a-f**) Electron micrographs of Lin28 tg, Dicer KO and controls from dorsal (L4d, **a-c**) and ventral (L4v, **d-f**) lumbar 4 roots at P5. (**g-o**) Electron micrographs of Lin28 tg, Dicer KO and controls at P14 from L4d (**g-i**), L4v (**j-l**) and SN (**m-o**); Myelinated axons (black arrows) and axons at the pro-myelinating stage (white arrows) are highlighted. Images are representatives from at least three biological replicates. Scale bar equals 2 μm (**a-o**).
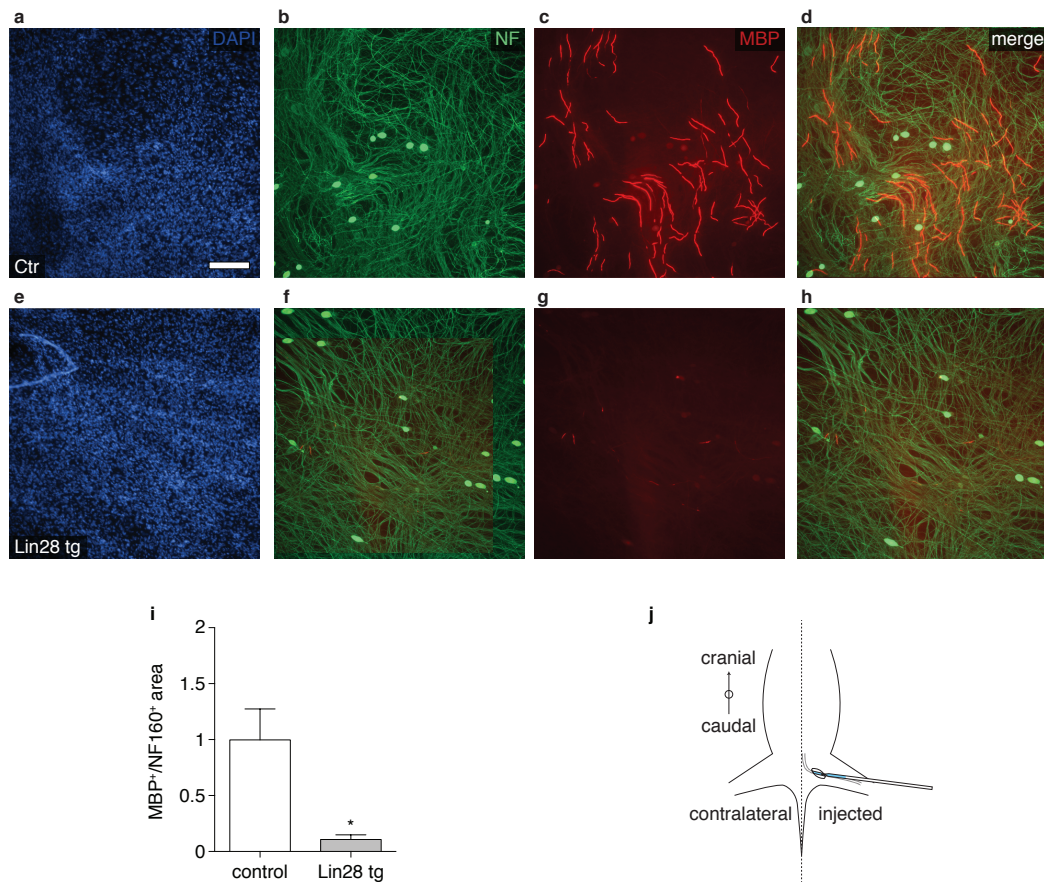
Figure 3.14 | Myelination is suppressed in Lin28 tg DRG explant cultures. (**a-h**) DRG explants from Lin28 tg and controls immunostained for NF (green) and MBP (red). Nuclei were stained with DAPI (blue). (**i**) Quantification of MBP+ area in Lin28 tg and controls after normalisation to NF+ area (n = 3). (**j**) Scheme of injection of lentivirus into SN; Scale bar equals 200 µm (**a-h**); n: Number of biological replicates used per condition. Error bars indicate standard error of the mean. Two-tailed Student's t-test *$P < 0.05$ (**i**).
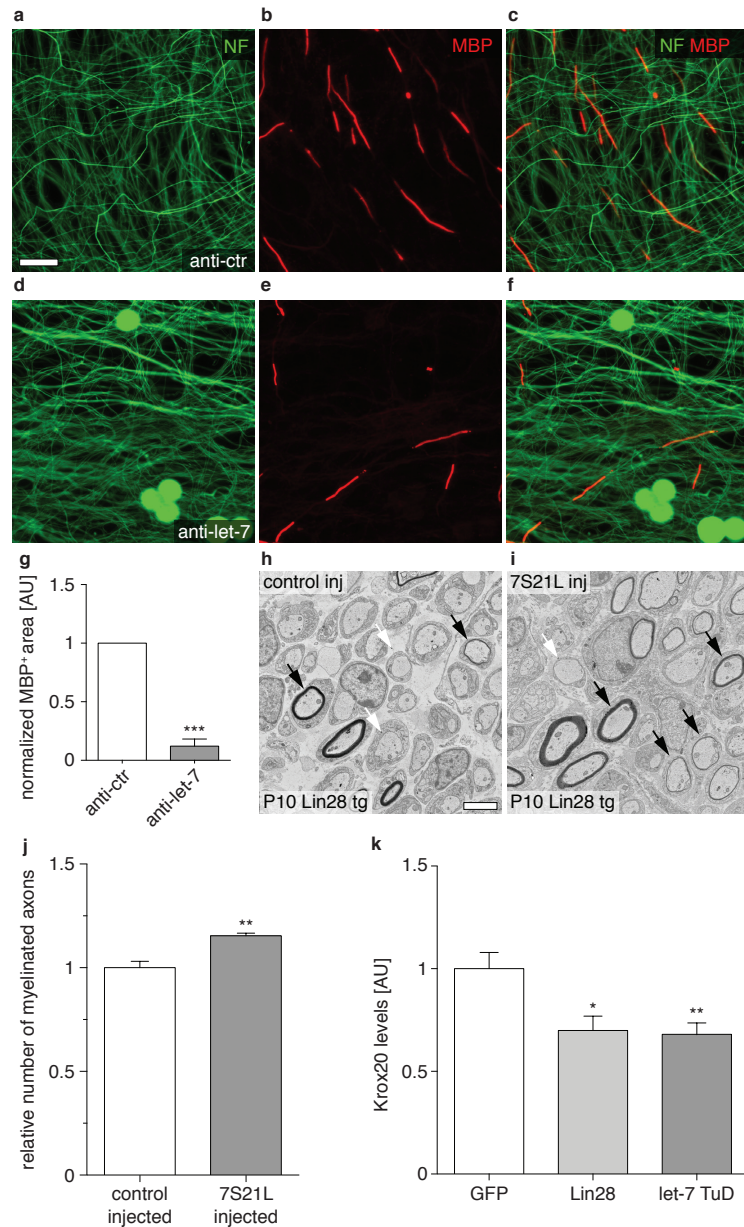
Figure 3.15 | Lin28B-dependent let-7 miRNAs are necessary for myelination and appropriate Krox20 expression. (**a-f**) Immunostainings for neurofilament (NF; green) and MBP (red) of wild-type DRG explants treated with anti-let-7 or control antagomir (anti-ctr), prior to induction of myelination (n = 3). (**g**) Quantification of MBP-positive area normalised to the NF-positive area. For individual embryonal culture, anti-ctr values were set to 1. (**h,i**) Electron micrographs of SN of Lin28 tg mice at P10, 7 days after injection with lentivirus expressing let-7S21L (7S21L inj) or control virus (control inj). Examples of myelinated axons (black arrows) and axons at the pro-myelinating stage (white arrows) are highlighted. (**j**) Quantification of the number of myelinated axons in 7S21L (n = 4) or control injected (n = 3) SN, normalised to the number in the respective contralateral nerve. (**k**) Levels of Krox20 mRNA in primary SC, induced for 1 h with Nrg1 48 h after transfection with Lin28, let-7 TuD, or GFP-expressing vector; Scale bars equal 50 µm (**a-f**) and 3 µm (**h,i**); two-tailed Student's t-test *$P < 0.05$, **$P < 0.01$; n: Number of biological replicates per condition; error bars indicate standard error of the mean (**g,j,k**).
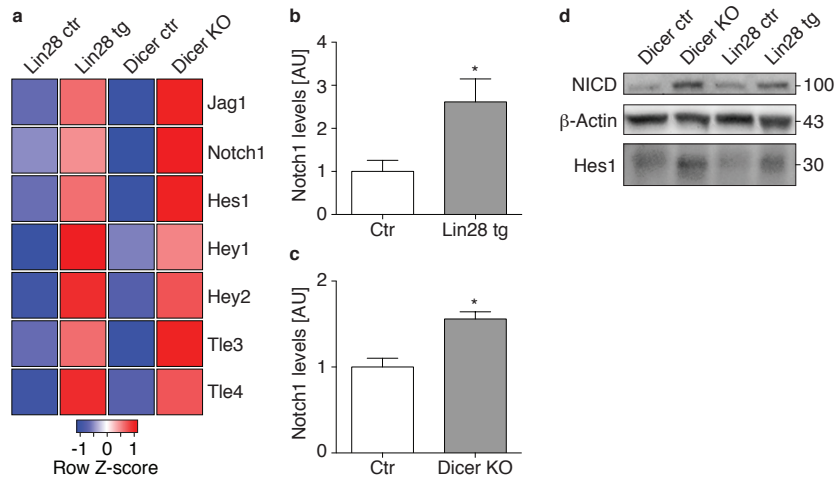
Figure 3.16 | The myelination-inhibiting Notch pathway is hyperactive in Lin28 tg and Dicer KO. (**a**) Heatmap representation of significantly ($P < 0.05$) regulated Notch pathway members in sequencing data from P1 Lin28 tg and Dicer KO versus control SN (n = 3). Colour intensities represent the Z-score for each row, red indicating upregulation and blue indicating downregulation. (**b,c**) Levels of Notch1 mRNA in SN of Lin28 tg (**b**) and in Dicer KO (**c**) at P5 (n = 3). (**d**) Immunoblots of NICD, Hes1, and β-Actin as a control, from P5 SN of Lin28 tg, Dicer KO and their respective controls. Numbers refer to molecular weight [kDa]. For quantification of 3 biological replicates, see Fig. 3.17g-j; n: Number of biological replicates. Error bars indicate standard error of the mean. Two-tailed Student's t-test *$P <$ 0.05 (**b,c**).

Our data show that Lin28B is developmentally repressed prior to the onset of myelination and that its sustained expression impairs the timely onset of myelination. The decline in Lin28B levels and concomitant induction of let-7 accumulation are in agreement with findings in other cellular systems showing that let-7 miRNAs are associated with more differentiated states, while Lin28 supports the maintenance of undifferentiated states [Thornton and Gregory, 2012]. Lin28B is itself a target of let-7 and this may partially explain the reduction of Lin28B expression during early Schwann cell development. Furthermore, Sox2 is an important regulator of glial lineage identity and is repressed prior to myelination [Le et al., 2005, Adameyko et al., 2012]. Since Sox2 promotes Lin28 expression in embryonic stem cells (ESCs) and neural progenitors [Cimadamore et al., 2013, Marson et al., 2008] Sox2 reduction might also contribute to the reduced Lin28B expression during Schwann cell lineage progression. In ESCs, Lin28 is part of the Sox2-Nanog-Oct4-Tcf3 network, which maintains ESCs in their pluripotent state while priming them for rapid let-7-mediated differentiation [Marson et al., 2008]. Whether a related concept applies to the regulation of nerve-associated Schwann cell precursors that can still give rise to multiple non-Schwann cell types, including skin melanocytes, odontoblasts, and parasympathetic neurons, remains to be elucidated [Adameyko et al., 2009, Dyachuk et al., 2014, Espinosa-Medina et al., 2014, Kaukua et al., 2014].
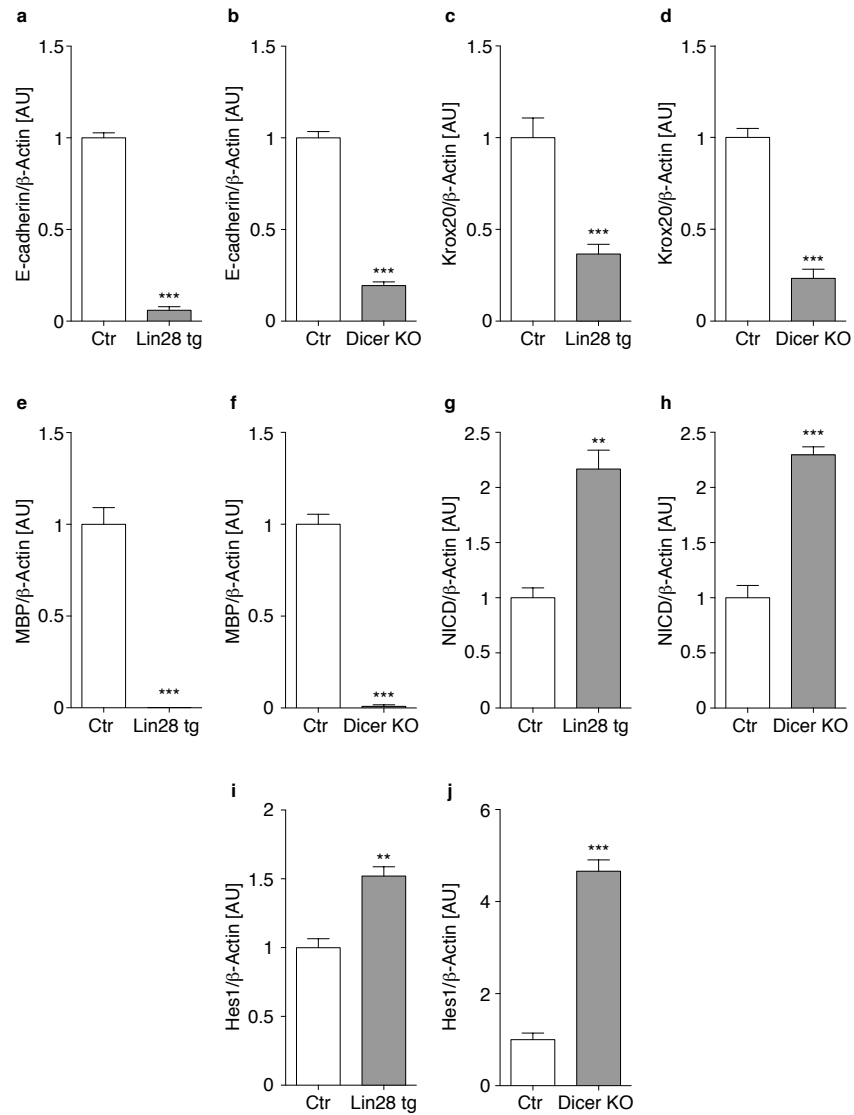
Figure 3.17 | Quantification of immunoblots. (**a-j**) Quantification of protein levels of E-cadherin in Lin28 tg and Dicer KO (**a,b**), Krox20 in Lin28 tg and Dicer KO (**c,d**), MBP in Lin28 tg and Dicer KO (**e,f**), NICD in Lin28 tg and Dicer KO (**g,h**) and Hes1 in Lin28 tg and Dicer KO (**i,j**); all levels were normalised to β-Actin levels. Three biological replicates were used for each condition. Error bars indicate standard error of the mean. Two-tailed Student's t-test *$P < 0.05$, **$P < 0.01$, ***$P < 0.001$ (**a-j**).
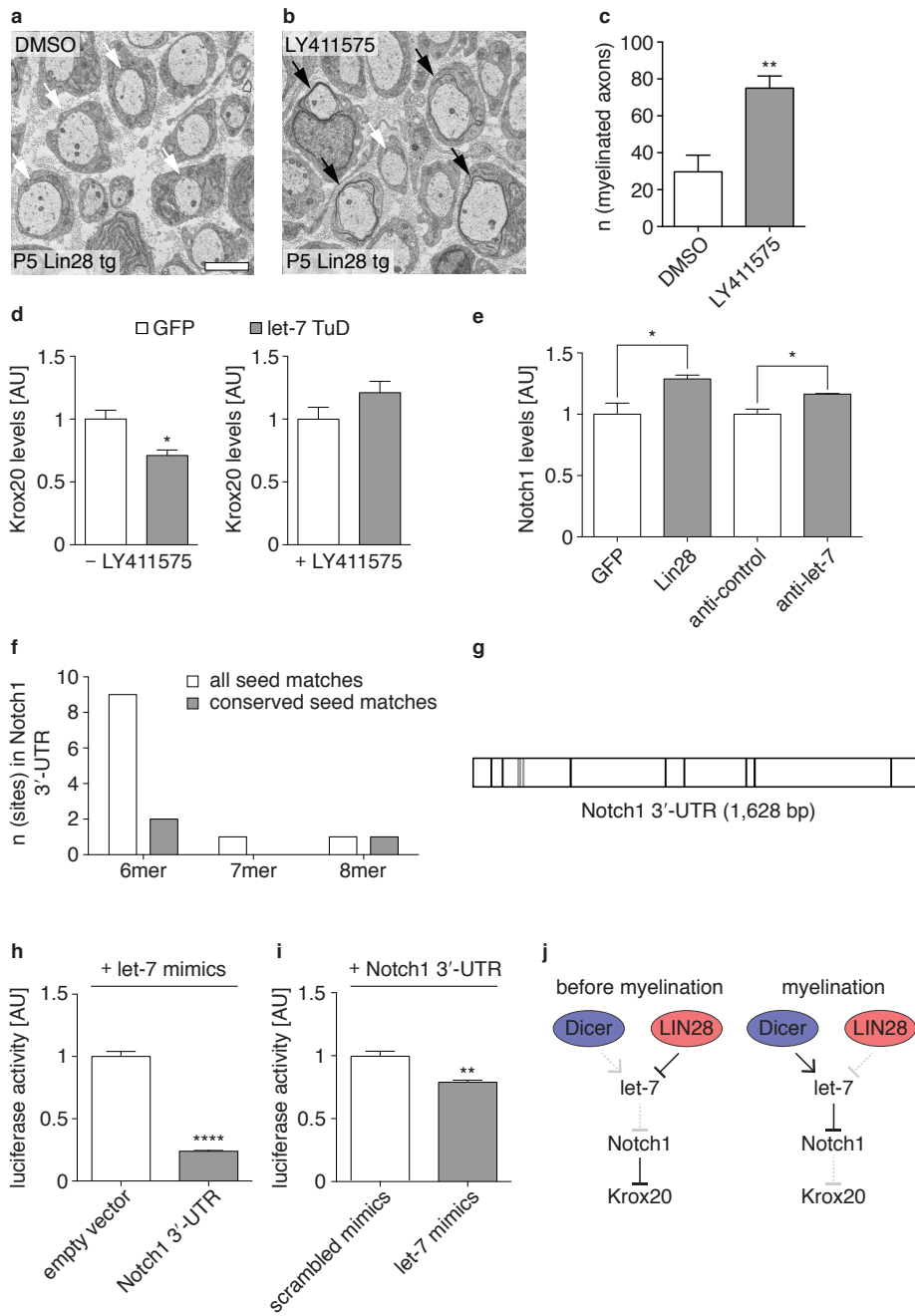
Sustained Lin28B expression caused a major arrest of the axon-Schwann cell unit at the promyelinating stage. The severity of the phenotype indicates a function of Lin28B as a negative regulator of PNS myelination, consistent with established criteria [Jessen and Mirsky, 2008]. These include expression before myelination and inactivation upon myelination. Furthermore, Lin28B opposes signals promoting myelination by negatively affecting let-7-mediated Notch pathway repression.

With the identification of the promoting function of let-7 in myelination, we follow up on findings demonstrating that global loss of Dicer-mediated miRNA biogenesis in SCs impairs myelination [Pereira et al., 2010, Bremer et al., 2010, Yun et al., 2010, Verrier et al., 2010]. The strong similarities of Lin28 tg and Dicer KO support a common regulatory defect, which we can now ascribe mainly to the loss of let-7 isoforms and the consequent ectopic expression of their targets. Furthermore, we have shown that let-7 miRNAs are necessary for myelination in DRG explants and in Lin28 tg. Nevertheless, we cannot fully exclude a contribution of let-7-independent functions of Lin28B in its role as a negative regulator of myelination.

Our studies revealed that targeting and downregulation of Notch signalling by let-7 contributes to the onset of myelination, based on the fact that Notch1 is known to prevent the timely onset of myelination by opposing Krox20 activation [Woodhoo et al., 2009]. Given the involvement of Notch signalling in many other aspects of metazoan development and disease, these findings warrant further studies of the relationship between Notch signalling and the antagonising role of let-7 in other systems. Likewise, potential functions of the Lin28 – let-7 regulatory axis during remyelination, after injury or in demyelinating diseases, also merit further investigations, particularly in the prospect of exploring novel therapeutic approaches for demyelinating diseases.

Figure 3.18 *(preceding page)* | Suppression of Notch1 by let-7 promotes myelination through Krox20 expression. (**a,b**) Electron micrographs of SN of Lin28 tg mice harvested at P5 after in situ injection of the Notch signalling inhibitor LY411575 or the solvent DMSO at P3 and P4. Myelinated axons (black arrows) and axons at the pro-myelinating stage (white arrows) are highlighted. (**c**) Quantification of the number of myelinated axons in LY411575- or DMSO-treated Lin28 tg per cross-section (n = 3). (**d**) Krox20 mRNA levels in primary SCs transduced with GFP or let-7 TuD-expressing lentivirus prior to 1 h of Nrg1 stimulation, with or without the prior application of 10 µM LY411575 (n = 3). (**e**) Notch1 mRNA levels 48 h after transfection of SpL201 cells with GFP or Lin28 expression vectors, or after application of control antagomir (anti-control) or let-7f antagomir (anti-let-7) (n = 3). (**f**) Number of predicted seed matches in the Notch1 3′-UTR and the fraction of those conserved among vertebrates. (**g**) Schematic representation of Notch1 3′-UTR containing all predicted seed matches. Conserved seed sequences are indicated in grey. (**h**) Luciferase activity of primary SC lysates, transfected 48h before with let-7 mimics and empty pmirGLO, or pmirGLO harbouring the Notch1 3′-UTR (n = 3). (**i**) Luciferase activity of primary SC lysates transfected 48 h earlier with pmirGLO harbouring the Notch1 3′-UTR, in the presence of scrambled or let-7 mimics (n = 3). (**j**) Schematic model summarising the role of the Lin28B – let-7 axis in myelination. Solid lines indicate active mechanisms and dotted lines indicate inactive mechanisms; Scale bar equals 2 µm (**a,b**); n: Number of biological replicates used per condition. Error bars indicate standard error of the mean. Two-tailed Student's t-test *$P < 0.05$, **$P < 0.01$, ***$P < 0.001$, ****$P < 0.0001$ (**c,d,e,g,h,i**).
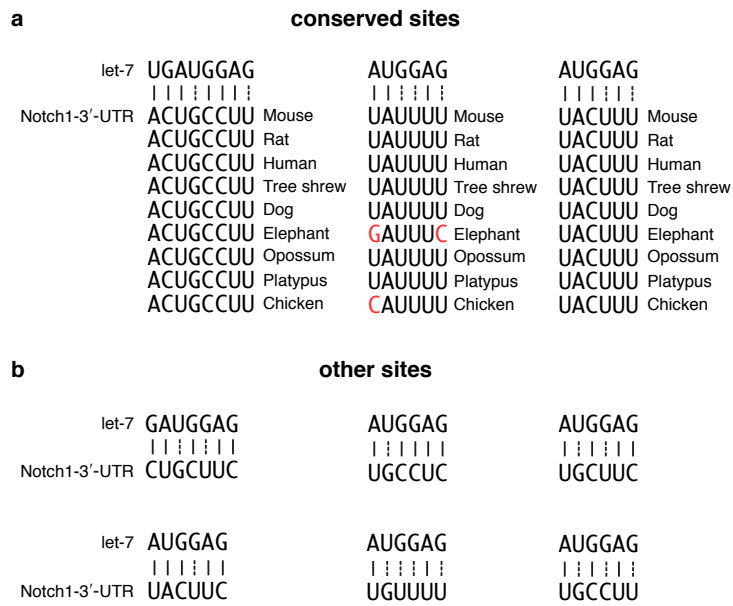
a   **conserved sites**

let-7	UGAUGGAG		AUGGAG		AUGGAG	
	∣∣∣∶∣∣∣∣		∣∣∣∶∣∣		∣∣∣∣∣	
Notch1-3′-UTR	ACUGCCUU	Mouse	UAUUUU	Mouse	UACUUU	Mouse
	ACUGCCUU	Rat	UAUUUU	Rat	UACUUU	Rat
	ACUGCCUU	Human	UAUUUU	Human	UACUUU	Human
	ACUGCCUU	Tree shrew	UAUUUU	Tree shrew	UACUUU	Tree shrew
	ACUGCCUU	Dog	UAUUUU	Dog	UACUUU	Dog
	ACUGCCUU	Elephant	GAUUUC	Elephant	UACUUU	Elephant
	ACUGCCUU	Opossum	UAUUUU	Opossum	UACUUU	Opossum
	ACUGCCUU	Platypus	UAUUUU	Platypus	UACUUU	Platypus
	ACUGCCUU	Chicken	CAUUUU	Chicken	UACUUU	Chicken

b   **other sites**

let-7	GAUGGAG	AUGGAG	AUGGAG
	∣∣∣∶∣∣∣	∣∶∣∣∣∣	∣∣∣∶∣∣
Notch1-3′-UTR	CUGCUUC	UGCCUC	UGCUUC

let-7	AUGGAG	AUGGAG	AUGGAG
	∣∣∣∣∶∣	∣∶∣∣∣∣	∣∣∣∣∶∣
Notch1-3′-UTR	UACUUC	UGUUUU	UGCCUU

Figure 3.19 | Seed matches of let-7 miRNAs in the 3′-UTR of Notch1. (**a,b**) Conserved (**a**) and unconserved (**b**) seed matches within the 3′-UTR of Notch1 predicted with RNAhybrid are shown in 5′-3′ direction. Each corresponding let-7 seed is shown in 3′-5′ direction. Unconserved nucleotides are highlighted in red. Watson-Crick base pairs are indicated by solid lines and Wobble base pairs are indicated by dashed lines.

4 Future Perspectives

The results in this thesis highlight multifaceted functions of the miRNA pathway during myelination. First, during a precise time window of radial sorting the microprocessor members DGCR8 and Drosha are necessary to protect SC survival by suppressing Shh signalling. Second, let-7 miRNAs promote the onset of myelination by suppressing Notch signalling (Fig. 4.1).
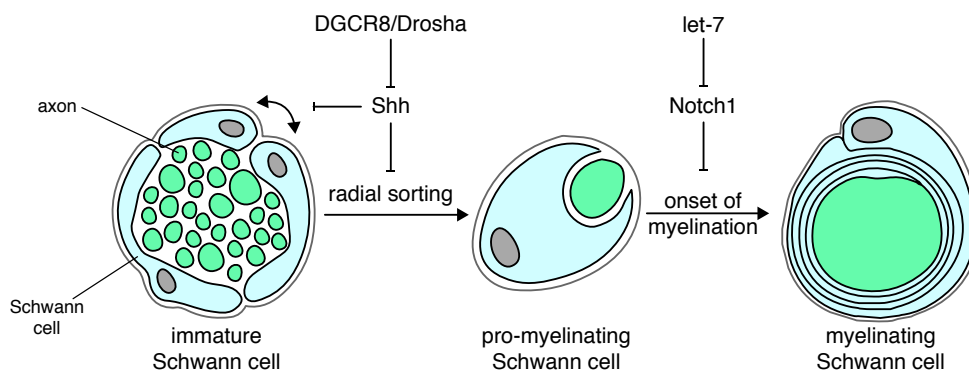

Figure 4.1 | Model of RNA interference-based regulation of myelination based on the obtained results in this thesis. The microprocessor members DGCR8 and Drosha protect SC survival during radial sorting by suppressing Shh signalling. Later in development let-7 miRNAs promote the onset of myelination by suppressing Notch signalling.

4.1 Non-canonical functions of the microprocessor

We found astrocytes and myelinating oligodendrocytes in the PNS roots of DGCR8 KO, suggesting an impairment of the CNS/PNS boundary (see 3.1, Fig. 3.2). The mechanisms underlying the formation of the CNS/PNS boundaries are not fully understood. It was shown that the absence of SCs could lead to an infiltration of oligodendrocytes into the PNS [Kucenas et al., 2009]. Furthermore transcription factor Sox10 is important in establishing the integrity of the boundary [Frob et al., 2012]. Besides its involvement in the death of SCs in DGCR8 mutants non-canonical functions of the microprocessor could also account for the impaired integrity of the boundary in another way, possibly by interfering with the function of Sox10. Future projects should address molecular players in SCs that promote the formation of the CNS/PNS boundary, including pathways downstream and upstream from Sox10. The next step would be to address whether direct post-transcriptional regulation by the microprocessor could influence these pathways.

The Shh pathway has crucial functions during embryonic development. Shh is silenced in SCs and other cell types upon terminal differentiation [Amakye et al., 2013]. The mechanisms underlying the suppression of this signalling axis remain largely unknown. Our results indicate a miRNA-independent and microprocessor-dependent mechanism of Shh repression in SCs during radial sorting (see 3.1). Whether this repression is due to direct processing of Shh mRNA by the microprocessor is not clear at this stage. Preliminary results have shown that Shh mRNA could be co-immunoprecipitated from lysates of adrenal glands, a tissue with high levels of Shh, using antibodies against DGCR8 (data not shown). Furthermore, published data obtained from DGCR8 cross-linked immunoprecipitation experiments in HEK cells could show Shh among potential mRNA substrates together with predicted hairpin structures within the precipitated region [Macias et al., 2012]. Further biochemical studies are necessary to test if direct binding and cutting of Shh mRNA by the microprocessor is the mechanism underlying Shh repression in SCs. Similar to the approaches used to validate binding of the microprocessor to neurogenin 2 [Knuckles et al., 2012], cells expressing Shh could be transiently transfected with FLAG-tagged Dgcr8 followed by co-immunoprecipitation of DGCR8 and interacting RNAs. Additionally, previously described *in vitro* processing assays [Han et al., 2009] could be used to validate the processing of potential substrate hairpin structures within the Shh mRNA.

The microprocessor was also shown to associate with certain loci in HeLa and suppress their transcription through induction of Pol II pausing [Wagschal et al., 2012]. Although in this study the *Shh* locus could not be identified among the microprocessor-interacting gene loci, a similar chromatin immunoprecipitation experiment could be performed in cultured SCs to validate possible additional interacting loci in SCs.

To address if microprocessor-dependent suppression of Shh could be a general way to achieve silencing of this embryonal pathway, this mechanism has to be further validated in other systems of terminal differentiation. It would make biological sense that various terminally differentiated cell types could access global mechanisms like microprocessor-mediated mRNA degradation to suppress certain loci that are associated with earlier developmental stages.

An additional explanation for the elevated Shh levels observed in DGCR8 KO (see 3.1) may be that it is due to active Wnt/β-catenin signalling. We could observe a significant increase in the protein levels of active β-catenin (ABC) exclusively in SNs of DGCR8 KO but not in Dicer KO (data not shown). ABC has been shown to induce apoptosis in SCs at a specific time frame during early events of radial sorting [Jacob et al., 2011]. However, the mechanisms by which ABC promotes apoptosis in SCs are not clear. During hair follicle morphogenesis, it was shown that both ABC and Shh are indispensable [Roop and Toftgard, 2008]. In fact, Shh is a target gene of ABC in this scenario [Gat et al., 1998, Lo Celso et al., 2004], which could also be the case in SCs. Preliminary results from DGCR8 co-immunoprecipitation experiments also suggest that Wnt mRNAs are interacting directly with DGCR8 (data not shown). An alternative mechanism of Wnt pathway regulation by the microprocessor could be through its interaction with certain gene loci. In fact the study reporting this additional microprocessor function identified several loci corresponding to Wnt ligands directly interacting with

Drosha [Wagschal et al., 2012]. Whether this is also true in SCs remains to be investigated. Therefore future studies should address whether DGCR8 can directly suppress Wnt expression and thereby, via ABC, can inhibit Shh-mediated SC apoptosis.

The detailed mechanism by which the microprocessor regulates non-miRNA substrates is still largely unclear. These substrates are predicted to have a pri-miRNA-like hairpin encoded within their primary structure, allowing them to be recognised by the microprocessor [Macias et al., 2013]. Binding by the microprocessor is then assumed to be followed by the degradation of the substrate [Ha and Kim, 2014]. Future studies need to address, the full set of core structural elements needed for microprocessor recognition, and whether degradation is a general outcome of microprocessor-substrate-assembly or if other consequences are possible such as subcellular sequestration of the substrate. In addition the nature of the degradation machinery involved in these processes needs to be characterised, including interacting protein partners, as well as the spatiotemporal resolution of the processing.

Loss of Dicer in SCs and therefore of canonical miRNAs leads only to very mild impairments during remyelination after injury [Viader et al., 2011]. It remains to be elucidated whether miRNA-independent functions of the microprocessor play a relevant role in this regeneration setting. Similar to the approach taken to analyse development (see 3.1), a side-by-side comparison of DGCR8- and Dicer mutants during injury and myelin maintenance would be appropriate to identify possible additional non-canonical functions of the microprocessor in the regulation of myelination. These functions could also include regulation of Shh by the microprocessor. The fact that Shh is expressed during injury [Hashimoto et al., 2008] suggests the presence of molecular mechanisms that protect Shh from suppression by the microprocessor under certain physiological conditions. Such mechanisms remain unexplored and largely depend on the outcome of the primary analysis of DGCR8 mutants during PNS injury and myelin maintenance. Such studies would widen our understanding of the specific regulatory mechanisms underlying developmental myelination and myelination after injury.

In oligodendrocytes miRNAs were also shown to be crucial for myelination [Zhao et al., 2010], but a regulatory role of the microprocessor beyond miRNAs has not been addressed. Based on our findings in the PNS there is a chance that the microprocessor has non-canonical functions also during myelination in the CNS. Therefore a similar side-by-side comparison of DGCR8- and Dicer mutant mice (see 3.1) in various regions of the CNS should be conducted. Should those studies reveal an aggravated phenotype of DGCR8 mutant mice, a transcriptomics approach similar to that used in this thesis (see 2.2.13) could be applied to pinpoint regulatory candidates causing the defects. It would be interesting to address whether Shh emerges as a suitable candidate. It was shown that Shh is necessary for the formation of early oligodendrocyte precursors [Rowitch and Kriegstein, 2010]; however, its role during developmental CNS myelination is not clear. Such studies would contribute to our understanding of the molecular mechanisms underlying CNS myelination and could reveal additional therapeutic targets for the treatment of demyelinating neuropathies in the CNS.

4.2 Lin28/let-7 in disease mechanisms

Many diseases including cancers involve miRNAs in particular also the Lin28/let-7 axis [Thornton and Gregory, 2012]. In 15% of all cancers analysed, Lin28 serves as an oncogene by suppressing let-7 [Viswanathan et al., 2009]. For instance, the prominent oncogene Myc is a known let-7 target and therefore can be activated by Lin28 [Thornton and Gregory, 2012]. The pathological role of Notch1 as an effector of the loss of let-7 should be addressed in these Lin28-expressing cancers, which could possibly reveal new venues for therapeutic purposes. It would also be worthwhile to investigate whether Lin28/let-7 is similarly involved in the disease mechanisms of SC-based diseases such as demyelinating neuropathies or gliomas. In gliomas, elevated Notch1 levels were identified as a prognostic factor for decreased survival of glioma patients [Engh, 2011]. Based on the mechanistic link highlighted in this thesis (see 3.2), a correlation of Notch1 and Lin28 expression should be addressed in glioma patients, as the knowledge to be gained has the potential to generate new therapeutic approaches or refine currently existing ones. Whether the levels of Lin28 or Notch1 are also elevated in certain demyelinating neuropathies is not known and should be addressed in such patients. Enforced SC-specific Notch1 expression in adult peripheral nerves has been shown to induce demyelination in mice [Woodhoo et al., 2009]. Whether this is also the case for enforced Lin28 expression and whether their actions are mechanistically linked remains to be addressed by similar approaches. SC-specific inducible transgenic NICD- [Woodhoo et al., 2009] and Lin28-expressing mice (see 2.2.9) could be generated by crossing each of them with mice expressing tamoxifen-inducible Cre under the control of the P0-Cx32 promoter [Leone et al., 2003]. After inducing these mice with tamoxifen during adulthood, possible mechanistic links between both phenotypes could be addressed in a side-by-side comparison. Such studies could contribute to our understanding of molecular mechanisms leading to demyelination and could reveal novel therapeutic targets for the treatment of demyelinating neuropathies.

The instructive role of let-7 miRNAs towards myelination demonstrated in this thesis also motivates the investigation of their potential as drugs to treat demyelinating neuropathies (see 3.2). In this context, let-7 mimic approaches [Zhang et al., 2013] could be used in disease models for SC-dependent demyelinating neuropathies. Such studies could begin with highly invasive approaches to deliver let-7, for example using lentiviral injections into the SN (see 2.2.8) to prove the concept, and then later use state-of-the-art mimic approaches that allow mimics to pass the blood-nerve barrier. Polyethyleneimine- or mesenchymal stem cell-based systems have been previously used successfully to deliver miRNA mimics to the nervous system [Zhang et al., 2013, Lee et al., 2013], and could also be tested in peripheral nerves. Promising approaches then could be considered for the use in clinical trials.

4.3 Lin28/let-7 in physiology

Although miR-219 and miR-338 were implicated in the promotion of oligodendrocyte differentiation [Zhao et al., 2010], a possible contribution of let-7 cannot be fully excluded. Strategies to genetically ablate miR-219 and/or miR-338 in oligodendrocytes and a comparison to the phenotype of Dicer-depleted oligodendrocytes would help to judge if miR-219 and miR-338 are the major physiologically relevant miRNAs in CNS myelination. Furthermore a small RNA sequencing approach comparing Dicer-depleted oligodendrocytes with controls could improve the accuracy and coverage of relevant oligodendrocyte-expressed miRNAs. Given the inhibitory function of Notch1 on CNS myelination [Zhang et al., 2009], a Lin28/let-7-mediated mechanism regulating Notch1 expression similar to that presented in this thesis in SCs (see 3.2) could be possible, and should be investigated in additional experiments.

The results presented in this thesis show a suppression of Notch1 by let-7 through targeting of the 3′-UTR which is necessary for myelination (see 3.2, Fig. 3.18). This targeting is likely occuring through non-canonical sites either involving G·U Wobble pairs as the predicted sites suggest or through other unpredicted non-canonical sites [Vo et al., 2010, Didiano and Hobert, 2006, Chi et al., 2012, Tay et al., 2008, Brennecke et al., 2005, Vella et al., 2004, Shin et al., 2010, Lal et al., 2009, Lu et al., 2010]. The physiological relevant binding sites among the predicted ones were not validated so far. Future studies should address this through mutating individual predicted sites and analysing the targeting by let-7 through luciferase assays. As 6mers in general do not efficiently induce target repression, the 8mer should be prioritised in this analysis. To identify possible unpredicted non-canonical sites, highly conserved areas of the Notch1-3′-UTR with partial complementarity to let-7 could be analysed by mutation in similar luciferase experiments. Ultimately photoactivatable-ribonucleoside-enhanced crosslinking and immunoprecipitation (PAR-CLIP) could be employed to identify AGO-bound let-7 targets in primary SCs. As we still cannot completely rule out an indirect mechanism of Notch1 regulation by let-7 through an intermediate factor, future studies should also take into account other let-7 targets that in turn are capable of directly regulating Notch1 expression.

We and others have shown that let-7 represses targets that are associated with earlier developmental stages [Thornton and Gregory, 2012]. During PNS injury Notch1 and other markers of dedifferentiation are re-expressed [Woodhoo et al., 2009, Pereira et al., 2012]. It remains to be elucidated if expression of Lin28 and consequently the suppression of let-7 contributes to dedifferentiation in SCs. As a first approach the differential expression of Lin28 and let-7 in injured vs. non-injured wild-type mice should be evaluated. Depending on the results, the physiological relevance of Lin28 during regeneration after injury in the PNS could be further validated by using inducible SC-specific Lin28 mutant mice (B6.Cg-*Lin28b*$^{tm1.2Gqda}$/J) carrying a tamoxifen-inducible Cre transgene under control of the P0-Cx32 promoter [Leone et al., 2003]. In this context the aforementioned SC-specific inducible transgenic Lin28-expressing mice (see 2.2.9) could be used to support a possible instructive function of Lin28 during SC dedifferentiation. In a similar approach the promoting role of Notch1 during regener-

ation after injury was shown [Woodhoo et al., 2009]. Whether this role of Notch1 is mechanistically linked to Lin28-dependent suppression of let-7 miRNAs as described in this thesis during developmental myelination (see 3.2), needs to be further investigated.

4.4 Other miRNA-related functions in the Schwann cell lineage

It is evident that miRNAs have fundamental regulatory functions during developmental myelination (see 3.2). However their role in earlier stages of the SC lineage could not be addressed with the experimental setup employed in this thesis. Studies should address functions of miRNAs in SC precursors and neural crest stem cells by employing an earlier cell-specific transgenic Cre mouse line, for example mice carrying a tamoxifen-inducible Cre under the control of the *Sox10* or *Plp* promoter [Dyachuk et al., 2014].

Asking about functions of miRNAs during earlier glial stages naturally leads to the question about their functions at later stages [Jessen and Mirsky, 2005]. Analyses of Dicer KO and Lin28 tg have clearly shown that let-7 miRNAs are necessary for the onset of myelination (see 3.2). However, the crucial role of let-7 miRNAs during this stage masks possible functions of let-7 or other miRNAs during later stages of developmental myelination, such as myelin progression and organisation of the polarised structure along the myelinated axon [Pereira et al., 2012]. Employing a mouse line which expresses Cre under the control of a promoter activated later in SC differentiation, such as the *Krox20* promoter, could help addressing the role of miRNAs during the formation of mature myelin domains [Voiculescu et al., 2000, Pereira et al., 2012]. The structural integrity of myelin is crucial for its proper function and is frequently compromised in demyelinating neuropathies [Niemann et al., 2006].

Analysis of Dicer KO mice has also shown that the survival of axons is compromised in SNs [Pereira et al., 2010]. This suggests a role of SC-specific miRNAs in trophic signalling or support towards the axon. Lin28 tg should be also analysed for axonal survival to address whether let-7 miRNAs do contribute to the observations made in Dicer KO. Future studies should include SC-derived miRNAs as a possible contributor to trophic signalling from SCs towards axons in the PNS. Molecular mechanisms of neuronal survival are of central interest for a detailed understanding of peripheral neuropathies such as certain types of Charcot-Marie-Tooth disease in which survival of axons is compromised [Niemann et al., 2006].

Comparative analysis of DGCR8 KO and Dicer KO mice in the sympathetic trunk has revealed an indispensable role of miRNAs during Remak bundle formation (see 3.1). Based on these data we suggested that the small unsorted bundles present in Dicer KO at P24 are meant to be engaged by non-myelinating SCs in Remak bundles. This hypothesis could be validated in future analyses by quantification of the total number of myelinated and not-myelinated 1:1 SC axon profiles in SNs of Dicer KO and controls. If the hypothesis would be true these numbers should match. Remak bundle formation is poorly understood and additional studies are needed to elucidate molecular mechanisms during differentiation of non-myelinating SCs [Jessen and Mirsky, 2005]. The sympathetic trunk has been shown to be an appropriate model system to perform such studies,

due to its enrichment in Remak bundles [Frank et al., 2000]. These nerves could be analysed at different time points during development using RNA sequencing, in order to obtain the expression pattern of possible regulatory candidates. Given the importance of miRNAs for Remak bundle maturation, the obtained list of candidates could be refined to mRNAs carrying predicted target sites in their 3′-UTR for abundant miRNAs at the same stage. The physiological relevance of promising candidate mRNAs could then be validated in loss-of-function mouse models. Non-myelinating SCs are essential for pain sensation in vertebrates, and pain itself is a major factor in human suffering and disability [Goldberg and McGee, 2011]. Therefore, a clear understanding of molecular mechanisms regulating the function of these fibres merits investigation in its own right, and may very well contribute to our knowledge of pain regulation in various disease scenarios.

5 Bibliography

[Adameyko et al., 2009] Adameyko, I., Lallemend, F., Aquino, J. B., Pereira, J. A., Topilko, P., Muller, T., Fritz, N., Beljajeva, A., Mochii, M., Liste, I., Usoskin, D., Suter, U., Birchmeier, C. and Ernfors, P. (2009). Schwann cell precursors from nerve innervation are a cellular origin of melanocytes in skin. Cell *139*, 366–79.

[Adameyko et al., 2012] Adameyko, I., Lallemend, F., Furlan, A., Zinin, N., Aranda, S., Kitambi, S. S., Blanchart, A., Favaro, R., Nicolis, S., Lubke, M., Muller, T., Birchmeier, C., Suter, U., Zaitoun, I., Takahashi, Y. and Ernfors, P. (2012). Sox2 and Mitf cross-regulatory interactions consolidate progenitor and melanocyte lineages in the cranial neural crest. Development *139*, 397–410.

[Agranat-Tamir et al., 2014] Agranat-Tamir, L., Shomron, N., Sperling, J. and Sperling, R. (2014). Interplay between pre-mRNA splicing and microRNA biogenesis within the supraspliceosome. Nucleic Acids Res *42*, 4640–51.

[Amakye et al., 2013] Amakye, D., Jagani, Z. and Dorsch, M. (2013). Unraveling the therapeutic potential of the Hedgehog pathway in cancer. Nat Med *19*, 1410–22.

[Ambros, 2004] Ambros, V. (2004). The functions of animal microRNAs. Nature *431*, 350–5.

[Ameres and Zamore, 2013] Ameres, S. L. and Zamore, P. D. (2013). Diversifying microRNA sequence and function. Nat Rev Mol Cell Biol *14*, 475–88.

[Anders and Huber, 2010] Anders, S. and Huber, W. (2010). Differential expression analysis for sequence count data. Genome Biol *11*, R106.

[Auyeung et al., 2013] Auyeung, V. C., Ulitsky, I., McGeary, S. E. and Bartel, D. P. (2013). Beyond secondary structure: primary-sequence determinants license pri-miRNA hairpins for processing. Cell *152*, 844–58.

[Babiarz et al., 2011] Babiarz, J. E., Hsu, R., Melton, C., Thomas, M., Ullian, E. M. and Blelloch, R. (2011). A role for noncanonical microRNAs in the mammalian brain revealed by phenotypic differences in Dgcr8 versus Dicer1 knockouts and small RNA sequencing. RNA *17*, 1489–501.

[Babiarz et al., 2008] Babiarz, J. E., Ruby, J. G., Wang, Y., Bartel, D. P. and Blelloch, R. (2008). Mouse ES cells express endogenous shRNAs, siRNAs, and other Microprocessor-independent, Dicer-dependent small RNAs. Genes Dev *22*, 2773–85.

[Baek et al., 2008] Baek, D., Villen, J., Shin, C., Camargo, F. D., Gygi, S. P. and Bartel, D. P. (2008). The impact of microRNAs on protein output. Nature *455*, 64–71.

[Bartel, 2009] Bartel, D. P. (2009). MicroRNAs: target recognition and regulatory functions. Cell *136*, 215–33.

[Bazzini et al., 2012] Bazzini, A. A., Lee, M. T. and Giraldez, A. J. (2012). Ribosome profiling shows that miR-430 reduces translation before causing mRNA decay in zebrafish. Science *336*, 233–7.

[Beirowski, 2013] Beirowski, B. (2013). Concepts for regulation of axon integrity by enwrapping glia. Front Cell Neurosci *7*, 256.

[Benninger et al., 2007] Benninger, Y., Thurnherr, T., Pereira, J. A., Krause, S., Wu, X., Chrostek-Grashoff, A., Herzog, D., Nave, K. A., Franklin, R. J., Meijer, D., Brakebusch, C., Suter, U. and Relvas, J. B. (2007). Essential and distinct roles for cdc42 and rac1 in the regulation of Schwann cell biology during peripheral nervous system development. J Cell Biol *177*, 1051–61.

[Berezikov, 2011] Berezikov, E. (2011). Evolution of microRNA diversity and regulation in animals. Nat Rev Genet *12*, 846–60.

[Berezikov et al., 2007] Berezikov, E., Chung, W. J., Willis, J., Cuppen, E. and Lai, E. C. (2007). Mammalian mirtron genes. Mol Cell *28*, 328–36.

[Berger et al., 2006] Berger, P., Niemann, A. and Suter, U. (2006). Schwann cells and the pathogenesis of inherited motor and sensory neuropathies (Charcot-Marie-Tooth disease). Glia *54*, 243–257.

[Bernstein et al., 2003] Bernstein, E., Kim, S. Y., Carmell, M. A., Murchison, E. P., Alcorn, H., Li, M. Z., Mills, A. A., Elledge, S. J., Anderson, K. V. and Hannon, G. J. (2003). Dicer is essential for mouse development. Nat Genet *35*, 215–7.

[Berti et al., 2011] Berti, C., Bartesaghi, L., Ghidinelli, M., Zambroni, D., Figlia, G., Chen, Z. L., Quattrini, A., Wrabetz, L. and Feltri, M. L. (2011). Non-redundant function of dystroglycan and beta1 integrins in radial sorting of axons. Development *138*, 4025–37.

[Betel et al., 2010] Betel, D., Koppal, A., Agius, P., Sander, C. and Leslie, C. (2010). Comprehensive modeling of microRNA targets predicts functional non-conserved and non-canonical sites. Genome Biol *11*, R90.

[Bezman et al., 2010] Bezman, N. A., Cedars, E., Steiner, D. F., Blelloch, R., Hesslein, D. G. and Lanier, L. L. (2010). Distinct requirements of microRNAs in NK cell activation, survival, and function. J Immunol *185*, 3835–46.

[Bohnsack et al., 2004] Bohnsack, M. T., Czaplinski, K. and Gorlich, D. (2004). Exportin 5 is a RanGTP-dependent dsRNA-binding protein that mediates nuclear export of pre-miRNAs. RNA *10*, 185–91.

[Braun et al., 2011] Braun, J. E., Huntzinger, E., Fauser, M. and Izaurralde, E. (2011). GW182 proteins directly recruit cytoplasmic deadenylase complexes to miRNA targets. Mol Cell *44*, 120–33.

[Bremer et al., 2010] Bremer, J., O'Connor, T., Tiberi, C., Rehrauer, H., Weis, J. and Aguzzi, A. (2010). Ablation of Dicer from murine Schwann cells increases their proliferation while blocking myelination. PLoS One *5*, e12450.

[Brennecke et al., 2005] Brennecke, J., Stark, A., Russell, R. B. and Cohen, S. M. (2005). Principles of microRNA-target recognition. PLoS Biol *3*, e85.

[Bruno et al., 2011] Bruno, I. G., Karam, R., Huang, L., Bhardwaj, A., Lou, C. H., Shum, E. Y., Song, H. W., Corbett, M. A., Gifford, W. D., Gecz, J., Pfaff, S. L. and Wilkinson, M. F. (2011). Identification of a microRNA that activates gene expression by repressing nonsense-mediated RNA decay. Mol Cell *42*, 500–10.

[Cai et al., 2004] Cai, X., Hagedorn, C. H. and Cullen, B. R. (2004). Human microRNAs are processed from capped, polyadenylated transcripts that can also function as mRNAs. RNA *10*, 1957–66.

[Chakravarthy et al., 2010] Chakravarthy, S., Sternberg, S. H., Kellenberger, C. A. and Doudna, J. A. (2010). Substrate-specific kinetics of Dicer-catalyzed RNA processing. J Mol Biol *404*, 392–402.

[Chakravarti et al., 2014] Chakravarti, D., Su, X., Cho, M. S., Bui, N. H., Coarfa, C., Venkatanarayan, A., Benham, A. L., Flores Gonzalez, R. E., Alana, J., Xiao, W., Leung, M. L., Vin, H., Chan, I. L., Aquino, A., Muller, N., Wang, H., Cooney, A. J., Parker-Thornburg, J., Tsai, K. Y., Gunaratne, P. H. and Flores, E. R. (2014). Induced multipotency in adult keratinocytes through down-regulation of DeltaNp63 or DGCR8. Proc Natl Acad Sci U S A *111*, E572–81.

[Chan et al., 2006] Chan, J. R., Jolicoeur, C., Yamauchi, J., Elliott, J., Fawcett, J. P., Ng, B. K. and Cayouette, M. (2006). The polarity protein Par-3 directly interacts with p75NTR to regulate myelination. Science *314*, 832–6.

[Chatterjee and Grosshans, 2009] Chatterjee, S. and Grosshans, H. (2009). Active turnover modulates mature microRNA activity in Caenorhabditis elegans. Nature *461*, 546–9.

[Chechneva et al., 2014] Chechneva, O. V., Mayrhofer, F., Daugherty, D. J., Krishnamurty, R. G., Bannerman, P., Pleasure, D. E. and Deng, W. (2014). A Smoothened receptor agonist is neuroprotective and promotes regeneration after ischemic brain injury. Cell Death Dis *5*, e1481.

[Chekulaeva et al., 2011] Chekulaeva, M., Mathys, H., Zipprich, J. T., Attig, J., Colic, M., Parker, R. and Filipowicz, W. (2011). miRNA repression involves GW182-mediated recruitment of CCR4-NOT through conserved W-containing motifs. Nat Struct Mol Biol *18*, 1218–26.

[Cheloufi et al., 2010] Cheloufi, S., Dos Santos, C. O., Chong, M. M. and Hannon, G. J. (2010). A dicer-independent miRNA biogenesis pathway that requires Ago catalysis. Nature *465*, 584–9.

[Chen et al., 2012] Chen, C. J., Servant, N., Toedling, J., Sarazin, A., Marchais, A., Duvernois-Berthet, E., Cognat, V., Colot, V., Voinnet, O., Heard, E., Ciaudo, C. and Barillot, E. (2012). ncPRO-seq: a tool for annotation and profiling of ncRNAs in sRNA-seq data. Bioinformatics *28*, 3147–9.

[Chen and Strickland, 2003] Chen, Z. L. and Strickland, S. (2003). Laminin gamma1 is critical for Schwann cell differentiation, axon myelination, and regeneration in the peripheral nerve. J Cell Biol *163*, 889–99.

[Cheng et al., 2014] Cheng, T. L., Wang, Z., Liao, Q., Zhu, Y., Zhou, W. H., Xu, W. and Qiu, Z. (2014). MeCP2 suppresses nuclear microRNA processing and dendritic growth by regulating the DGCR8/Drosha complex. Dev Cell *28*, 547–60.

[Chi et al., 2012] Chi, S. W., Hannon, G. J. and Darnell, R. B. (2012). An alternative mode of microRNA target recognition. Nat Struct Mol Biol *19*, 321–7.

[Chi et al., 2009] Chi, S. W., Zang, J. B., Mele, A. and Darnell, R. B. (2009). Argonaute HITS-CLIP decodes microRNA-mRNA interaction maps. Nature *460*, 479–86.

[Chong et al., 2008] Chong, M. M., Rasmussen, J. P., Rudensky, A. Y. and Littman, D. R. (2008). The RNAseIII enzyme Drosha is critical in T cells for preventing lethal inflammatory disease. J Exp Med *205*, 2005–17.

[Chong et al., 2010] Chong, M. M., Zhang, G., Cheloufi, S., Neubert, T. A., Hannon, G. J. and Littman, D. R. (2010). Canonical and alternate functions of the microRNA biogenesis machinery. Genes Dev *24*, 1951–60.

[Cimadamore et al., 2013] Cimadamore, F., Amador-Arjona, A., Chen, C., Huang, C. T. and Terskikh, A. V. (2013). SOX2-LIN28/let-7 pathway regulates proliferation and neurogenesis in neural precursors. Proc Natl Acad Sci U S A *110*, E3017–26.

[Cotter et al., 2010] Cotter, L., Ozcelik, M., Jacob, C., Pereira, J. A., Locher, V., Baumann, R., Relvas, J. B., Suter, U. and Tricaud, N. (2010). Dlg1-PTEN interaction regulates myelin thickness to prevent damaging peripheral nerve overmyelination. Science *328*, 1415–8.

[D'Antonio et al., 2006] D'Antonio, M., Droggiti, A., Feltri, M. L., Roes, J., Wrabetz, L., Mirsky, R. and Jessen, K. R. (2006). TGFbeta type II receptor signaling controls Schwann cell death and proliferation in developing nerves. J Neurosci *26*, 8417–27.

[Davis et al., 2008] Davis, B. N., Hilyard, A. C., Lagna, G. and Hata, A. (2008). SMAD proteins control DROSHA-mediated microRNA maturation. Nature *454*, 56–61.

[Davis et al., 2010] Davis, B. N., Hilyard, A. C., Nguyen, P. H., Lagna, G. and Hata, A. (2010). Smad proteins bind a conserved RNA sequence to promote microRNA maturation by Drosha. Mol Cell *39*, 373–84.

[Delloye-Bourgeois et al., 2014] Delloye-Bourgeois, C., Rama, N., Brito, J., Le Douarin, N. and Mehlen, P. (2014). Sonic Hedgehog promotes the survival of neural crest cells by limiting apoptosis induced by the dependence receptor CDON during branchial arch development. Biochem Biophys Res Commun *452*, 655–60.

[Dennler et al., 2007] Dennler, S., Andre, J., Alexaki, I., Li, A., Magnaldo, T., ten Dijke, P., Wang, X. J., Verrecchia, F. and Mauviel, A. (2007). Induction of sonic hedgehog mediators by transforming growth factor-beta: Smad3-dependent activation of Gli2 and Gli1 expression in vitro and in vivo. Cancer Res *67*, 6981–6.

[Didiano and Hobert, 2006] Didiano, D. and Hobert, O. (2006). Perfect seed pairing is not a generally reliable predictor for miRNA-target interactions. Nat Struct Mol Biol *13*, 849–51.

[Dweep et al., 2011] Dweep, H., Sticht, C., Pandey, P. and Gretz, N. (2011). miRWalk–database: prediction of possible miRNA binding sites by "walking" the genes of three genomes. J Biomed Inform *44*, 839–47.

[Dyachuk et al., 2014] Dyachuk, V., Furlan, A., Shahidi, M. K., Giovenco, M., Kaukua, N., Konstantinidou, C., Pachnis, V., Memic, F., Marklund, U., Muller, T., Birchmeier, C., Fried, K., Ernfors, P. and Adameyko, I. (2014). Neurodevelopment. Parasympathetic neurons originate from nerve-associated peripheral glial progenitors. Science *345*, 82–7.

[Ebert and Sharp, 2012] Ebert, M. S. and Sharp, P. A. (2012). Roles for microRNAs in conferring robustness to biological processes. Cell *149*, 515–24.

[Ecke et al., 2008] Ecke, I., Rosenberger, A., Obenauer, S., Dullin, C., Aberger, F., Kimmina, S., Schweyer, S. and Hahn, H. (2008). Cyclopamine treatment of full-blown Hh/Ptch-associated RMS partially inhibits Hh/Ptch signaling, but not tumor growth. Mol Carcinog *47*, 361–72.

[Ender et al., 2008] Ender, C., Krek, A., Friedlander, M. R., Beitzinger, M., Weinmann, L., Chen, W., Pfeffer, S., Rajewsky, N. and Meister, G. (2008). A human snoRNA with microRNA-like functions. Mol Cell *32*, 519–28.

[Engh, 2011] Engh, J. A. (2011). Notch1 identified as a prognostic factor for glioma patients. Neurosurgery *68*, N22–3.

[Espinosa-Medina et al., 2014] Espinosa-Medina, I., Outin, E., Picard, C. A., Chettouh, Z., Dymecki, S., Consalez, G. G., Coppola, E. and Brunet, J. F. (2014). Neurodevelopment. Parasympathetic ganglia derive from Schwann cell precursors. Science *345*, 87–90.

[Fabian et al., 2011] Fabian, M. R., Cieplak, M. K., Frank, F., Morita, M., Green, J., Srikumar, T., Nagar, B., Yamamoto, T., Raught, B., Duchaine, T. F. and Sonenberg, N. (2011). miRNA-mediated deadenylation is orchestrated by GW182 through two conserved motifs that interact with CCR4-NOT. Nat Struct Mol Biol *18*, 1211–7.

[Farh et al., 2005] Farh, K. K., Grimson, A., Jan, C., Lewis, B. P., Johnston, W. K., Lim, L. P., Burge, C. B. and Bartel, D. P. (2005). The widespread impact of mammalian MicroRNAs on mRNA repression and evolution. Science *310*, 1817–21.

[Faroni et al., 2014] Faroni, A., Castelnovo, L. F., Procacci, P., Caffino, L., Fumagalli, F., Melfi, S., Gambarotta, G., Bettler, B., Wrabetz, L. and Magnaghi, V. (2014). Deletion of GABA-B receptor in Schwann cells regulates remak bundles and small nociceptive C-fibers. Glia *62*, 548–65.

[Feltri et al., 2002] Feltri, M. L., Graus Porta, D., Previtali, S. C., Nodari, A., Migliavacca, B., Cassetti, A., Littlewood-Evans, A., Reichardt, L. F., Messing, A., Quattrini, A., Mueller, U. and Wrabetz, L. (2002). Conditional disruption of beta 1 integrin in Schwann cells impedes interactions with axons. J Cell Biol *156*, 199–209.

[Feltri and Wrabetz, 2005] Feltri, M. L. and Wrabetz, L. (2005). Laminins and their receptors in Schwann cells and hereditary neuropathies. J Peripher Nerv Syst *10*, 128–43.

[Francia et al., 2012] Francia, S., Michelini, F., Saxena, A., Tang, D., de Hoon, M., Anelli, V., Mione, M., Carninci, P. and d'Adda di Fagagna, F. (2012). Site-specific DICER and DROSHA RNA products control the DNA-damage response. Nature *488*, 231–5.

[Frank et al., 2000] Frank, M., Atanasoski, S., Sancho, S., Magyar, J. P., Rulicke, T., Schwab, M. E. and Suter, U. (2000). Progressive segregation of unmyelinated axons in peripheral nerves, myelin alterations in the CNS, and cyst formation in the kidneys of myelin and lymphocyte protein-overexpressing mice. J Neurochem *75*, 1927–39.

[Friedman et al., 2009] Friedman, R. C., Farh, K. K., Burge, C. B. and Bartel, D. P. (2009). Most mammalian mRNAs are conserved targets of microRNAs. Genome Res *19*, 92–105.

[Frob et al., 2012] Frob, F., Bremer, M., Finzsch, M., Kichko, T., Reeh, P., Tamm, E. R., Charnay, P. and Wegner, M. (2012). Establishment of myelinating Schwann cells and barrier integrity between central and peripheral nervous systems depend on Sox10. Glia *60*, 806–19.

[Fukuda et al., 2007] Fukuda, T., Yamagata, K., Fujiyama, S., Matsumoto, T., Koshida, I., Yoshimura, K., Mihara, M., Naitou, M., Endoh, H., Nakamura, T., Akimoto, C., Yamamoto, Y., Katagiri, T., Foulds, C., Takezawa, S., Kitagawa, H., Takeyama, K., O'Malley, B. W. and Kato, S. (2007). DEAD-box RNA helicase subunits of the Drosha complex are required for processing of rRNA and a subset of microRNAs. Nat Cell Biol *9*, 604–11.

[Fukunaga et al., 2012] Fukunaga, R., Han, B. W., Hung, J. H., Xu, J., Weng, Z. and Zamore, P. D. (2012). Dicer partner proteins tune the length of mature miRNAs in flies and mammals. Cell *151*, 533–46.

[Gat et al., 1998] Gat, U., DasGupta, R., Degenstein, L. and Fuchs, E. (1998). De Novo hair follicle morphogenesis and hair tumors in mice expressing a truncated beta-catenin in skin. Cell *95*, 605–14.

[Goldberg and McGee, 2011] Goldberg, D. S. and McGee, S. J. (2011). Pain as a global public health priority. BMC Public Health *11*, 770.

[Gottwein et al., 2011] Gottwein, E., Corcoran, D. L., Mukherjee, N., Skalsky, R. L., Hafner, M., Nusbaum, J. D., Shamulailatpam, P., Love, C. L., Dave, S. S., Tuschl, T., Ohler, U. and Cullen, B. R. (2011). Viral microRNA targetome of KSHV-infected primary effusion lymphoma cell lines. Cell Host Microbe *10*, 515–26.

[Griffiths-Jones et al., 2006] Griffiths-Jones, S., Grocock, R. J., van Dongen, S., Bateman, A. and Enright, A. J. (2006). miRBase: microRNA sequences, targets and gene nomenclature. Nucleic Acids Res *34*, D140–4.

[Grigoryan et al., 2013] Grigoryan, T., Stein, S., Qi, J., Wende, H., Garratt, A. N., Nave, K. A., Birchmeier, C. and Birchmeier, W. (2013). Wnt/Rspondin/beta-catenin signals control axonal sorting and lineage progression in Schwann cell development. Proc Natl Acad Sci U S A *110*, 18174–9.

[Grimson et al., 2007] Grimson, A., Farh, K. K., Johnston, W. K., Garrett-Engele, P., Lim, L. P. and Bartel, D. P. (2007). MicroRNA targeting specificity in mammals: determinants beyond seed pairing. Mol Cell *27*, 91–105.

[Gromak et al., 2013] Gromak, N., Dienstbier, M., Macias, S., Plass, M., Eyras, E., Caceres, J. F. and Proudfoot, N. J. (2013). Drosha regulates gene expression independently of RNA cleavage function. Cell Rep *5*, 1499–510.

[Grove et al., 2007] Grove, M., Komiyama, N. H., Nave, K. A., Grant, S. G., Sherman, D. L. and Brophy, P. J. (2007). FAK is required for axonal sorting by Schwann cells. J Cell Biol *176*, 277–82.

[Guan et al., 2008] Guan, W., Wang, G., Scott, S. A. and Condic, M. L. (2008). Shh influences cell number and the distribution of neuronal subtypes in dorsal root ganglia. Dev Biol *314*, 317–28.

[Guil and Caceres, 2007] Guil, S. and Caceres, J. F. (2007). The multifunctional RNA-binding protein hnRNP A1 is required for processing of miR-18a. Nat Struct Mol Biol *14*, 591–6.

[Guo et al., 2010] Guo, H., Ingolia, N. T., Weissman, J. S. and Bartel, D. P. (2010). Mammalian microRNAs predominantly act to decrease target mRNA levels. Nature *466*, 835–40.

[Ha and Kim, 2014] Ha, M. and Kim, V. N. (2014). Regulation of microRNA biogenesis. Nat Rev Mol Cell Biol *15*, 509–24.

[Hafner et al., 2010] Hafner, M., Landthaler, M., Burger, L., Khorshid, M., Hausser, J., Berninger, P., Rothballer, A., Ascano, M., J., Jungkamp, A. C., Munschauer, M., Ulrich, A., Wardle, G. S., Dewell, S., Zavolan, M. and Tuschl, T. (2010). Transcriptome-wide identification of RNA-binding protein and microRNA target sites by PAR-CLIP. Cell *141*, 129–41.

[Hagan et al., 2009] Hagan, J. P., Piskounova, E. and Gregory, R. I. (2009). Lin28 recruits the TUTase Zcchc11 to inhibit let-7 maturation in mouse embryonic stem cells. Nat Struct Mol Biol *16*, 1021–5.

[Hammond et al., 2001] Hammond, S. M., Boettcher, S., Caudy, A. A., Kobayashi, R. and Hannon, G. J. (2001). Argonaute2, a link between genetic and biochemical analyses of RNAi. Science *293*, 1146–50.

[Han et al., 2014] Han, C., Liu, Y., Wan, G., Choi, H. J., Zhao, L., Ivan, C., He, X., Sood, A. K., Zhang, X. and Lu, X. (2014). The RNA-binding protein DDX1 promotes primary microRNA maturation and inhibits ovarian tumor progression. Cell Rep *8*, 1447–60.

[Han et al., 2004] Han, J., Lee, Y., Yeom, K. H., Kim, Y. K., Jin, H. and Kim, V. N. (2004). The Drosha-DGCR8 complex in primary microRNA processing. Genes Dev *18*, 3016–27.

[Han et al., 2006] Han, J., Lee, Y., Yeom, K. H., Nam, J. W., Heo, I., Rhee, J. K., Sohn, S. Y., Cho, Y., Zhang, B. T. and Kim, V. N. (2006). Molecular basis for the recognition of primary microRNAs by the Drosha-DGCR8 complex. Cell *125*, 887–901.

[Han et al., 2009] Han, J., Pedersen, J. S., Kwon, S. C., Belair, C. D., Kim, Y. K., Yeom, K. H., Yang, W. Y., Haussler, D., Blelloch, R. and Kim, V. N. (2009). Posttranscriptional crossregulation between Drosha and DGCR8. Cell *136*, 75–84.

[Haraguchi et al., 2009] Haraguchi, T., Ozaki, Y. and Iba, H. (2009). Vectors expressing efficient RNA decoys achieve the long-term suppression of specific microRNA activity in mammalian cells. Nucleic Acids Res *37*, e43.

[Hashimoto et al., 2008] Hashimoto, M., Ishii, K., Nakamura, Y., Watabe, K., Kohsaka, S. and Akazawa, C. (2008). Neuroprotective effect of sonic hedgehog up-regulated in Schwann cells following sciatic nerve injury. J Neurochem *107*, 918–27.

[Havens et al., 2014] Havens, M. A., Reich, A. A. and Hastings, M. L. (2014). Drosha promotes splicing of a pre-microRNA-like alternative exon. PLoS Genet *10*, e1004312.

[He et al., 2010] He, Y., Kim, J. Y., Dupree, J., Tewari, A., Melendez-Vasquez, C., Svaren, J. and Casaccia, P. (2010). Yy1 as a molecular link between neuregulin and transcriptional modulation of peripheral myelination. Nat Neurosci *13*, 1472–80.

[Helwak et al., 2013] Helwak, A., Kudla, G., Dudnakova, T. and Tollervey, D. (2013). Mapping the human miRNA interactome by CLASH reveals frequent noncanonical binding. Cell *153*, 654–65.

[Heo et al., 2009] Heo, I., Joo, C., Kim, Y. K., Ha, M., Yoon, M. J., Cho, J., Yeom, K. H., Han, J. and Kim, V. N. (2009). TUT4 in concert with Lin28 suppresses microRNA biogenesis through pre-microRNA uridylation. Cell *138*, 696–708.

[Heras et al., 2013] Heras, S. R., Macias, S., Plass, M., Fernandez, N., Cano, D., Eyras, E., Garcia-Perez, J. L. and Caceres, J. F. (2013). The Microprocessor controls the activity of mammalian retrotransposons. Nat Struct Mol Biol *20*, 1173–81.

[Herbert et al., 2013] Herbert, K. M., Pimienta, G., DeGregorio, S. J., Alexandrov, A. and Steitz, J. A. (2013). Phosphorylation of DGCR8 increases its intracellular stability and induces a progrowth miRNA profile. Cell Rep *5*, 1070–81.

[Hertel et al., 2006] Hertel, J., Lindemeyer, M., Missal, K., Fried, C., Tanzer, A., Flamm, C., Hofacker, I. L., Stadler, P. F. and Students of Bioinformatics Computer Labs, a. (2006). The expansion of the metazoan microRNA repertoire. BMC Genomics *7*, 25.

[Hutvagner et al., 2001] Hutvagner, G., McLachlan, J., Pasquinelli, A. E., Balint, E., Tuschl, T. and Zamore, P. D. (2001). A cellular function for the RNA-interference enzyme Dicer in the maturation of the let-7 small temporal RNA. Science *293*, 834–8.

[Jacob et al., 2011] Jacob, C., Christen, C. N., Pereira, J. A., Somandin, C., Baggiolini, A., Lotscher, P., Ozcelik, M., Tricaud, N., Meijer, D., Yamaguchi, T., Matthias, P. and Suter, U. (2011). HDAC1 and HDAC2 control the transcriptional program of myelination and the survival of Schwann cells. Nat Neurosci *14*, 429–36.

[Jaegle et al., 2003] Jaegle, M., Ghazvini, M., Mandemakers, W., Piirsoo, M., Driegen, S., Levavasseur, F., Raghoenath, S., Grosveld, F. and Meijer, D. (2003). The POU proteins Brn-2 and Oct-6 share important functions in Schwann cell development. Genes Dev *17*, 1380–91.

[Jessen and Mirsky, 2005] Jessen, K. R. and Mirsky, R. (2005). The origin and development of glial cells in peripheral nerves. Nat Rev Neurosci *6*, 671–82.

[Jessen and Mirsky, 2008] Jessen, K. R. and Mirsky, R. (2008). Negative regulation of myelination: relevance for development, injury, and demyelinating disease. Glia *56*, 1552–65.

[Ji et al., 2007] Ji, Z., Mei, F. C., Xie, J. and Cheng, X. (2007). Oncogenic KRAS activates hedgehog signaling pathway in pancreatic cancer cells. J Biol Chem *282*, 14048–55.

[Jung et al., 2014] Jung, E., Seong, Y., Seo, J. H., Kwon, Y. S. and Song, H. (2014). Cell cycle-dependent regulation of Aurora kinase B mRNA by the Microprocessor complex. Biochem Biophys Res Commun *446*, 241–7.

[Kadener et al., 2009] Kadener, S., Rodriguez, J., Abruzzi, K. C., Khodor, Y. L., Sugino, K., Marr, M. T., n., Nelson, S. and Rosbash, M. (2009). Genome-wide identification of targets of the drosha-pasha/DGCR8 complex. RNA *15*, 537–45.

[Kanellopoulou et al., 2005] Kanellopoulou, C., Muljo, S. A., Kung, A. L., Ganesan, S., Drapkin, R., Jenuwein, T., Livingston, D. M. and Rajewsky, K. (2005). Dicer-deficient mouse embryonic stem cells are defective in differentiation and centromeric silencing. Genes Dev *19*, 489–501.

[Kao et al., 2009] Kao, S. C., Wu, H., Xie, J., Chang, C. P., Ranish, J. A., Graef, I. A. and Crabtree, G. R. (2009). Calcineurin/NFAT signaling is required for neuregulin-regulated Schwann cell differentiation. Science *323*, 651–4.

[Kataoka et al., 2009] Kataoka, N., Fujita, M. and Ohno, M. (2009). Functional association of the Microprocessor complex with the spliceosome. Mol Cell Biol *29*, 3243–54.

[Kaukua et al., 2014] Kaukua, N., Shahidi, M. K., Konstantinidou, C., Dyachuk, V., Kaucka, M., Furlan, A., An, Z., Wang, L., Hultman, I., Ahrlund-Richter, L., Blom, H., Brismar, H., Lopes, N. A., Pachnis, V., Suter, U., Clevers, H., Thesleff, I., Sharpe, P., Ernfors, P., Fried, K. and Adameyko, I. (2014). Glial origin of mesenchymal stem cells in a tooth model system. Nature *513*, 551–4.

[Khorshid et al., 2013] Khorshid, M., Hausser, J., Zavolan, M. and van Nimwegen, E. (2013). A biophysical miRNA-mRNA interaction model infers canonical and non-canonical targets. Nat Methods *10*, 253–5.

[Khvorova et al., 2003] Khvorova, A., Reynolds, A. and Jayasena, S. D. (2003). Functional siRNAs and miRNAs exhibit strand bias. Cell *115*, 209–16.

[Kim et al., 2009] Kim, V. N., Han, J. and Siomi, M. C. (2009). Biogenesis of small RNAs in animals. Nat Rev Mol Cell Biol *10*, 126–39.

[Knuckles et al., 2012] Knuckles, P., Vogt, M. A., Lugert, S., Milo, M., Chong, M. M., Hautbergue, G. M., Wilson, S. A., Littman, D. R. and Taylor, V. (2012). Drosha regulates neurogenesis by controlling neurogenin 2 expression independent of microRNAs. Nat Neurosci *15*, 962–9.

[Kozomara and Griffiths-Jones, 2014] Kozomara, A. and Griffiths-Jones, S. (2014). miRBase: annotating high confidence microRNAs using deep sequencing data. Nucleic Acids Res *42*, D68–73.

[Krutzfeldt et al., 2005] Krutzfeldt, J., Rajewsky, N., Braich, R., Rajeev, K. G., Tuschl, T., Manoharan, M. and Stoffel, M. (2005). Silencing of microRNAs in vivo with 'antagomirs'. Nature *438*, 685–9.

[Kucenas et al., 2009] Kucenas, S., Wang, W. D., Knapik, E. W. and Appel, B. (2009). A selective glial barrier at motor axon exit points prevents oligodendrocyte migration from the spinal cord. J Neurosci *29*, 15187–94.

[Lal et al., 2009] Lal, A., Navarro, F., Maher, C. A., Maliszewski, L. E., Yan, N., O'Day, E., Chowdhury, D., Dykxhoorn, D. M., Tsai, P., Hofmann, O., Becker, K. G., Gorospe, M., Hide, W. and Lieberman, J. (2009). miR-24 Inhibits cell proliferation by targeting E2F2, MYC, and other cell-cycle genes via binding to "seedless" 3'UTR microRNA recognition elements. Mol Cell *35*, 610–25.

[Lamouille et al., 2014] Lamouille, S., Xu, J. and Derynck, R. (2014). Molecular mechanisms of epithelial-mesenchymal transition. Nat Rev Mol Cell Biol *15*, 178–96.

[Landgraf et al., 2007] Landgraf, P., Rusu, M., Sheridan, R., Sewer, A., Iovino, N., Aravin, A., Pfeffer, S., Rice, A., Kamphorst, A. O., Landthaler, M., Lin, C., Socci, N. D., Hermida, L., Fulci, V., Chiaretti, S., Foa, R., Schliwka, J., Fuchs, U., Novosel, A., Muller, R. U., Schermer, B., Bissels, U., Inman, J., Phan, Q., Chien, M., Weir, D. B., Choksi, R., De Vita, G., Frezzetti, D., Trompeter, H. I., Hornung, V., Teng, G., Hartmann, G., Palkovits, M., Di Lauro, R., Wernet, P., Macino, G., Rogler, C. E., Nagle, J. W., Ju, J., Papavasiliou, F. N., Benzing, T., Lichter, P., Tam, W., Brownstein, M. J., Bosio, A., Borkhardt, A., Russo, J. J., Sander, C., Zavolan, M. and Tuschl, T. (2007). A mammalian microRNA expression atlas based on small RNA library sequencing. Cell *129*, 1401–14.

[Le et al., 2005] Le, N., Nagarajan, R., Wang, J. Y., Araki, T., Schmidt, R. E. and Milbrandt, J. (2005). Analysis of congenital hypomyelinating Egr2Lo/Lo nerves identifies Sox2 as an inhibitor of Schwann cell differentiation and myelination. Proc Natl Acad Sci U S A *102*, 2596–601.

[Lee et al., 2013] Lee, H. K., Finniss, S., Cazacu, S., Bucris, E., Ziv-Av, A., Xiang, C., Bobbitt, K., Rempel, S. A., Hasselbach, L., Mikkelsen, T., Slavin, S. and Brodie, C. (2013). Mesenchymal stem cells deliver synthetic microRNA mimics to glioma cells and glioma stem cells and inhibit their cell migration and self-renewal. Oncotarget *4*, 346–61.

[Lee et al., 1993] Lee, R. C., Feinbaum, R. L. and Ambros, V. (1993). The C. elegans heterochronic gene lin-4 encodes small RNAs with antisense complementarity to lin-14. Cell *75*, 843–54.

[Lee et al., 2003] Lee, Y., Ahn, C., Han, J., Choi, H., Kim, J., Yim, J., Lee, J., Provost, P., Radmark, O., Kim, S. and Kim, V. N. (2003). The nuclear RNase III Drosha initiates microRNA processing. Nature *425*, 415–9.

[Lee et al., 2004] Lee, Y., Kim, M., Han, J., Yeom, K. H., Lee, S., Baek, S. H. and Kim, V. N. (2004). MicroRNA genes are transcribed by RNA polymerase II. EMBO J *23*, 4051–60.

[Leone et al., 2003] Leone, D. P., Genoud, S., Atanasoski, S., Grausenburger, R., Berger, P., Metzger, D., Macklin, W. B., Chambon, P. and Suter, U. (2003). Tamoxifeninducible glia-specific Cre mice for somatic mutagenesis in oligodendrocytes and Schwann cells. Mol Cell Neurosci *22*, 430–40.

[Lewis et al., 2005] Lewis, B. P., Burge, C. B. and Bartel, D. P. (2005). Conserved seed pairing, often flanked by adenosines, indicates that thousands of human genes are microRNA targets. Cell *120*, 15–20.

[Li and Dewey, 2011] Li, B. and Dewey, C. N. (2011). RSEM: accurate transcript quantification from RNA-Seq data with or without a reference genome. BMC Bioinformatics *12*, 323.

[Lim et al., 2005] Lim, L. P., Lau, N. C., Garrett-Engele, P., Grimson, A., Schelter, J. M., Castle, J., Bartel, D. P., Linsley, P. S. and Johnson, J. M. (2005). Microarray analysis shows that some microRNAs downregulate large numbers of target mRNAs. Nature *433*, 769–73.

[Lindeboom et al., 2003] Lindeboom, F., Gillemans, N., Karis, A., Jaegle, M., Meijer, D., Grosveld, F. and Philipsen, S. (2003). A tissue-specific knockout reveals that Gata1 is not essential for Sertoli cell function in the mouse. Nucleic Acids Res *31*, 5405–12.

[Liu et al., 2005] Liu, J., Valencia-Sanchez, M. A., Hannon, G. J. and Parker, R. (2005). MicroRNA-dependent localization of targeted mRNAs to mammalian P-bodies. Nat Cell Biol *7*, 719–23.

[Lo Celso et al., 2004] Lo Celso, C., Prowse, D. M. and Watt, F. M. (2004). Transient activation of beta-catenin signalling in adult mouse epidermis is sufficient to induce new hair follicles but continuous activation is required to maintain hair follicle tumours. Development *131*, 1787–99.

[Lobsiger et al., 2001] Lobsiger, C. S., Smith, P. M., Buchstaller, J., Schweitzer, B., Franklin, R. J., Suter, U. and Taylor, V. (2001). SpL201: a conditionally immortalized Schwann cell precursor line that generates myelin. Glia *36*, 31–47.

[Loeb et al., 2012] Loeb, G. B., Khan, A. A., Canner, D., Hiatt, J. B., Shendure, J., Darnell, R. B., Leslie, C. S. and Rudensky, A. Y. (2012). Transcriptome-wide miR-155 binding map reveals widespread noncanonical microRNA targeting. Mol Cell *48*, 760–70.

[Lu et al., 2010] Lu, L. F., Boldin, M. P., Chaudhry, A., Lin, L. L., Taganov, K. D., Hanada, T., Yoshimura, A., Baltimore, D. and Rudensky, A. Y. (2010). Function of miR-146a in controlling Treg cell-mediated regulation of Th1 responses. Cell *142*, 914–29.

[Luhur et al., 2014] Luhur, A., Chawla, G., Wu, Y. C., Li, J. and Sokol, N. S. (2014). Drosha-independent DGCR8/Pasha pathway regulates neuronal morphogenesis. Proc Natl Acad Sci U S A *111*, 1421–6.

[Lund et al., 2004] Lund, E., Guttinger, S., Calado, A., Dahlberg, J. E. and Kutay, U. (2004). Nuclear export of microRNA precursors. Science *303*, 95–8.

[Macias et al., 2013] Macias, S., Cordiner, R. A. and Caceres, J. F. (2013). Cellular functions of the microprocessor. Biochem Soc Trans *41*, 838–43.

[Macias et al., 2012] Macias, S., Plass, M., Stajuda, A., Michlewski, G., Eyras, E. and Caceres, J. F. (2012). DGCR8 HITS-CLIP reveals novel functions for the Microprocessor. Nat Struct Mol Biol *19*, 760–6.

[Macrae et al., 2006] Macrae, I. J., Zhou, K., Li, F., Repic, A., Brooks, A. N., Cande, W. Z., Adams, P. D. and Doudna, J. A. (2006). Structural basis for double-stranded RNA processing by Dicer. Science *311*, 195–8.

[Mahindroo et al., 2009] Mahindroo, N., Punchihewa, C. and Fujii, N. (2009). Hedgehog-Gli signaling pathway inhibitors as anticancer agents. J Med Chem *52*, 3829–45.

[Marson et al., 2008] Marson, A., Levine, S. S., Cole, M. F., Frampton, G. M., Brambrink, T., Johnstone, S., Guenther, M. G., Johnston, W. K., Wernig, M., Newman, J., Calabrese, J. M., Dennis, L. M., Volkert, T. L., Gupta, S., Love, J., Hannett, N., Sharp, P. A., Bartel, D. P., Jaenisch, R. and Young, R. A. (2008). Connecting microRNA genes to the core transcriptional regulatory circuitry of embryonic stem cells. Cell *134*, 521–33.

[Matise and Wang, 2011] Matise, M. P. and Wang, H. (2011). Sonic hedgehog signaling in the developing CNS where it has been and where it is going. Curr Top Dev Biol *97*, 75–117.

[Mendell and Olson, 2012] Mendell, J. T. and Olson, E. N. (2012). MicroRNAs in stress signaling and human disease. Cell *148*, 1172–87.

[Michailov et al., 2004] Michailov, G. V., Sereda, M. W., Brinkmann, B. G., Fischer, T. M., Haug, B., Birchmeier, C., Role, L., Lai, C., Schwab, M. H. and Nave, K. A. (2004). Axonal neuregulin-1 regulates myelin sheath thickness. Science *304*, 700–3.

[Miranda et al., 2006] Miranda, K. C., Huynh, T., Tay, Y., Ang, Y. S., Tam, W. L., Thomson, A. M., Lim, B. and Rigoutsos, I. (2006). A pattern-based method for the identification of MicroRNA binding sites and their corresponding heteroduplexes. Cell *126*, 1203–17.

[Miyagoe-Suzuki et al., 2000] Miyagoe-Suzuki, Y., Nakagawa, M. and Takeda, S. (2000). Merosin and congenital muscular dystrophy. Microsc Res Tech *48*, 181–91.

[Miyoshi et al., 2010] Miyoshi, K., Miyoshi, T. and Siomi, H. (2010). Many ways to generate microRNA-like small RNAs: non-canonical pathways for microRNA production. Mol Genet Genomics *284*, 95–103.

[Molenaar et al., 2012] Molenaar, J. J., Domingo-Fernandez, R., Ebus, M. E., Lindner, S., Koster, J., Drabek, K., Mestdagh, P., van Sluis, P., Valentijn, L. J., van Nes, J., Broekmans, M., Haneveld, F., Volckmann, R., Bray, I., Heukamp, L., Sprussel, A.,

Thor, T., Kieckbusch, K., Klein-Hitpass, L., Fischer, M., Vandesompele, J., Schramm, A., van Noesel, M. M., Varesio, L., Speleman, F., Eggert, A., Stallings, R. L., Caron, H. N., Versteeg, R. and Schulte, J. H. (2012). LIN28B induces neuroblastoma and enhances MYCN levels via let-7 suppression. Nat Genet *44*, 1199–206.

[Montani et al., 2014] Montani, L., Buerki-Thurnherr, T., de Faria, J. P., Pereira, J. A., Dias, N. G., Fernandes, R., Goncalves, A. F., Braun, A., Benninger, Y., Bottcher, R. T., Costell, M., Nave, K. A., Franklin, R. J., Meijer, D., Suter, U. and Relvas, J. B. (2014). Profilin 1 is required for peripheral nervous system myelination. Development *141*, 1553–61.

[Mori et al., 2014] Mori, M., Triboulet, R., Mohseni, M., Schlegelmilch, K., Shrestha, K., Camargo, F. D. and Gregory, R. I. (2014). Hippo signaling regulates microprocessor and links cell-density-dependent miRNA biogenesis to cancer. Cell *156*, 893–906.

[Murchison et al., 2005] Murchison, E. P., Partridge, J. F., Tam, O. H., Cheloufi, S. and Hannon, G. J. (2005). Characterization of Dicer-deficient murine embryonic stem cells. Proc Natl Acad Sci U S A *102*, 12135–40.

[Nakao et al., 1997] Nakao, J., Shinoda, J., Nakai, Y., Murase, S. and Uyemura, K. (1997). Apoptosis regulates the number of Schwann cells at the premyelinating stage. J Neurochem *68*, 1853–62.

[Nam et al., 2011] Nam, Y., Chen, C., Gregory, R. I., Chou, J. J. and Sliz, P. (2011). Molecular basis for interaction of let-7 microRNAs with Lin28. Cell *147*, 1080–91.

[Newbern et al., 2011] Newbern, J. M., Li, X., Shoemaker, S. E., Zhou, J., Zhong, J., Wu, Y., Bonder, D., Hollenback, S., Coppola, G., Geschwind, D. H., Landreth, G. E. and Snider, W. D. (2011). Specific functions for ERK/MAPK signaling during PNS development. Neuron *69*, 91–105.

[Niemann et al., 2006] Niemann, A., Berger, P. and Suter, U. (2006). Pathomechanisms of mutant proteins in Charcot-Marie-Tooth disease. Neuromolecular Med *8*, 217–42.

[Nodari et al., 2007] Nodari, A., Zambroni, D., Quattrini, A., Court, F. A., D'Urso, A., Recchia, A., Tybulewicz, V. L., Wrabetz, L. and Feltri, M. L. (2007). beta1 integrin activates Rac1 in Schwann cells to generate radial lamellae during axonal sorting and myelination. J Cell Biol *177*, 1063–75.

[Norrmen et al., 2014] Norrmen, C., Figlia, G., Lebrun-Julien, F., Pereira, J. A., Trotzmuller, M., Kofeler, H. C., Rantanen, V., Wessig, C., van Deijk, A. L., Smit, A. B., Verheijen, M. H., Ruegg, M. A., Hall, M. N. and Suter, U. (2014). mTORC1 Controls PNS Myelination along the mTORC1-RXRgamma-SREBP-Lipid Biosynthesis Axis in Schwann Cells. Cell Rep *9*, 646–60.

[Oppenheim et al., 1999] Oppenheim, R. W., Homma, S., Marti, E., Prevette, D., Wang, S., Yaginuma, H. and McMahon, A. P. (1999). Modulation of early but not later stages

of programmed cell death in embryonic avian spinal cord by sonic hedgehog. Mol Cell Neurosci *13*, 348–61.

[Orita et al., 2013] Orita, S., Henry, K., Mantuano, E., Yamauchi, K., De Corato, A., Ishikawa, T., Feltri, M. L., Wrabetz, L., Gaultier, A., Pollack, M., Ellisman, M., Takahashi, K., Gonias, S. L. and Campana, W. M. (2013). Schwann cell LRP1 regulates remak bundle ultrastructure and axonal interactions to prevent neuropathic pain. J Neurosci *33*, 5590–602.

[Ozcelik et al., 2010] Ozcelik, M., Cotter, L., Jacob, C., Pereira, J. A., Relvas, J. B., Suter, U. and Tricaud, N. (2010). Pals1 is a major regulator of the epithelial-like polarization and the extension of the myelin sheath in peripheral nerves. J Neurosci *30*, 4120–31.

[Ozsolak et al., 2008] Ozsolak, F., Poling, L. L., Wang, Z., Liu, H., Liu, X. S., Roeder, R. G., Zhang, X., Song, J. S. and Fisher, D. E. (2008). Chromatin structure analyses identify miRNA promoters. Genes Dev *22*, 3172–83.

[Panman and Zeller, 2003] Panman, L. and Zeller, R. (2003). Patterning the limb before and after SHH signalling. J Anat *202*, 3–12.

[Parkinson et al., 2008] Parkinson, D. B., Bhaskaran, A., Arthur-Farraj, P., Noon, L. A., Woodhoo, A., Lloyd, A. C., Feltri, M. L., Wrabetz, L., Behrens, A., Mirsky, R. and Jessen, K. R. (2008). c-Jun is a negative regulator of myelination. J Cell Biol *181*, 625–37.

[Parmantier et al., 1999] Parmantier, E., Lynn, B., Lawson, D., Turmaine, M., Namini, S. S., Chakrabarti, L., McMahon, A. P., Jessen, K. R. and Mirsky, R. (1999). Schwann cell-derived Desert hedgehog controls the development of peripheral nerve sheaths. Neuron *23*, 713–24.

[Pellegatta et al., 2013] Pellegatta, M., De Arcangelis, A., D'Urso, A., Nodari, A., Zambroni, D., Ghidinelli, M., Matafora, V., Williamson, C., Georges-Labouesse, E., Kreidberg, J., Mayer, U., McKee, K. K., Yurchenco, P. D., Quattrini, A., Wrabetz, L. and Feltri, M. L. (2013). alpha6beta1 and alpha7beta1 integrins are required in Schwann cells to sort axons. J Neurosci *33*, 17995–8007.

[Pereira et al., 2010] Pereira, J. A., Baumann, R., Norrmen, C., Somandin, C., Miehe, M., Jacob, C., Luhmann, T., Hall-Bozic, H., Mantei, N., Meijer, D. and Suter, U. (2010). Dicer in Schwann cells is required for myelination and axonal integrity. J Neurosci *30*, 6763–75.

[Pereira et al., 2009] Pereira, J. A., Benninger, Y., Baumann, R., Goncalves, A. F., Ozcelik, M., Thurnherr, T., Tricaud, N., Meijer, D., Fassler, R., Suter, U. and Relvas, J. B. (2009). Integrin-linked kinase is required for radial sorting of axons and Schwann cell remyelination in the peripheral nervous system. J Cell Biol *185*, 147–61.

[Pereira et al., 2012] Pereira, J. A., Lebrun-Julien, F. and Suter, U. (2012). Molecular mechanisms regulating myelination in the peripheral nervous system. Trends Neurosci *35*, 123–34.

[Peters and Muir, 1959] Peters, A. and Muir, A. R. (1959). The relationship between axons and Schwann cells during development of peripheral nerves in the rat. Q J Exp Physiol Cogn Med Sci *44*, 117–30.

[Piskounova et al., 2008] Piskounova, E., Viswanathan, S. R., Janas, M., LaPierre, R. J., Daley, G. Q., Sliz, P. and Gregory, R. I. (2008). Determinants of microRNA processing inhibition by the developmentally regulated RNA-binding protein Lin28. J Biol Chem *283*, 21310–4.

[Poy et al., 2009] Poy, M. N., Hausser, J., Trajkovski, M., Braun, M., Collins, S., Rorsman, P., Zavolan, M. and Stoffel, M. (2009). miR-375 maintains normal pancreatic alpha- and beta-cell mass. Proc Natl Acad Sci U S A *106*, 5813–8.

[Quintes et al., 2010] Quintes, S., Goebbels, S., Saher, G., Schwab, M. H. and Nave, K. A. (2010). Neuron-glia signaling and the protection of axon function by Schwann cells. J Peripher Nerv Syst *15*, 10–6.

[Rehmsmeier et al., 2004] Rehmsmeier, M., Steffen, P., Hochsmann, M. and Giegerich, R. (2004). Fast and effective prediction of microRNA/target duplexes. RNA *10*, 1507–17.

[Riobo et al., 2006] Riobo, N. A., Lu, K., Ai, X., Haines, G. M. and Emerson, C. P., J. (2006). Phosphoinositide 3-kinase and Akt are essential for Sonic Hedgehog signaling. Proc Natl Acad Sci U S A *103*, 4505–10.

[Rodriguez et al., 2004] Rodriguez, A., Griffiths-Jones, S., Ashurst, J. L. and Bradley, A. (2004). Identification of mammalian microRNA host genes and transcription units. Genome Res *14*, 1902–10.

[Rodriguez et al., 2007] Rodriguez, A., Vigorito, E., Clare, S., Warren, M. V., Couttet, P., Soond, D. R., van Dongen, S., Grocock, R. J., Das, P. P., Miska, E. A., Vetrie, D., Okkenhaug, K., Enright, A. J., Dougan, G., Turner, M. and Bradley, A. (2007). Requirement of bic/microRNA-155 for normal immune function. Science *316*, 608–11.

[Roop and Toftgard, 2008] Roop, D. and Toftgard, R. (2008). Hedgehog in Wnterland. Nat Genet *40*, 1040–1.

[Roush and Slack, 2008] Roush, S. and Slack, F. J. (2008). The let-7 family of microRNAs. Trends Cell Biol *18*, 505–16.

[Rowitch and Kriegstein, 2010] Rowitch, D. H. and Kriegstein, A. R. (2010). Developmental genetics of vertebrate glial-cell specification. Nature *468*, 214–22.

[Salzer, 2012] Salzer, J. L. (2012). Axonal regulation of Schwann cell ensheathment and myelination. J Peripher Nerv Syst *17 Suppl 3*, 14–9.

[Sanz-Ezquerro and Tickle, 2000] Sanz-Ezquerro, J. J. and Tickle, C. (2000). Autoregulation of Shh expression and Shh induction of cell death suggest a mechanism for modulating polarising activity during chick limb development. Development *127*, 4811–23.

[Scales and de Sauvage, 2009] Scales, S. J. and de Sauvage, F. J. (2009). Mechanisms of Hedgehog pathway activation in cancer and implications for therapy. Trends Pharmacol Sci *30*, 303–12.

[Schweigreiter et al., 2006] Schweigreiter, R., Roots, B. I., Bandtlow, C. E. and Gould, R. M. (2006). Understanding myelination through studying its evolution. Int Rev Neurobiol *73*, 219–73.

[Selbach et al., 2008] Selbach, M., Schwanhausser, B., Thierfelder, N., Fang, Z., Khanin, R. and Rajewsky, N. (2008). Widespread changes in protein synthesis induced by microRNAs. Nature *455*, 58–63.

[Sellier et al., 2013] Sellier, C., Freyermuth, F., Tabet, R., Tran, T., He, F., Ruffenach, F., Alunni, V., Moine, H., Thibault, C., Page, A., Tassone, F., Willemsen, R., Disney, M. D., Hagerman, P. J., Todd, P. K. and Charlet-Berguerand, N. (2013). Sequestration of DROSHA and DGCR8 by expanded CGG RNA repeats alters microRNA processing in fragile X-associated tremor/ataxia syndrome. Cell Rep *3*, 869–80.

[Shin et al., 2010] Shin, C., Nam, J. W., Farh, K. K., Chiang, H. R., Shkumatava, A. and Bartel, D. P. (2010). Expanding the microRNA targeting code: functional sites with centered pairing. Mol Cell *38*, 789–802.

[Shin et al., 2014] Shin, Y. K., Jang, S. Y., Park, S. Y., Park, J. Y., Kim, J. K., Kim, J. P., Suh, D. J., Lee, H. J. and Park, H. T. (2014). Grb2-associated binder-1 is required for neuregulin-1-induced peripheral nerve myelination. J Neurosci *34*, 7657–62.

[Shiohama et al., 2007] Shiohama, A., Sasaki, T., Noda, S., Minoshima, S. and Shimizu, N. (2007). Nucleolar localization of DGCR8 and identification of eleven DGCR8-associated proteins. Exp Cell Res *313*, 4196–207.

[Siggins et al., 2009] Siggins, S. L., Nguyen, N. Y., McCormack, M. P., Vasudevan, S., Villani, R., Jane, S. M., Wainwright, B. J. and Curtis, D. J. (2009). The Hedgehog receptor Patched1 regulates myeloid and lymphoid progenitors by distinct cell-extrinsic mechanisms. Blood *114*, 995–1004.

[Skalsky et al., 2012] Skalsky, R. L., Corcoran, D. L., Gottwein, E., Frank, C. L., Kang, D., Hafner, M., Nusbaum, J. D., Feederle, R., Delecluse, H. J., Luftig, M. A., Tuschl, T., Ohler, U. and Cullen, B. R. (2012). The viral and cellular microRNA targetome in lymphoblastoid cell lines. PLoS Pathog *8*, e1002484.

[Suzuki et al., 2009] Suzuki, H. I., Yamagata, K., Sugimoto, K., Iwamoto, T., Kato, S. and Miyazono, K. (2009). Modulation of microRNA processing by p53. Nature *460*, 529–33.

[Syroid et al., 2000] Syroid, D. E., Maycox, P. J., Soilu-Hanninen, M., Petratos, S., Bucci, T., Burrola, P., Murray, S., Cheema, S., Lee, K. F., Lemke, G. and Kilpatrick, T. J. (2000). Induction of postnatal schwann cell death by the low-affinity neurotrophin receptor in vitro and after axotomy. J Neurosci *20*, 5741–7.

[Tabara et al., 1999] Tabara, H., Sarkissian, M., Kelly, W. G., Fleenor, J., Grishok, A., Timmons, L., Fire, A. and Mello, C. C. (1999). The rde-1 gene, RNA interference, and transposon silencing in C. elegans. Cell *99*, 123–32.

[Tang et al., 2011] Tang, X., Li, M., Tucker, L. and Ramratnam, B. (2011). Glycogen synthase kinase 3 beta (GSK3beta) phosphorylates the RNAase III enzyme Drosha at S300 and S302. PLoS One *6*, e20391.

[Tang et al., 2013] Tang, X., Wen, S., Zheng, D., Tucker, L., Cao, L., Pantazatos, D., Moss, S. F. and Ramratnam, B. (2013). Acetylation of drosha on the N-terminus inhibits its degradation by ubiquitination. PLoS One *8*, e72503.

[Tay et al., 2008] Tay, Y., Zhang, J., Thomson, A. M., Lim, B. and Rigoutsos, I. (2008). MicroRNAs to Nanog, Oct4 and Sox2 coding regions modulate embryonic stem cell differentiation. Nature *455*, 1124–8.

[Teta et al., 2012] Teta, M., Choi, Y. S., Okegbe, T., Wong, G., Tam, O. H., Chong, M. M., Seykora, J. T., Nagy, A., Littman, D. R., Andl, T. and Millar, S. E. (2012). Inducible deletion of epidermal Dicer and Drosha reveals multiple functions for miRNAs in postnatal skin. Development *139*, 1405–16.

[Thornton and Gregory, 2012] Thornton, J. E. and Gregory, R. I. (2012). How does Lin28 let-7 control development and disease? Trends Cell Biol *22*, 474–82.

[Topilko et al., 1994] Topilko, P., Schneider-Maunoury, S., Levi, G., Baron-Van Evercooren, A., Chennoufi, A. B., Seitanidou, T., Babinet, C. and Charnay, P. (1994). Krox-20 controls myelination in the peripheral nervous system. Nature *371*, 796–9.

[Triboulet et al., 2009] Triboulet, R., Chang, H. M., Lapierre, R. J. and Gregory, R. I. (2009). Post-transcriptional control of DGCR8 expression by the Microprocessor. RNA *15*, 1005–11.

[Varjosalo and Taipale, 2008] Varjosalo, M. and Taipale, J. (2008). Hedgehog: functions and mechanisms. Genes Dev *22*, 2454–72.

[Vella et al., 2004] Vella, M. C., Choi, E. Y., Lin, S. Y., Reinert, K. and Slack, F. J. (2004). The C. elegans microRNA let-7 binds to imperfect let-7 complementary sites from the lin-41 3'UTR. Genes Dev *18*, 132–7.

[Verrier et al., 2010] Verrier, J. D., Semple-Rowland, S., Madorsky, I., Papin, J. E. and Notterpek, L. (2010). Reduction of Dicer impairs Schwann cell differentiation and myelination. J Neurosci Res *88*, 2558–68.

[Viader et al., 2011] Viader, A., Chang, L. W., Fahrner, T., Nagarajan, R. and Milbrandt, J. (2011). MicroRNAs modulate Schwann cell response to nerve injury by reinforcing transcriptional silencing of dedifferentiation-related genes. J Neurosci *31*, 17358–69.

[Viswanathan et al., 2009] Viswanathan, S. R., Powers, J. T., Einhorn, W., Hoshida, Y., Ng, T. L., Toffanin, S., O'Sullivan, M., Lu, J., Phillips, L. A., Lockhart, V. L., Shah, S. P., Tanwar, P. S., Mermel, C. H., Beroukhim, R., Azam, M., Teixeira, J., Meyerson, M., Hughes, T. P., Llovet, J. M., Radich, J., Mullighan, C. G., Golub, T. R., Sorensen, P. H. and Daley, G. Q. (2009). Lin28 promotes transformation and is associated with advanced human malignancies. Nat Genet *41*, 843–8.

[Vo et al., 2010] Vo, N. K., Dalton, R. P., Liu, N., Olson, E. N. and Goodman, R. H. (2010). Affinity purification of microRNA-133a with the cardiac transcription factor, Hand2. Proc Natl Acad Sci U S A *107*, 19231–6.

[Voiculescu et al., 2000] Voiculescu, O., Charnay, P. and Schneider-Maunoury, S. (2000). Expression pattern of a Krox-20/Cre knock-in allele in the developing hindbrain, bones, and peripheral nervous system. Genesis *26*, 123–6.

[Wada et al., 2012] Wada, T., Kikuchi, J. and Furukawa, Y. (2012). Histone deacetylase 1 enhances microRNA processing via deacetylation of DGCR8. EMBO Rep *13*, 142–9.

[Wagschal et al., 2012] Wagschal, A., Rousset, E., Basavarajaiah, P., Contreras, X., Harwig, A., Laurent-Chabalier, S., Nakamura, M., Chen, X., Zhang, K., Meziane, O., Boyer, F., Parrinello, H., Berkhout, B., Terzian, C., Benkirane, M. and Kiernan, R. (2012). Microprocessor, Setx, Xrn2, and Rrp6 co-operate to induce premature termination of transcription by RNAPII. Cell *150*, 1147–57.

[Wang et al., 2007] Wang, Y., Medvid, R., Melton, C., Jaenisch, R. and Blelloch, R. (2007). DGCR8 is essential for microRNA biogenesis and silencing of embryonic stem cell self-renewal. Nat Genet *39*, 380–5.

[Wang et al., 2009] Wang, Z., Gerstein, M. and Snyder, M. (2009). RNA-Seq: a revolutionary tool for transcriptomics. Nat Rev Genet *10*, 57–63.

[Watanabe et al., 2008] Watanabe, T., Totoki, Y., Toyoda, A., Kaneda, M., Kuramochi-Miyagawa, S., Obata, Y., Chiba, H., Kohara, Y., Kono, T., Nakano, T., Surani, M. A., Sakaki, Y. and Sasaki, H. (2008). Endogenous siRNAs from naturally formed dsRNAs regulate transcripts in mouse oocytes. Nature *453*, 539–43.

[Webster et al., 1973] Webster, H. D., Martin, R. and O'Connell, M. F. (1973). The relationships between interphase Schwann cells and axons before myelination: a quantitative electron microscopic study. Dev Biol *32*, 401–16.

[Wheeler et al., 2009] Wheeler, B. M., Heimberg, A. M., Moy, V. N., Sperling, E. A., Holstein, T. W., Heber, S. and Peterson, K. J. (2009). The deep evolution of metazoan microRNAs. Evol Dev *11*, 50–68.

[Wienholds et al., 2005] Wienholds, E., Kloosterman, W. P., Miska, E., Alvarez-Saavedra, E., Berezikov, E., de Bruijn, E., Horvitz, H. R., Kauppinen, S. and Plasterk, R. H. (2005). MicroRNA expression in zebrafish embryonic development. Science *309*, 310–1.

[Woodhoo et al., 2009] Woodhoo, A., Alonso, M. B., Droggiti, A., Turmaine, M., D'Antonio, M., Parkinson, D. B., Wilton, D. K., Al-Shawi, R., Simons, P., Shen, J., Guillemot, F., Radtke, F., Meijer, D., Feltri, M. L., Wrabetz, L., Mirsky, R. and Jessen, K. R. (2009). Notch controls embryonic Schwann cell differentiation, postnatal myelination and adult plasticity. Nat Neurosci *12*, 839–47.

[Wu et al., 2010] Wu, H., Sun, S., Tu, K., Gao, Y., Xie, B., Krainer, A. R. and Zhu, J. (2010). A splicing-independent function of SF2/ASF in microRNA processing. Mol Cell *38*, 67–77.

[Wu et al., 2000] Wu, H., Xu, H., Miraglia, L. J. and Crooke, S. T. (2000). Human RNase III is a 160-kDa protein involved in preribosomal RNA processing. J Biol Chem *275*, 36957–65.

[Xie et al., 2013] Xie, M., Li, M., Vilborg, A., Lee, N., Shu, M. D., Yartseva, V., Sestan, N. and Steitz, J. A. (2013). Mammalian 5'-capped microRNA precursors that generate a single microRNA. Cell *155*, 1568–80.

[Xie et al., 2005] Xie, X., Lu, J., Kulbokas, E. J., Golub, T. R., Mootha, V., Lindblad-Toh, K., Lander, E. S. and Kellis, M. (2005). Systematic discovery of regulatory motifs in human promoters and 3' UTRs by comparison of several mammals. Nature *434*, 338–45.

[Yang et al., 2005] Yang, D., Bierman, J., Tarumi, Y. S., Zhong, Y. P., Rangwala, R., Proctor, T. M., Miyagoe-Suzuki, Y., Takeda, S., Miner, J. H., Sherman, L. S., Gold, B. G. and Patton, B. L. (2005). Coordinate control of axon defasciculation and myelination by laminin-2 and -8. J Cell Biol *168*, 655–66.

[Yang and Lai, 2011] Yang, J. S. and Lai, E. C. (2011). Alternative miRNA biogenesis pathways and the interpretation of core miRNA pathway mutants. Mol Cell *43*, 892–903.

[Yeom et al., 2006] Yeom, K. H., Lee, Y., Han, J., Suh, M. R. and Kim, V. N. (2006). Characterization of DGCR8/Pasha, the essential cofactor for Drosha in primary miRNA processing. Nucleic Acids Res *34*, 4622–9.

[Yi et al., 2009] Yi, R., Pasolli, H. A., Landthaler, M., Hafner, M., Ojo, T., Sheridan, R., Sander, C., O'Carroll, D., Stoffel, M., Tuschl, T. and Fuchs, E. (2009). DGCR8-

dependent microRNA biogenesis is essential for skin development. Proc Natl Acad Sci U S A *106*, 498–502.

[Yi et al., 2003] Yi, R., Qin, Y., Macara, I. G. and Cullen, B. R. (2003). Exportin-5 mediates the nuclear export of pre-microRNAs and short hairpin RNAs. Genes Dev *17*, 3011–6.

[Yu et al., 2005] Yu, W. M., Feltri, M. L., Wrabetz, L., Strickland, S. and Chen, Z. L. (2005). Schwann cell-specific ablation of laminin gamma1 causes apoptosis and prevents proliferation. J Neurosci *25*, 4463–72.

[Yu et al., 2009] Yu, W. M., Yu, H., Chen, Z. L. and Strickland, S. (2009). Disruption of laminin in the peripheral nervous system impedes nonmyelinating Schwann cell development and impairs nociceptive sensory function. Glia *57*, 850–9.

[Yun et al., 2010] Yun, B., Anderegg, A., Menichella, D., Wrabetz, L., Feltri, M. L. and Awatramani, R. (2010). MicroRNA-deficient Schwann cells display congenital hypomyelination. J Neurosci *30*, 7722–8.

[Zamudio et al., 2014] Zamudio, J. R., Kelly, T. J. and Sharp, P. A. (2014). Argonaute-bound small RNAs from promoter-proximal RNA polymerase II. Cell *156*, 920–34.

[Zhang et al., 2004] Zhang, H., Kolb, F. A., Jaskiewicz, L., Westhof, E. and Filipowicz, W. (2004). Single processing center models for human Dicer and bacterial RNase III. Cell *118*, 57–68.

[Zhang et al., 2009] Zhang, Y., Argaw, A. T., Gurfein, B. T., Zameer, A., Snyder, B. J., Ge, C., Lu, Q. R., Rowitch, D. H., Raine, C. S., Brosnan, C. F. and John, G. R. (2009). Notch1 signaling plays a role in regulating precursor differentiation during CNS remyelination. Proc Natl Acad Sci U S A *106*, 19162–7.

[Zhang et al., 2013] Zhang, Y., Wang, Z. and Gemeinhart, R. A. (2013). Progress in microRNA delivery. J Control Release *172*, 962–74.

[Zhao et al., 2010] Zhao, X., He, X., Han, X., Yu, Y., Ye, F., Chen, Y., Hoang, T., Xu, X., Mi, Q. S., Xin, M., Wang, F., Appel, B. and Lu, Q. R. (2010). MicroRNA-mediated control of oligodendrocyte differentiation. Neuron *65*, 612–26.

[Zisoulis et al., 2010] Zisoulis, D. G., Lovci, M. T., Wilbert, M. L., Hutt, K. R., Liang, T. Y., Pasquinelli, A. E. and Yeo, G. W. (2010). Comprehensive discovery of endogenous Argonaute binding sites in Caenorhabditis elegans. Nat Struct Mol Biol *17*, 173–9.

[Zuzarte-Luis and Hurle, 2005] Zuzarte-Luis, V. and Hurle, J. M. (2005). Programmed cell death in the embryonic vertebrate limb. Semin Cell Dev Biol *16*, 261–9.

Acknowledgements